

Using Co-Disposal Techniques to Achieve Stable “Dry-Stacked” Tailings: Geotechnical
Properties of Blended Waste Rock and Tailings in Oil Sands and Metal Mining

by

Ralph Burden

A thesis submitted in partial fulfillment of the requirements for the degree of

Doctor of Philosophy

Geo-Environmental Engineering

Department of Civil and Environmental Engineering
University of Alberta

© Ralph Burden, 2021

ABSTRACT

Mine “tailings”, waste produced by the extraction process, are most typically stored in impoundments behind dams which are often constructed from the tailings themselves. These structures pose a serious geotechnical risk and are difficult to successfully reclaim at the end of mining. As highly destructive, tragic failures of tailings dams continue to occur, the mining industry and society at large seek more sustainable methods of waste management. In response, an increasingly common alternative to traditional tailings disposal is “dry stacking”: the placement of dewatered tailings in a self-supporting stack. This thesis investigates the application of co-disposal techniques, the blending of waste rock and tailings, to dry stacking. Two distinct applications are considered: blending filtered gold tailings with waste rock to improve the geotechnical performance of the stack and blending of oil sands tailings with Clearwater shale overburden material.

The addition of waste rock to a filtered tailings stack by blending the rock and tailings has the potential to offer significant advantage over established dry stacking methods. A conceptual model was developed to describe the behaviour of filtered tailings and waste rock blends, based upon particle packing arrangement. The model may be used to predict the structure and behaviour of the blend, based on mix ratio and density. In addition, the thesis presents the results of experimental investigations on filtered tailings and waste rock blends. The compression behaviour and pore pressure response under self-weight consolidation of blends at a range of mix ratios was investigated using an innovative methodology that was developed to simulate the placement of stacks, using a controlled rate of loading test. Large scale direct shear tests were undertaken to investigate the

relationship between shear strength and mix ratio. Blends of waste rock and tailings were observed that have higher drained shear strength than waste rock alone. Shear strength was observed to increase with rock content, up to a limiting value of 1 : 1 rock to tailings by dry mass. At higher stresses, or with weaker rocks, the strength of the blend has the potential to be higher than rockfill alone. The addition of waste rock to filtered tailings reduces the build-up of pore pressure when loaded in compression with an incrementally increasing load. This suggests that co-disposal of filtered tailings with rock will reduce the build-up of pore pressure during stacking, improving stability and allowing more rapid deposition or deposition in higher lifts.

The oil sands of Northern Alberta present their own unique waste management challenge: very large volumes of fluid fine tailings (FFT) that are challenging to dewater by normal methods. A promising solution to this problem is co-disposal of FFT with the clay shale overburden found in the area. It has been demonstrated that clay shale overburden can be blended with FFT to create trafficable deposits. This study investigates the compression behaviour and pore pressure response of stacked clay shale – FFT blends, using the sample consolidation cell used in the filtered gold tailings study. Volume change behaviour and pore pressure response of Clearwater shale – FFT blends were found to be a complex, time-dependent process, governed by both consolidation and by transfer of moisture from the FFT into the shale lumps. Further study is recommended to characterise this process, including development of an unsaturated, double-porosity consolidation numerical consolidation model.

ACKNOWLEDGEMENTS

I am very grateful to my supervisor, Dr Ward Wilson, and to Dr David Williams of the University of Queensland, for the guidance and support they have provided throughout the process of production of this thesis. I would also like to thank everyone at the University of Alberta, especially Dr Louis Kabwe, Christine Hereygers and David Barsi for their help with the laboratory work, Annette Busenius and Jen Stogowski for running the place, and Vivian Giang for her grant writing and also running the place. Thanks also to all the staff and students at the University of Queensland for making me feel welcome while I was there, in particular Sebastian Quintero and Jennifer Speer for their assistance in the lab (and for providing me with a roof over my head!).

Special thanks to everyone at Peñasquito Mine and Newmont Goldcorp who helped to make the field work happen, in particular Ross Hunsaker, Mike Jacobs and Manuel Apparicio. Also thanks to Nan Wang at Syncrude for his support and for provision of the oil sands samples.

I would also like to thank the Natural Sciences and Engineering Research Council of Canada (NSERC) and Canadian Oil Sands Innovation Alliance (COSIA) for assistance in funding this research.

TABLE OF CONTENTS

Abstract.....	i
Acknowledgements	iii
Table of contents.....	iv
List of tables	viii
List of figures.....	x
List of symbols and acronyms	xv
1 Introduction	1
1.1 Background	1
1.1.1 Metal mining – Filtered tailings and waste rock blends.....	2
1.1.2 Oil sands co-disposal.....	3
1.2 Scope and objectives of the thesis	4
1.2.1 Objectives of the research	4
1.2.2 Scope of the research.....	5
1.3 Layout of the thesis	6
2 Mix design theory for filtered tailings and waste rock blends	8
2.1 Introduction	8
2.2 Background	9
2.2.1 Filtered tailings	9
2.2.2 Co-disposal of waste rock and tailings.....	12
2.2.3 Blended co-disposal	13
2.3 Objective	15
2.4 Phase relationships.....	15
2.5 Mix ratio.....	17
2.6 Ternary diagram.....	18
2.6.1 Estimation of material property boundaries	20
2.6.2 Estimation of the “just filled” line	22

2.7	Structure and compression behaviour of stacked filtered tailings and waste rock blends	24
2.7.1	Construction of the material property boundary chart.....	29
2.8	Summary and conclusions	31
	References.....	33
3	A novel method of simulating “dry stacked” tailings deposition using CRL tests	36
3.1	Introduction	36
3.2	Method	39
3.2.1	Equipment	39
3.2.2	Theoretical approach.....	42
3.2.3	Materials.....	45
3.2.4	Summary of tests performed	50
3.3	Results	54
3.3.1	Test series 1	54
3.3.2	Test series 2.....	61
3.4	Analysis and discussion	68
3.4.1	Pore pressure response	68
3.4.2	Density.....	72
3.4.3	Blend structure and configuration.....	73
3.4.4	Container wall effects	82
3.4.5	Other issues identified with the slurry consolidometer test	88
3.5	Further discussion and conclusions	89
	References.....	92
4	The shear strength of filtered tailings and waste rock blends	95
4.1	Introduction	95
4.2	Background.....	96
4.3	Objective	98
4.4	Materials.....	98
4.4.1	Sampling.....	98
4.4.2	Basic characterisation.....	105
4.4.3	Sample preparation and blending.....	110

4.5	Method	115
4.6	Results	118
4.6.1	Summary	118
4.6.2	Shear stress – strain behaviour	120
4.6.3	Moisture content and density.....	124
4.6.4	Particle size distributions	126
4.7	Discussion.....	127
4.8	Conclusions.....	132
	References.....	133
5	Co-disposal in the oil sands: Geotechnical testing on Clearwater shale and fluid fine tailings blends	136
5.1	Introduction	136
5.2	Background	137
5.2.1	Geological background	137
5.2.2	Previous studies on Clearwater shale – FFT blends	138
5.3	Mix design theory for Clearwater Shale – FFT blends.....	141
5.3.1	Blend structure and configuration	141
5.3.2	Phase relationships	143
5.3.3	Mix ratio	145
5.3.4	Predicting blend configuration from mix ratio.....	147
5.4	Experimental Investigations	147
5.4.1	Material Characterisation.....	148
5.4.2	Mixing trial	154
5.4.3	Slurry consolidometer testing	157
5.5	Further discussion and conclusions	174
	References.....	176
6	Conclusions and recommendations.....	178
6.1	Conclusion	178
6.2	Contributions of the thesis.....	179
6.3	Recommendations for further research.....	180
	References (Combined)	182

LIST OF TABLES

Table 2-1: Input parameters for Figure 2-10.....	31
Table 3-1: Index properties	46
Table 3-2: Summary of tests performed in series 1 (rapid deposition)	51
Table 3-3: Summary of tests performed in series 2 (slow deposition)	52
Table 3-4: Test series 2 load steps and load rates.....	54
Table 3-5: Initial and final moisture content and density properties for test series 1	55
Table 3-6: Initial and final moisture content and density properties for test series 2	61
Table 3-7: Wall friction losses in slurry consolidometer tests	82
Table 4-1 Gravimetric moisture content of waste rock and filtered tailings.....	106
Table 4-2: Atterberg limits for filtered tailings	106
Table 4-3 Specific gravity of soil solids for waste rock and filtered tailings.....	107
Table 4-4: Fredlund – Xing curve fitting parameters.....	109
Table 4-5: Maximum recommended particle size parameters for a 300 x 300 x 200 mm direct shear test.....	111
Table 4-6: D_{50} and D_{max} parameters for blends tested	111
Table 4-7: Effective (after scalping) mix ratios for blends produced.....	112
Table 4-8: Peak shear stress	119
Table 4-9: Friction angles.....	120
Table 4-10: Moisture content and density of direct shear samples.....	125
Table 5-1: Gravimetric moisture content of oil sands materials.....	148
Table 5-2 Atterberg limits of Syncrude centrifuge cake (after Schafer 2018)	149

Table 5-3 Atterberg limits for the Clearwater formation (after Zadar and Chalaturnyk 2015)	149
Table 5-4: Specific gravity of solids for oil sands materials	152
Table 5-5: MBI for Clearwater shale (after Mikula, Wang et al. 2016)	152
Table 5-6: XRD analysis for Clearwater shale and FFT (after Mikula, Wang et al. 2016)	153
Table 5-7: Dean Stark test results for oil sands tailings	153
Table 5-8: Summary of slurry consolidometer tests on oil sand materials	161
Table 5-9: Initial and final void ratios for oil sands slurry consolidometer tests	162

LIST OF FIGURES

Figure 2-1: The tailings continuum (after Davies and Rice (2001) and Jewell and Fourie (2006)).....	10
Figure 2-2: Blend configurations (after Wickand et al. 2006).....	13
Figure 2-3: “paste rock” mix design theory (after Wickland et al. 2006)	14
Figure 2-4: Phase diagram for waste rock – tailings blends	16
Figure 2-5: Ternary diagram for waste rock – fine tailings blends	20
Figure 2-6: Ternary diagram showing blend configuration vs mix ratio for fine tailings – waste rock blends.....	21
Figure 2-7: Ternary diagram showing blend configuration vs mix ratio for different tailings dewatering technologies.....	22
Figure 2-8: Literature review of reported values for maximum void ratio of granular materials.....	23
Figure 2-9: Structure and compression behaviour of filtered tailings – waste rock blends	25
Figure 2-10: Material property boundary chart for filtered tailings – waste rock blend (per input parameters given in Table 2-1).....	28
Figure 3-1 Waste rock sampling.....	100
Figure 3-2 Waste rock sampling.....	101
Figure 3-3 Waste rock sampling.....	102
Figure 3-4 Waste rock sampling.....	103
Figure 3-5 Pilot-scale filter plant schematic.....	104
Figure 3-6: Pilot-scale filter plant.....	104
Figure 3-7: Filter press	105

Figure 3-8: Particle size distribution	107
Figure 3-9: Soil water characteristic curve for filtered tailings	109
Figure 3-10: Particle size distributions for blended materials scalped to 37 mm	113
Figure 3-11: Blending apparatus	114
Figure 3-12: 1:1 rock to tailings blend scalped to 37 mm	115
Figure 3-13: Large scale direct shear box containing an $R = 0.4$ sample.....	117
Figure 3-14: Collection of moisture sample from sheared material	118
Figure 3-15: Shear box test results summary.....	119
Figure 3-16: Direct shear test results at 250 kPa confining stress.....	121
Figure 3-17: Direct shear test results at 500 kPa confining stress.....	122
Figure 3-18: Direct shear test results at 1000 kPa confining stress.....	123
Figure 3-19 Particle size distributions of sheared waste rock samples	127
Figure 3-20: Direct shear tests plotted on property boundary chart	129
Figure 3-21: Comparison between saturated and unsaturated direct shear box test results ($R=1$ blend, 500 kPa confining stress)	131
Figure 4-1: Slurry consolidometer schematic (dimensions in mm)	40
Figure 4-2: Slurry consolidometer	41
Figure 4-3: Placement of filtered tailings sample in slurry consolidometer.....	41
Figure 4-4: Particle size distribution	47
Figure 4-5: Blending apparatus	48
Figure 4-6: Preparation of blend.....	49
Figure 4-7: Particle size distributions for blended materials	50
Figure 4-8: Test 1-1 – Initial sample height 100 mm	56
Figure 4-9: Test 1-2 – Initial sample height 30 mm	57

Figure 4-10: Base pore pressure against simulated field time for samples with different initial height	59
Figure 4-11: Normalised base pore pressure against simulated field time for samples with different initial height	60
Figure 4-12: Test 2-1 – Filtered tailings.....	62
Figure 4-13: Test 2-1 – $R = 1$ Blend	63
Figure 4-14: Test 2-1 – $R = 1.8$ Blend	64
Figure 4-15: Test 2-1 – Filtered tailings (plotted on simulated field time axis).....	65
Figure 4-16: Test 2-1 – $R = 1$ blend (plotted on simulated field time axis)	66
Figure 4-17: Test 2-3 – $R = 1.8$ blend (plotted on simulated field time axis)	67
Figure 4-18: Normalised base pore pressure against time.....	69
Figure 4-19: Normalised base pore pressure against simulated field time	70
Figure 4-20: Typical vertical total stress distributions in (a) Tailings stack, and (b) Slurry consolidometer cell.....	71
Figure 4-21: Void ratio – average normal stress relationship	73
Figure 4-22: Slurry consolidometer tests plotted on property boundary chart	74
Figure 4-23: Test 2-1 (Pure FT) dry density – applied stress and pore water pressure plot	75
Figure 4-24: Test 2-2 ($R = 1$ blend) dry density – applied stress and pore water pressure plot	76
Figure 4-25: Test 2-2 ($R = 1.8$ blend) dry density – applied stress and pore water pressure plot	77
Figure 4-26: Test 2-1 (Filtered tailings) average vertical stress – dry density plot.....	79
Figure 4-27: Test 2-2 ($R = 1$ blend) average vertical stress – dry density plot	80
Figure 4-28: Test 2-3 ($R = 1.8$ blend) average vertical stress – dry density plot	81

Figure 4-29: Measured and computed base stress for test 2-1 (pure tailings)	85
Figure 4-30: Measured and computed base stress for test 2-2 (1R:1T blend)	86
Figure 4-31: Measured and computed base stress for test 2-2 (1.8R:1T blend)	87
Figure 5-1: Particle structure configurations for Clearwater shale - FFT blends: (a) Shale lumps only; (b) Shale lump matrix partly filled with FFT; (c) "Just filled" condition; (d) "Floating" shale lumps in an FFT matrix; (e) FFT only	142
Figure 5-2: Schematic showing internal structure of shale "lump"	143
Figure 5-3: Phase diagram for Clearwater shale – FFT blends.....	144
Figure 5-4: Mass proportion with respect to mix ratio for a typical FFT – Clearwater shale blend	146
Figure 5-5: Bulk Mass Ratio (BMR) and solids content (s) with respect to dry mass ratio (R) for a typical FFT-Clearwater shale blend ($w_s = 20\%$, $w_t = 200\%$, $b = 8\%$).....	147
Figure 5-6: Particle size distribution for Clearwater shale samples	150
Figure 5-7: Particle size distribution for Syncrude centrifuge cake (after Schafer 2018)	151
Figure 5-8: Standard Proctor compaction curve for Clearwater shale – FFT blend.....	155
Figure 5-9: Dry density with respect to mix ratio for Centrifuge cake – KCA Clearwater shale blends compacted using the standard and modified Proctor method	156
Figure 5-10: Slurry consolidometer schematic (dimensions in mm)	159
Figure 5-11: Slurry consolidometer	160
Figure 5-12: Test 1 – 72% solids 108 mm sample height.....	163
Figure 5-13: Test 2 – 71% solids 104 mm sample height.....	164
Figure 5-14: Test 3 – 71% solids 264 mm sample height.....	165
Figure 5-15: Test 4 – 71% solids 35 mm sample height.....	166
Figure 5-16: Test 5 – 72% solids 191 mm sample height.....	167

Figure 5-17: Test 6 – 72% solids 192 mm sample height (left to cure for 1 week prior to test)	168
Figure 5-18: Normalised base pore against time for Test 1 and Test 2.....	169
Figure 5-19: Normalised base pore pressure against time for samples at a range of sample heights	170
Figure 5-20: Base pore pressure against time for Test 5 and Test 6.....	172
Figure 5-21: Normalised base pore pressure against time for Test 5 and Test 6.....	173

LIST OF SYMBOLS AND ACRONYMS

ARD	Acid rock drainage
BMR	Bulk mass ratio
CRL	Controlled rate of loading
CU	Consolidated undrained
FFT	Fluid fine tailings
LVDT	Linear variable differential transformer
MBI	Methylene blue index
SWCC	Soil-water characteristic curve
TSWR	Tailing solids – water ratio
XRD	X-ray diffraction
a	Dimensionless fitting parameter for Fredlund – Xing (1994) equation
b	Bitumen content (geotechnical definition)
c'	Effective cohesion
c_v	Coefficient of consolidation
d	Field drainage path length
D_{max}	Maximum grain size
D_{50}	Sieve diameter which 50% of particles pass
e	Void ratio
e_r	Waste rock skeleton void ratio
e_s	Internal lump void ratio
e_t	Tailings void ratio
e_t^*	Equivalent tailings void ratio (Borja 2019, Thevanayagam 2007)
G_s	Specific gravity of solids
G_{sr}	Specific gravity of rock solids
G_{st}	Specific gravity of tailings solids
h	Slurry consolidometer sample height
H	Direct shear box sample height

K	Coefficient of horizontal earth pressure
m	Rate of rise
m	Dimensionless fitting parameter for Fredlund – Xing (1994) equation
M	Total mass
M_{bit}	Mass of bitumen
M_r	Mass of rock
M_{rs}	Mass of rock solids
M_{rw}	Mass of rock porewater
M_t	Mass of tailings
M_{ts}	Mass of tailings mineral solids
M_{tw}	Mass of tailings porewater
n	Dimensionless fitting parameter for Fredlund – Xing (1994) equation
n_r	Waste rock skeleton porosity
n_{rmax}	Maximum porosity of waste rock skeleton
R	Mix ratio by dry mass
R_{opt}	“Just-filled” mix ratio
s	Solids content (geotechnical definition)
s_m	Solids content (mining definition)
S_r	Degree of saturation
t	Simulated field time
T	Time
T_s	Time scaling factor
u	Excess porewater pressure
u_a	Air pressure
u_b	Excess porewater pressure at sample base
u_i	Initial excess porewater pressure
u_w	Porewater pressure
V	Volume
V_{bit}	Volume of bitumen
V_r	Volume of rock

V_{rs}	Volume of rock solids
V_{rw}	Volume of rock porewater
V_{ma}	Volume of macro-scale air voids
V_t	Volume of tailings
V_{ta}	Volume of air voids in tailings
V_{ts}	Volume of tailings mineral solids
V_{tw}	Volume of tailings water
w	Moisture content
w_r	Rock moisture content
w_t	Tailings moisture content
W	Direct shear box width
γ	Unit weight
ρ_{bulk}	Bulk density
ρ_d	Dry density
σ	Vertical stress
$\bar{\sigma}$	Average vertical stress
φ'	Effective friction angle
ψ_r	Matric suction at residual water content
Θ	Volumetric water content
Θ_s	Volumetric water content at saturation

1 INTRODUCTION

1.1 Background

The extraction of mineral resources is a necessary function of society. Driven by global development and population growth, demand for the products of the mining industry is now greater than ever. Mining is an inherently waste-producing activity; in open pit mining, large quantities of overburden material are often stripped before ore can be mined. Furthermore, the majority of the ore also becomes a waste product; even high grade deposits contain only a few grams per tonne of recoverable metal. In typical metal mining operations, ore is recovered in a wet extraction process. The by-product, “tailings”, is discharged from the mill in the form of a fluid slurry, typically about 20-40% solids by mass. Conventionally, these are stored behind dams often constructed from the tailings themselves (Vick 1990). These structures can present a challenge for reclamation and closure, and are a long-term geotechnical risk and liability. Several large, high-profile and sometimes tragic failures have occurred in recent years, such as Mount Polley (Morgenstern, Vick et al. 2015), Fundão (Morgenstern, Vick et al. 2016) and Feijão (Robertson, de Melo et al. 2019), the latter of which resulted in the loss of over 250 lives. In response, traditional tailings dams are increasingly becoming seen as unacceptable by many stakeholders, and tailings management practices are now coming under scrutiny by major investors (COE 2019).

A promising new approach is “dry stacking”: the deposition of tailings in a self-supporting pile that has the potential to eliminate or reduce the need for a dam. Dry stacking has now been successfully applied in many commercial-scale mining operations (AMEC

2008, Newman, Arnold et al. 2010, Butikofer, Erickson et al. 2017, Wickland and Longo 2017, Crystal and Hore 2018). In the majority of cases, creating stackable tailings is achieved by using pressure- or vacuum-filtration to rapidly dewater the tailings, usually to around 80% solids by mass. The filtered tailings are typically transported to the disposal site by truck or conveyor, dried and then spread compacted using standard construction equipment.

Another emerging mine waste management technology is co-disposal of tailings and waste rock or overburden material. Co-disposal refers to the practice of disposing of tailings and waste rock in the same facility. Co-disposal can take a variety of forms; potential advantages include increased geochemical stability by encapsulation of acid generating rock, increased geotechnical stability and reduced overall waste volume. Co-disposal has been applied at several mines around the world (Habte and Bocking 2017) and has been the subject of numerous field- and laboratory-scale trials that have demonstrated its potential benefits over traditional means of disposal (Wickland and Wilson 2005, Wickland 2006, Wijewickreme, Khalili et al. 2010, Jehring and Bareither 2016, Antonaki, Abdoun et al. 2018, Bareither, Gorakhki et al. 2018). This thesis focuses on the application of co-disposal technology to achieve geotechnically stable dry stacks.

The thesis considers two distinct applications: one in conventional metal mining and one in oil sands mining. These are discussed in the following sections.

1.1.1 Metal mining – Filtered tailings and waste rock blends

Whilst numerous examples exist of successful filtered tailings stacking operations, it has thus far only been applied at small- to medium-sized mines; the largest mines currently

operating have throughputs of around 30,000 tonnes per day (Crystal and Hore 2018, Amoah 2019). A potential barrier to the successful scale-up of filtered tailings is the cost and operation complexity involved in the placement and compaction of filtered tailings using conventional construction equipment. The addition of waste rock to a filtered tailings stack during transit, using the same conveyor system used to transport the material to create a blended material, has the potential to offer significant advantages over established dry stacking methods, which may make large-scale dry stacking more economically viable. Understanding the geotechnical properties and behaviour of these materials is required to design safe and stable stacks.

1.1.2 Oil sands co-disposal

The Athabasca oil sands in Northern Alberta present their own unique tailings management challenges, most notably the very large volumes of fine tailings that have thus far proven very resistant to dewatering by normal methods. As of 2016, the industry as a whole managed an inventory of Fluid Fine Tailings (FFT), estimated to be 1.13 billion m³ (AER 2016). Unlike conventional metal mine tailings which can be effectively dewatered by filtration, dewatering of FFT remains a significant, largely unresolved challenge and represents a barrier to reclamation and closure. Whilst most approaches for dewatering FFT currently in use or under development aim to increase the solids content of the FFT by removing water, co-disposal with overburden increases the solids content by adding solids. This has great potential because of the high water demand of the clay shale overburden material found in the region. Upon mixing, water is transferred from the FFT to the shale, promoting rapid dewatering and strength gain. Co-disposal is

perhaps the only method currently under development that has the demonstrated potential to produce “dry stacks” of oil sand tailings quickly (Mikula, Wang et al. 2016, Wang, Cleminson et al. 2017), although it has yet to be implemented commercially at large scale. Whilst successful stacking of clay shale – FFT blends has been demonstrated, the geotechnical properties of the material are still not well understood. There is a particular need to understand the compression behaviour and the build-up and dissipation of excess pore pressures during stacking.

1.2 Scope and objectives of the thesis

1.2.1 *Objectives of the research*

The general goal of the research is to advance the understanding of the geotechnical behaviour of dry stacks of blended mine wastes. The research focusses on two specific co-disposal technologies: filtered tailings – waste rock blends and clay shale – oil sands tailings blends. Specific objectives include:

- Provide a state-of-the-art literature review on co-disposal research, with an emphasis on filtered tailings – waste rock blends, and oil sands tailings – clay shale blends;
- Develop an extended conceptual model, based on the model proposed by Wickland, Wilson et al. (2006) for understanding the behaviour of filtered tailings – waste rock blends and oil sands tailings – clay shale blends, with respect to particle structure;

- Investigate the compression behaviour of rapidly placed “dry stacks” of blended filtered tailings and waste rock, by developing an experimental method to predict pore pressure response and density under self-weight consolidation;
- Investigate the relationship between mix ratio and the shear strength of filtered tailings and waste rock blends; and
- Investigate the compression behaviour of rapidly placed “dry stacks” of blended Clearwater clay shale and FFT.

1.2.2 Scope of the research

This thesis presents laboratory-based investigations on two types of tailings, two types of waste rock or overburden material, and mixtures thereof. In addition, the thesis contains a literature review on filtered tailings and the co-disposal of waste rock and tailings, with a focus on co-disposal of waste rock and filtered tailings, and oil sands co-disposal.

The investigations into filtered gold tailings and waste rock blends include drained shear strength and compression behaviour, including the development of a new test methodology to simulate the placement of dry stacks. The investigations into FFT – Clearwater shale blends include compression behaviour.

The research does not include any investigations of operational considerations, such as large-scale blending, quantitative economic analysis or cost benefit analysis, geochemistry, hydraulic conductivity, water retention properties or static and seismic liquefaction potential, although it is acknowledged that such investigations would be critical to implementation and evaluation of these technologies.

1.3 Layout of the thesis

The major findings of this thesis are documented in four manuscripts to be submitted to peer-reviewed journals and conferences. Each manuscript is presented as a chapter. Some of the background materials are repeated between manuscripts.

Chapter 2 deals with the mix design of filtered tailings and waste rock blends. An extended theoretical model to predict the structure and behaviour of blends of waste rock and tailings is presented, based upon both mix ratio and density. It is based upon the co-disposal mix design theory developed by Wickland, Wilson et al. (2006) but is extended to consider the case of loosely placed materials and to consider the effect of volume change on structural configuration.

Chapter 3 presents a new method of simulating self-weight consolidation of tailings stacks in the laboratory, using Controlled Rate of Loading (CRL) tests where an incrementally increasing load rate is applied as the stress increases, to account for the increase in drainage path length as the tailings stack rises in the field. A procedure for calculating a series of load rates to simulate the required deposition rate is given, and the results of experimental trials on filtered gold tailings intended to verify this approach are presented. A second experimental trial is presented, which demonstrates the application of this method to the evaluation of different stack designs. Tests were carried out on co-mingled blends of waste rock and filtered tailings at a range of mix ratios, using a simulated constant deposition rate, to investigate the influence of rock addition on the geotechnical behaviour of stacked filtered tailings.

Chapter 4 investigates the relationship between mix ratio and shear strength for filtered tailings – waste rock blends. The results of large-scale direct shear tests carried out on blends at a range of mix ratios are presented.

Chapter 5 deals with the application of co-disposal to the dry stacking of oil sands tailings, specifically to the properties of Clearwater shale – FFT blends. A conceptual model, similar to the one presented in Chapter 2, is presented for the special case of oil sands materials. It is proposed that the mix ratio can be used as the principle parameter to control the properties of a blend and that the conceptual model can be used to predict the properties of a blend of a given mix ratio. It is shown how simple compaction tests can be used to estimate the relationship between mix ratio and configuration at the time of placement. In the second part of chapter, the properties of "dry stacked" Clearwater shale and FFT deposits are evaluated using the slurry consolidometer method presented in Chapter 3.

Finally, the materials presented in Chapters 2 through 5 are summarised in Chapter 6. Original contributions arising from this research and suggestions for further advancement are made in Chapter 6.

2 MIX DESIGN THEORY FOR FILTERED TAILINGS AND WASTE ROCK BLENDS

2.1 Introduction

Traditionally, mine tailings are discharged as slurry and stored behind dams often constructed from the tailings themselves (Vick 1990). These structures can present a challenge for reclamation and closure, and are a long-term geotechnical risk and liability. Several large, high-profile and sometimes tragic failures have occurred in recent years, such as Mount Polley (Morgenstern, Vick et al. 2015), Fundão (Morgenstern, Vick et al. 2016) and Feijão (Robertson, de Melo et al. 2019), the latter of which resulted in the loss of over 250 lives. In response, traditional tailings dams are increasingly becoming seen as unacceptable by many stakeholders.

A promising new approach is “dry stacking”, the deposition of tailings in a self-supporting pile that has the potential to eliminate or reduce the need for a dam. Dry stacking has now been successfully applied in many commercial-scale mining operations (AMEC 2008, Newman, Arnold et al. 2010, Butikofer, Erickson et al. 2017, Wickland and Longo 2017, Crystal and Hore 2018). In the majority of cases, creating stackable tailings is achieved by using pressure- or vacuum-filtration to rapidly dewater the tailings, usually to around 80% solids by mass. The filtered tailings are typically transported to the disposal site by truck or conveyor, dried and then spread compacted using standard construction equipment.

Whilst numerous examples exist of successful filtered tailings stacking operations, it has thus far only been applied at small- to medium sized mines; the largest of such currently operating mines have throughputs of around 30,000 tonnes per day (Crystal and Hore 2018, Amoah 2019). A potential barrier to the successful scale-up of filtered tailings is the cost and operation complexity involved in the placement and compaction of filtered tailings using conventional construction equipment. The addition of waste rock to a filtered tailings stack during transit, using the same conveyor system used to transport the material to create a blended material, has the potential to offer significant advantage over established dry stacking methods, which may make large-scale dry stacking more economically viable. Understanding the geotechnical properties and behaviour of these materials is required to design safe and stable stacks.

2.2 Background

2.2.1 *Filtered tailings*

Densified tailings technologies are broadly divided into three categories based on the mechanical properties and method of dewatering: thickened tailings (typically ~50-65% solids), paste tailings (typically 70-80% solids) and filtered tailings (>80% solids). A good overall summary of densified tailings technologies is given by Bussiere (2007). Figure 2-1 summarises the properties, and pros and cons, of different densified tailings technologies.

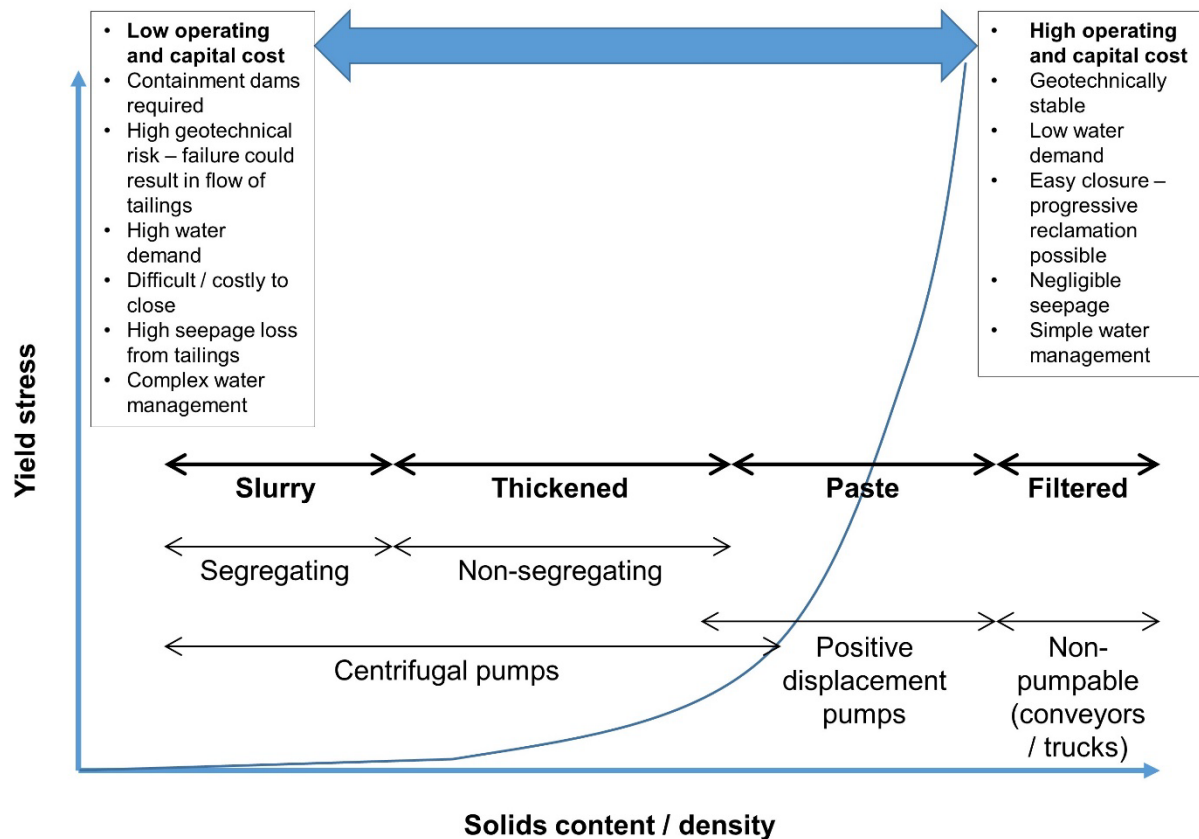


Figure 2-1: The tailings continuum (after Davies and Rice (2001) and Jewell and Fourie (2006))

Thickened and paste tailings technologies have many potential benefits, namely reduced water consumption, reduced waste volumes and improved geotechnical stability, whilst maintaining relatively low operating costs and good geochemical performance (Jewell and Fourie 2006, Williams, Seddon et al. 2008). However, some form of containment structure is still required for the deposition of thickened tailings or paste tailings alone. Construction of a stable, self-supporting “dry stack” requires filtration or co-disposal technologies.

Filtration is widely used in many fields to separate solids and liquids. The material is placed on a porous medium (such as filter paper or cloth) and a pressure gradient is

applied across the medium, causing the flow of filtrate through the medium and leaving behind a densified “cake”. A good summary of the literature on the general principles of filtration is given by Wang, Harbottle et al. (2014).

The pressure gradient may be applied by vacuum, mechanical squeezing action or via the feed pump. The most commonly used filter plant configurations are drums, stacked plates in either horizontal or vertical alignment, or horizontal belts (Davies and Rice 2001). Filtration performance is critically dependent upon the solids content of the feed. Consequently, the tailings are typically run through a conventional thickener prior to filtration. The filter cake is often left to dry to the optimum moisture content, or slightly dry of optimum, before compaction into the stack. The efficiency of the process is very much dependent upon the properties of the tailings feed. Low fines content, low clay content and high specific gravity are preferable for filtration; this gives lower filtration time requirement and consequently lower operating costs (Lara, Pornillos et al. 2013).

Filtered tailings “dry stacking” is becoming an increasingly popular alternative to traditional methods of tailings disposal and is now widespread in practice (Davies and Rice 2001, Jewell and Fourie 2006, Wickland and Longo 2017).

The first published use of filtered tailings technology is in the coal mining industry (Green 1981). Coal tailings, produced in the washing of coal, have a high fines content and low permeability, which makes de-watering by more conventional means difficult. As of 2008, there were reported to be 37 operating mines worldwide employing filtered tailings technologies, with production rates up to 24,000 t/day (AMEC 2008). The number of operating facilities has undoubtedly increased in recent years, although no

comprehensive list exists in the literature. Crystal and Hore (2018) prepared an inventory of 19 currently operating dry stacks, although almost all of them are small operations below 10,000 t/day. The largest currently operational mine employing filtered tailings is understood to be Karara (Amoah 2019) in Western Australia, a 30,000 t/day magnetite mine. Tailings are pressure filtered using vertical plates to around 85% solids, whereupon they are transported using an overland conveyor system and stacked in a radial pattern using conveyors and stackers.

Published literature on the geotechnical properties of filtered tailings is sparse and generally restricted to case histories (Lupo and Hall 2010, Newman, Arnold et al. 2010, Butikofer, Erickson et al. 2017, Robertson, da Fonseca et al. 2017). Generally speaking, filtered metal mine tailings have been shown to have similar behaviour to an unsaturated silty sand which is amenable to compaction and stacking.

2.2.2 Co-disposal of waste rock and tailings

The earliest use of co-disposal is probably in underground backfills, often combined with a binder such as Portland cement (Brawner and Argall 1978). Pumped co-disposal has also been implemented successfully at several coal mines around the world and has been shown to reduce waste volumes and the need for containment (Williams 1997). Other approaches that have been demonstrated include layered co-disposal, or “co-mingling”, which typically involves the placement of fine tailings layers inside a waste rock pile to act as a barrier to seepage or oxygen flux, and waste rock “inclusions” which are waste rock dykes placed inside tailings ponds as the ponds are raised to promote drainage and improve overall stability and seismic resistance. A summary of these techniques is given

by Bussiere (2007). More recent research at metal mines has focussed on producing homogenous blends to create an engineered material which has favourable properties, known as “paste rock” (Wilson et al. 2008). Blended co-disposal is the focus of this research.

2.2.3 Blended co-disposal

Wickland et al. (2006) present a theoretical basis for the design of “paste rock” blends, based on particle structure, as well as methods for predicting blend structure and properties from the mix ratio. The optimum mix ratio was found to be the “just filled” point, where tailings slurry fills the voids between the waste rock particles. Figure 2-2 shows structural configurations of “paste rock”-style blends.

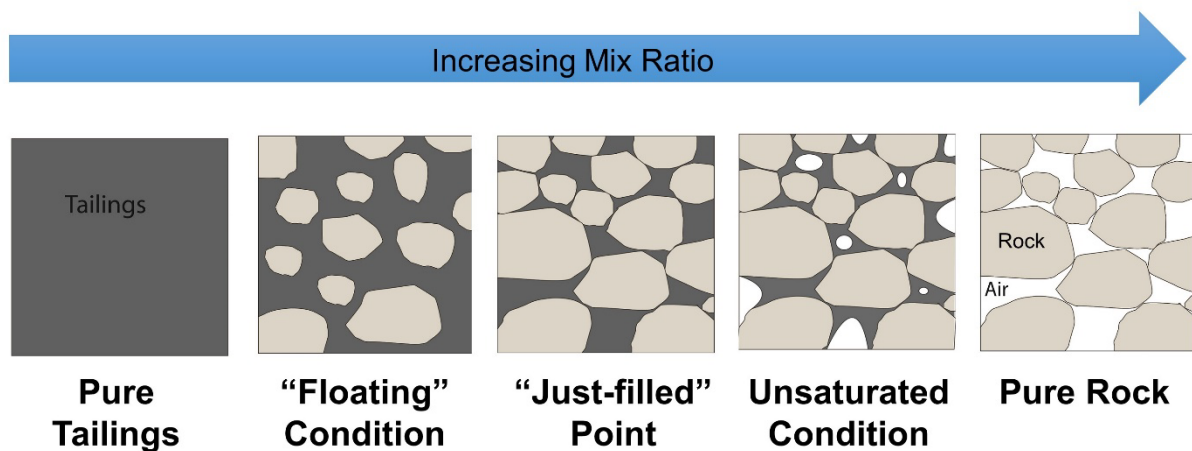


Figure 2-2: Blend configurations (after Wickand et al. 2006)

Figure 2-3 shows the general relationship between the density and mix ratio for “paste rock” blends. The optimum mix ratio is a function of the tailings density, the waste rock skeleton porosity and the waste rock moisture content. Increasing rock porosity and tailings density results in an optimum mix ratio with lower rock content.

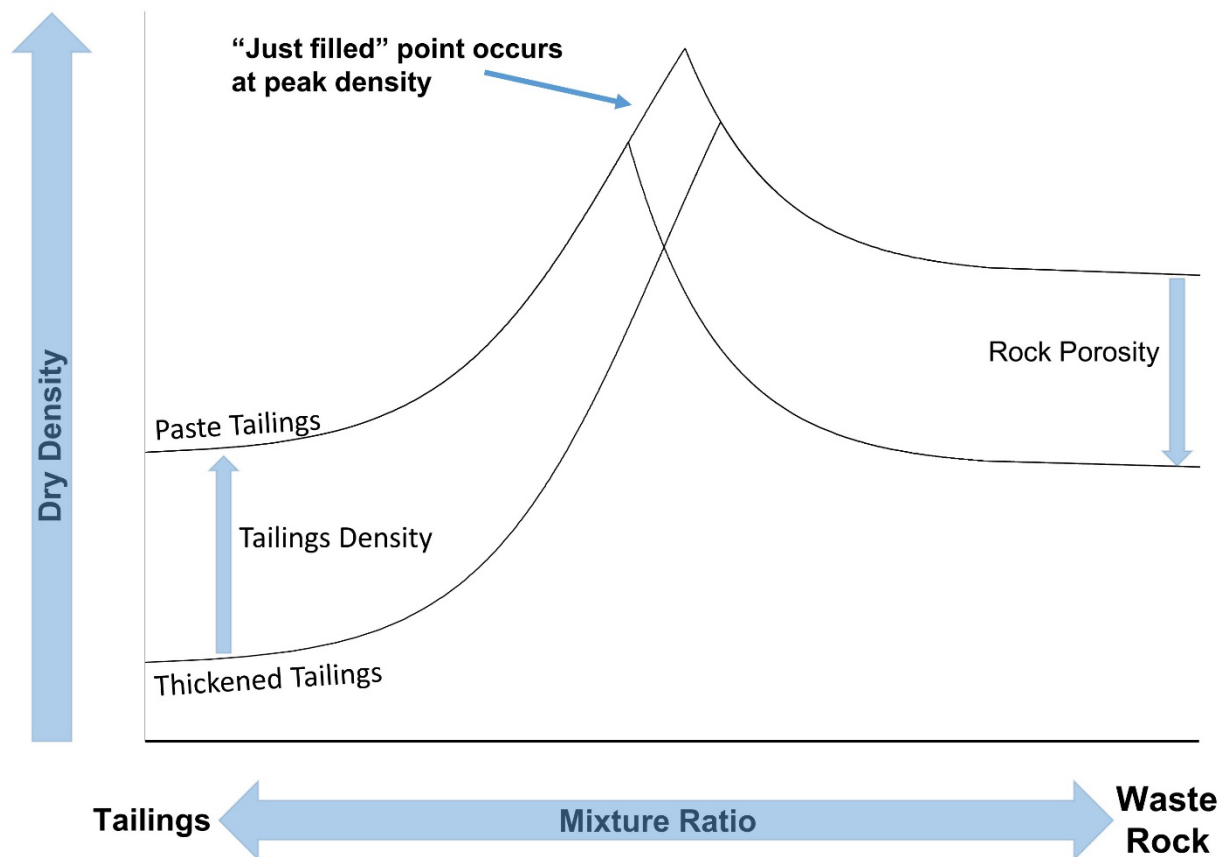


Figure 2-3: “paste rock” mix design theory (after Wickland et al. 2006)

The theoretical work was supported by laboratory mixing trials, compression tests (Wickland, Wilson et al. 2010) and a two year meso-scale column study of self-weight consolidation (Wickland and Wilson 2005). It was found that the blends at the optimum mix ratio had a compressibility similar to the waste rock skeleton and a permeability similar to the tailings alone. “paste rock” research generally focussed on blends of waste rock and paste tailings, although the theoretical principles could equally be applied to waste rock blended with any non-segregating fluid tailings. At the time, the primary application of the research was seen as in encapsulation of potentially acid generating waste rock in saturated tailings to mitigate the risk of acid rock drainage (ARD). This

research approaches the problem with a view to assess how the addition of rock enhances the stability of a “dry-stacked” tailings deposit; nevertheless, many of the underlying principles remain the same.

2.3 Objective

The objective of this paper is to extend the established co-disposal mix design theory to cover the case of filtered tailings and waste rock blends, and to present a theoretical model to predict the structure and behaviour of blends of waste rock and tailings, based upon mix ratio and density. It is based upon the mix design theory developed by Wickland, Wilson et al. (2006) but is extended to consider the case of loosely placed materials and to consider the effect of volume change on structural configuration.

Section 2.4 defines the phase relationships and notation used in this paper. Section 2.5 defines the mix ratio parameters used in this paper. Section 2.6 introduces the concept of using ternary diagrams to represent tailings and waste rock blends. Section 2.7 presents a theoretical model to predict the particle structure and behaviour of blends of waste rock and filtered tailings, based upon mix ratio and density.

2.4 Phase relationships

The phase relationships and notation used in this paper are given in this section. Figure 2-4 shows the mass and volume relations for the constituents of the blend. It may be useful, particularly in the case of filtered tailings, to consider entrained air in the void space of the tailings to be a separate air phase, as shown in Figure 2-4.

Mass M	Rock mass M_r	Rock solids M_{rs}
		Rock water M_{rw}
	Tailings mass M_t	Tailings solids M_{ts}
		Tailings water M_{tw}

Volume V	Rock volume V_r	Rock solids V_{rs}
		Rock water V_{rw}
	Tailings volume V_t	Tailings solids V_{ts}
		Tailings water V_{tw}
		Tailings air voids V_{ta}
	Macro air voids V_{ma}	

Figure 2-4: Phase diagram for waste rock – tailings blends

The blend can be characterised using a global void ratio, defined as follows:

$$e = \frac{\text{Total volume of voids}}{\text{Total volume of solids}} \quad \text{or} \quad e = \frac{V_{rw} + V_{tw} + V_{ta} + V_{ma}}{V_{rs} + V_{ts}} \quad (2-1)$$

The geotechnical moisture content of the blend, denoted w , is defined as follows:

$$w = \frac{\text{Mass of water}}{\text{Mass of solids}} = \frac{M_w}{M_s} \quad (2-2)$$

The “macro scale”, or waste rock skeleton void ratio, is defined as follows:

$$e_r = \frac{V_t + V_{ma}}{V_{rs}} \quad (2-3)$$

The waste rock skeleton void ratio is commonly expressed as porosity, defined as follows:

$$n_r = \frac{V_t + V_{ma}}{V} \quad (2-4)$$

The tailings void ratio is defined as follows:

$$e_t = \frac{V_{tw} + V_{ta}}{V_{ts}} \quad (2-5)$$

2.5 Mix ratio

All mix ratios are given by dry mass, defined as follows, after Wickland, Wilson et al. (2006):

$$R = \frac{\text{Mass of rock solids}}{\text{Mass of tailings solids}} \quad \text{or} \quad R = \frac{M_{rs}}{M_{ts}} \quad (2-6)$$

A convenient mix ratio parameter for producing blends in practice is Bulk Mass Ratio (BMR), defined as follows:

$$BMR = \frac{\text{Bulk mass of rock}}{\text{Bulk mass of tailings}} \quad \text{or} \quad BMR = \frac{M_{rs} + M_{rw}}{M_{ts} + M_{tw}} \quad (2-7)$$

The geotechnical moisture contents of the waste rock and filtered tailings, denoted w_r and w_t , respectively, may be defined as follows:

$$w_r = \frac{\text{Mass of rock pore water}}{\text{Mass of rock solids}} = \frac{M_{rw}}{M_{rs}} \quad (2-8)$$

$$w_t = \frac{\text{Mass of tailings pore water}}{\text{Mass of tailings solids}} = \frac{M_{tw}}{M_{ts}} \quad (2-9)$$

Based on equations 2.6, 2.7, 2.8 and 2.9, the following expressions can be derived which may be found useful. The moisture content of the blend (w) can be calculated as follows:

$$w = \frac{w_t + R w_r}{1 + R} \quad (2-10)$$

The bulk ratio can be calculated as follows:

$$BMR = \frac{R + R w_r}{1 + w_t} \quad (2-11)$$

2.6 Ternary diagram

Ternary diagrams constructed using the approach developed by Charles and Charles (1971) are widely used in the oil sands industry (COSIA 2012) to describe the structure and behaviour of composite tailings, which contain a fines and a sand component. The same approach provides a useful framework to describe the structure and behaviour of waste rock – tailings blends, with respect to mass relations. Any theoretical combination of rock solids, tailings solids and water can be represented by a point inside the triangle. In this section, it is shown that the ternary diagram approach provides a simple and effective tool for quickly estimating the bulk properties of a blend of a given tailings solids content and mix ratio, which may assist in high level tailings planning and conceptual design.

The construction of the ternary diagram is shown in Figure 2-5. The apices of the triangle represent 100% by mass water (top), rock solids (bottom left) and tailings solids (bottom right). Points inside the triangle represent a three phase blend. Points along the axis connecting 100% water and 100% tailings apices represent tailings only. Straight lines drawn from this line to the 100% rock apex (shown in magenta on Figure 2-5) represent blends with constant tailings solids – water ratio (*TSWR*), defined as follows:

$$TSWR = \frac{\text{Mass of tailings solids}}{\text{Mass of tailings solids} + \text{Mass of water}} = \frac{M_{ts}}{M_{ts} + M_{tw} + M_{rw}} \quad (2-12)$$

For blends where the waste rock moisture content is dry or negligible, *TSWR* may be considered equivalent to tailings solids content, defined as follows:

$$\text{Tailings solids content} = \frac{\text{Mass of tailings solids}}{\text{Mass of tailings solids} + \text{Mass of tailings water}} = \frac{M_{ts}}{M_{ts} + M_{tw}} \quad (2-13)$$

Tailings solids content (also referred to as pulp density) is widely used in industry to describe tailings.

Straight lines drawn from the bottom axis to the 100% water apex represent the constant mix ratio. For ternary diagram construction purposes, the mix ratio is expressed as rock content, defined as follows:

$$\text{Rock content} = \frac{\text{Mass of rock solids}}{\text{Mass of tailings solids} + \text{Mass of rock solids}} = \frac{M_{rs}}{M_{ts} + M_{rs}} \quad (2-14)$$

Rock content may be related to the mix ratio (R) (Equation 2.6) using the following expression:

$$\text{Rock content} = \frac{R}{1 + R} \quad (2-15)$$

The constant mix ratio lines (shown in green on Figure 2-5) represent blends with constant particle size distributions but varying solids content. Horizontal lines (shown in blue on Figure 2-5) represent lines of constant overall solids content.

It should be noted that unlike ternary diagrams used in the oil sands industry which consider coarse solids and fine solids as defined by a specific particle size, the diagrams discussed in this paper consider rock solids and tailings solids as defined by origin.

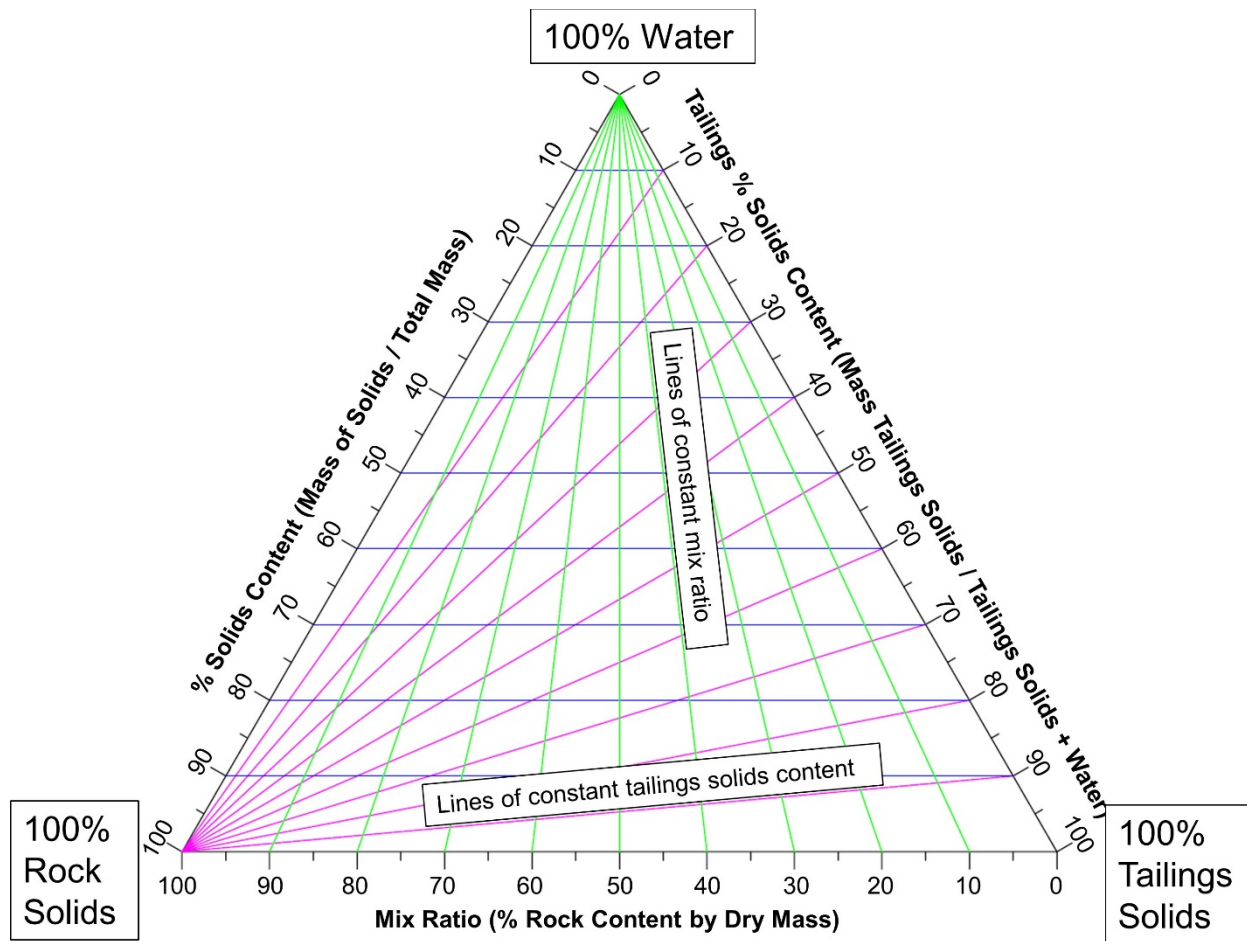


Figure 2-5: Ternary diagram for waste rock – fine tailings blends

2.6.1 Estimation of material property boundaries

Figure 2-6 shows the ternary diagram annotated with general material property and blend configuration boundaries. The figure was generated using a waste rock moisture content of zero and specific gravity of tailings and waste rock solids of 2.7. The solid black lines show the “just-filled” point, or optimum mix ratio described by Wickland, Wilson et al. (2006), for waste rock skeleton porosities of 40% and 50%, calculated based upon the assumption that the tailings are fully saturated at the “just filled” point. These lines define

the division between blends whose behaviour is dominated by fines (blends in the “floating” condition) and blends whose behaviour is rock-dominated (blends with a continuous phase of rock particles in contact). Further discussion around the determination of the “just filled” lines is given in Section 2.6.2. The dashed lines show assumed tailings property boundaries based on solids content. For consistency with the rest of this thesis and with other researchers, the mix ratio is expressed as R (Equation 2.6) instead of rock content as shown in Figure 2-5.

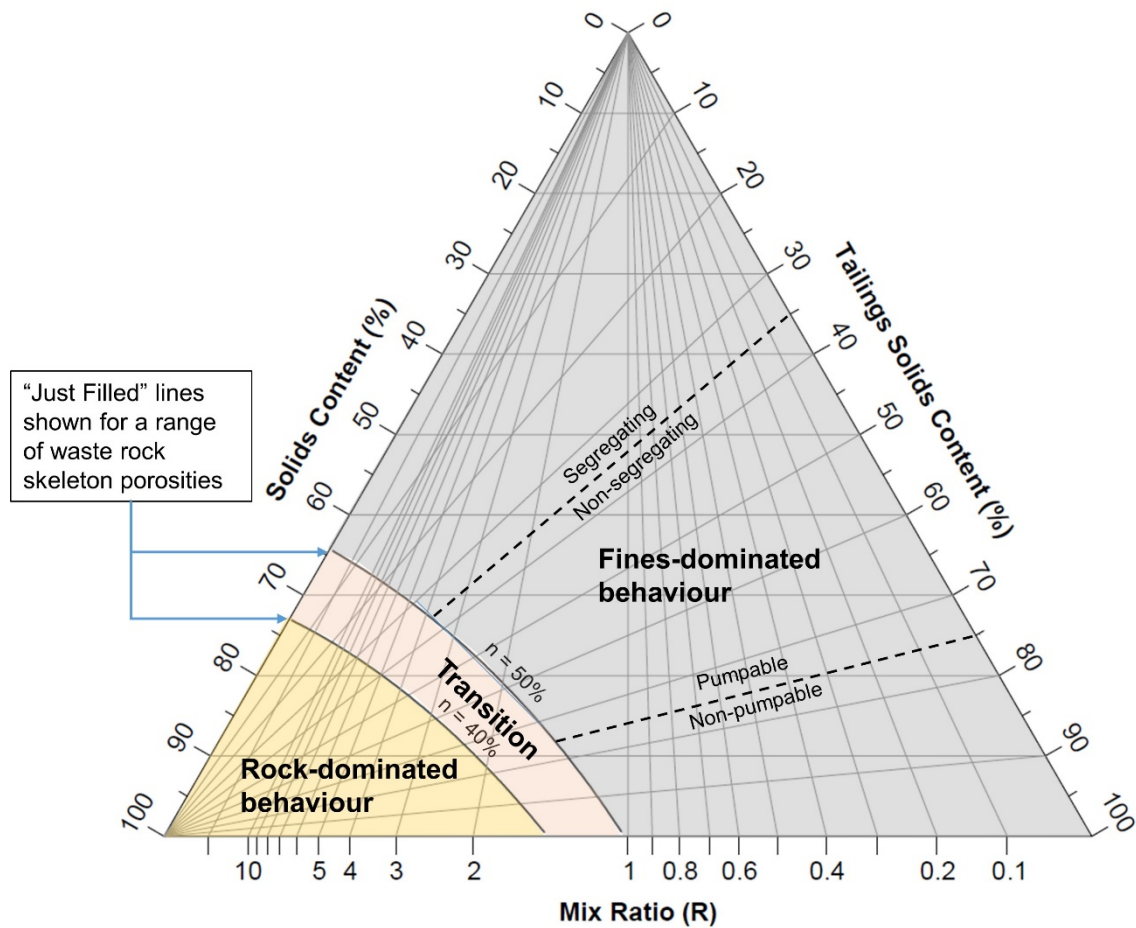


Figure 2-6: Ternary diagram showing blend configuration vs mix ratio for fine tailings – waste rock blends

Figure 2-7 shows the ternary diagram annotated with typical solids contents of different tailings dewatering technologies.

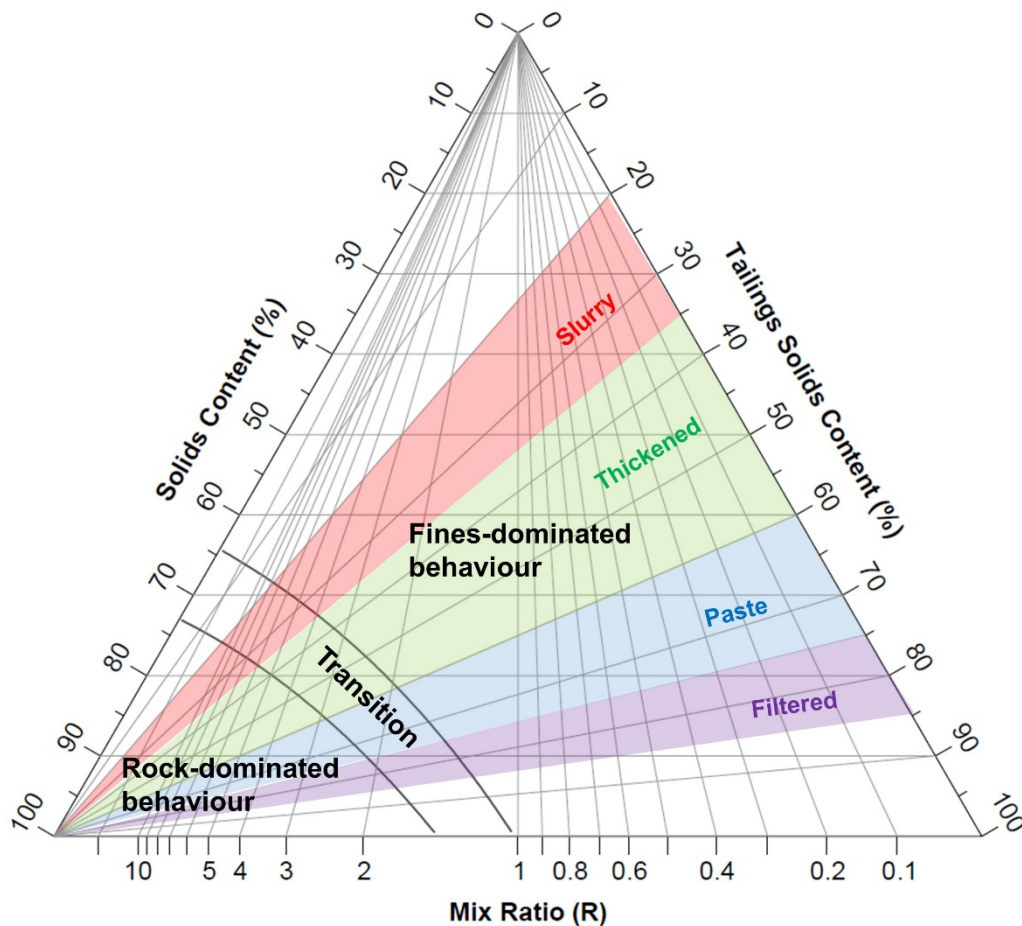


Figure 2-7: Ternary diagram showing blend configuration vs mix ratio for different tailings dewatering technologies

2.6.2 Estimation of the “just filled” line

At the “just filled” line, also termed the “coarse solids matrix boundary” (COSIA 2012), the rock structure is at the maximum void ratio (loosest possible state), whilst still maintaining clast-to-clast contact. Fundamentally, the maximum void ratio of granular materials is governed by the particle size distribution and the particle shape, i.e. roundness or angularity (Youd 1973, Rousé, Fannin et al. 2008). Various methods have been proposed

for the prediction of porosity from the particle size distribution, including empirical correlations (Tsirel 1997) and mathematical models (Peronius and Sweeting 1985, Åberg 1992, Yu and Standish 1993). A good summary is given by Latham, Munjiza et al. (2002). However, there is no method that has currently found widespread favour in geotechnical or mining practice.

The maximum void ratio of granular materials can readily be measured using standardised methods (ASTM 2016), and numerous values have been reported in the literature. An extensive review is given by Bolton (1986) and Rousé, Fannin et al. (2008); the values reported from these papers are plotted in Figure 2-8.

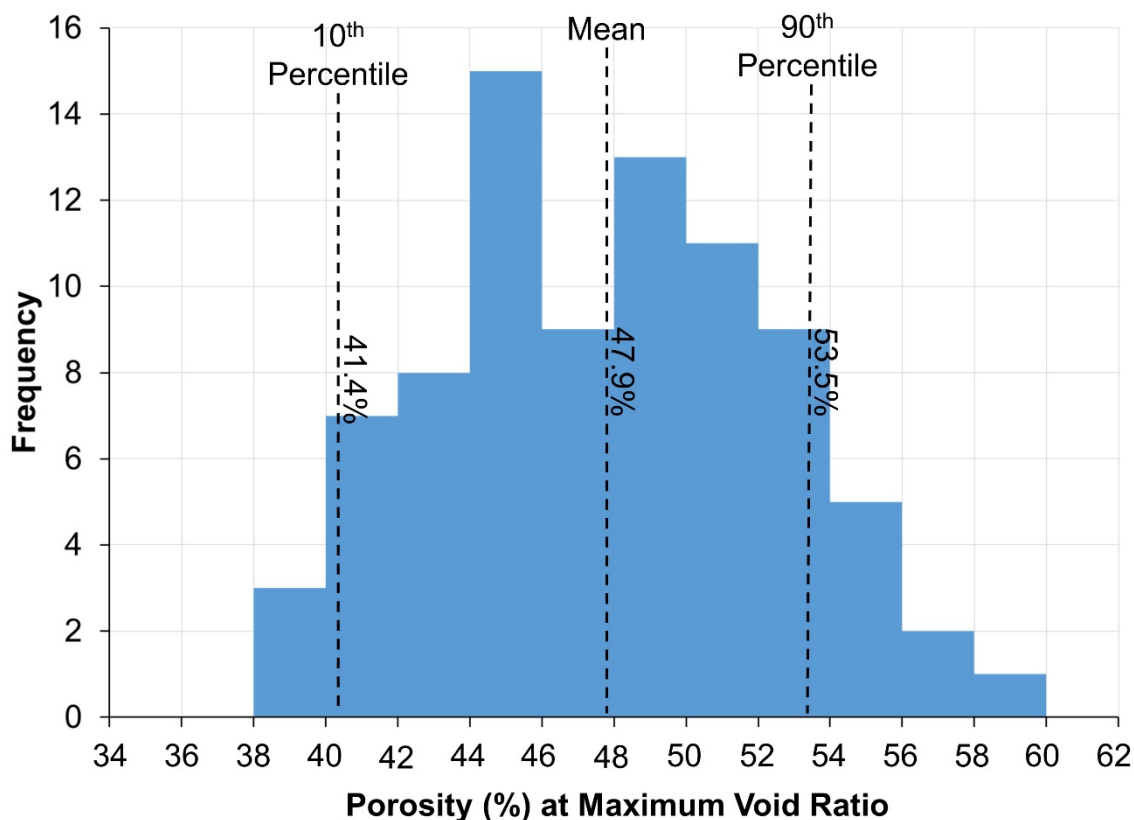


Figure 2-8: Literature review of reported values for maximum void ratio of granular materials

Figure 2-8 shows porosity at maximum void ratio for 83 granular materials reported by Rousé, Fannin et al. (2008) and Bolton (1986). The materials included sands, gravels, crushed rockfills and glass beads. It can be seen that, given the range of materials tested, there is relatively low variance, with the majority falling between 40% and 55%.

2.7 Structure and compression behaviour of stacked filtered tailings and waste rock blends

When in an un-compacted state, filtered tailings and waste rock blends consist of discrete “lumps” of filter cake, rock particles and macro-scale (inter-lump) air voids. The “lumps” typically consist of compact to dense, saturated (or close to saturated) fines. In general terms, the geotechnical behaviour of the blend is controlled by the structural configuration of the blend. The structural configuration is dependent upon the mix ratio and the packing density.

The model proposed here is intended for mixtures where the waste rock has a low fines content and low moisture content, and the tailings are saturated and predominately fine. This is typical for run-of-mine waste rock blended with tailings in a hard rock, metal mining operation. The model presented here is not considered to be applicable for cases where the waste rock has a high fines content, high moisture content, high clay content or may be considered a very weak, soil-like rock that is prone to weathering. Considerations relating to these cases, for example in an oil sands operation, are discussed in Chapter 5.

The structural configurations, and key processes that govern volume change under compression, are shown in Figure 2-9 and defined below.

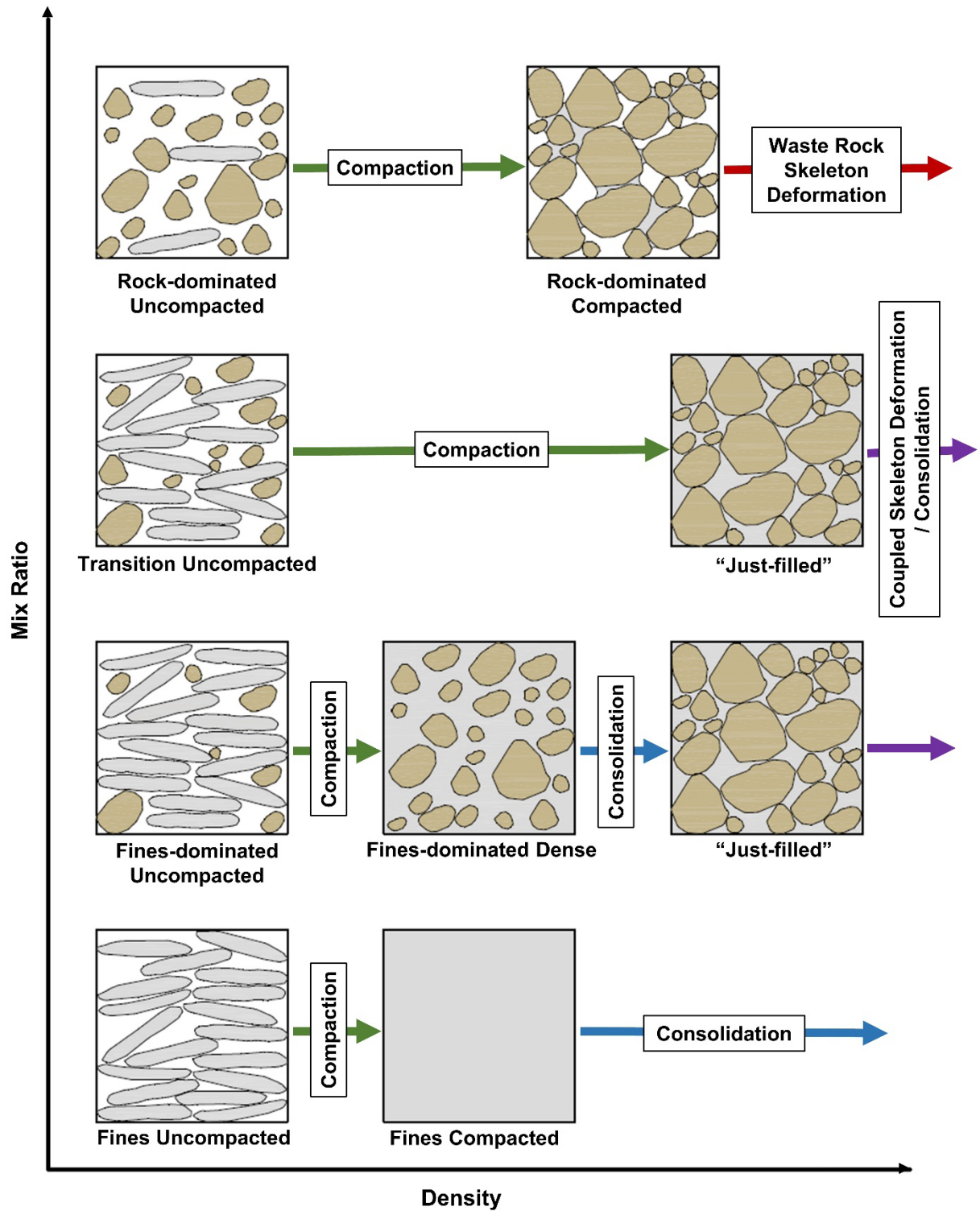


Figure 2-9: Structure and compression behaviour of filtered tailings – waste rock blends

Figure 2-9 presents a theoretical framework for describing the behaviour of the blends, with respect to mass and volume relations. Five key structural configurations are proposed:

- ***Rock-dominated uncompacted;***
- ***Fines-dominated uncompacted;***
- ***Rock-dominated compacted;***
- ***Fines-dominated compacted;*** and
- ***“Just-filled”***.

Just-filled refers to a condition where a continuous, load-bearing waste rock “skeleton” exists, with the void spaces between the rock particles fully occupied with tailings. *Fines-dominated compacted* refers to a condition where a discontinuous waste rock phase is “floating” in a continuous tailings matrix. *Rock-dominated compacted* refers to a condition with a continuous rock “skeleton”, where tailings and air voids take up the void space between rock particles. *Uncompacted* blends (rock or fines dominated) consist of lumps of filter cake, rock particles and air voids.

Four distinct processes that govern volume change under compression are proposed:

- ***Compaction*** (shown as green arrows on Figure 2-9);
- ***Waste rock skeleton deformation***, or deformation of a continuous waste rock phase (shown as red arrows on Figure 2-9);
- ***Tailings consolidation***, or deformation of a continuous tailings phase (shown as blue arrows on Figure 2-9); and

- ***Coupled consolidation and skeleton deformation*** (shown as purple arrows on Figure 2-9).

Compaction refers to the process of removing large, inter-lump air voids by the deformation and breakdown of the filter cake lumps. *Skeleton deformation* refers to the deformation of the load-bearing waste rock skeleton after filter cakes are de-structured. Creep occurs due to the re-arrangement of the waste rock particle structure and particle breakage. *Consolidation* refers to the gradual reduction of the volume of the tailings fraction of the blend, due to drainage of pore water caused by an increase in pore pressure due to applied stress. Once the blend is in the “just-filled” condition, i.e. a continuous waste rock-skeleton with the voids fully occupied by fine tailings, the compression behaviour is governed by both *consolidation* and *skeleton deformation*. It is likely that the presence of tailings occupying the void space will have a significant influence on the deformation behaviour of the waste rock skeleton, due to a reduction in stress at clast to clast contacts and the consequent reduction in particle breakage effects. Material property boundaries can be defined based on the initial tailings solids content and minimum void ratio of the waste rock skeleton, shown below in Figure 2-10.

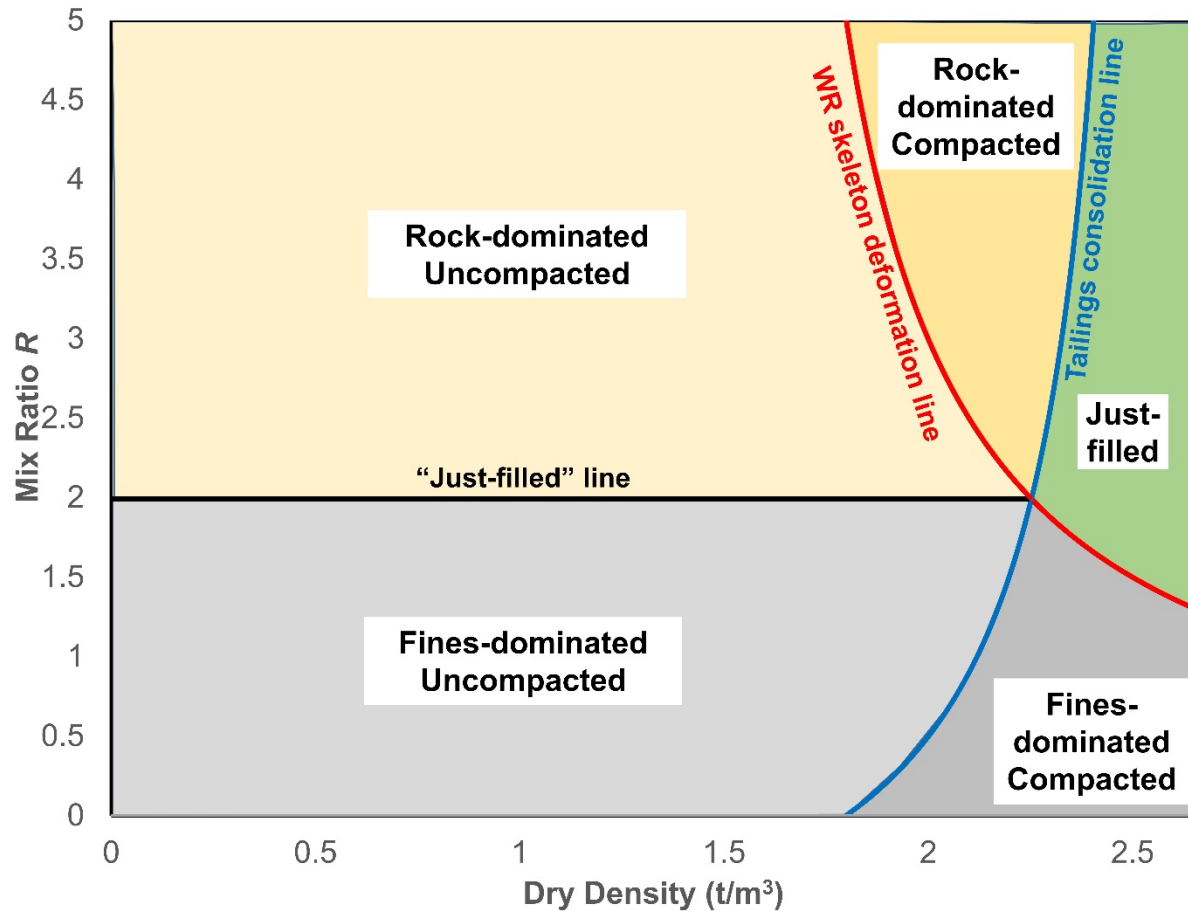


Figure 2-10: Material property boundary chart for filtered tailings – waste rock blend (per input parameters given in Table 2-1)

Figure 2-10 shows the full range of possible conditions for blends of waste rock and tailings with $0 \leq R \leq 5$. The chart defines the structural configuration, and dominant volume change mechanism, of a blend of a given mix ratio and density. A blend of a given mix ratio will trace a path horizontally across the chart from its initial dry density, as it compresses. The blue line (tailings consolidation line) represents the point at which the blend becomes fully saturated, positive pore pressures are generated and the tailings start to consolidate. The position of this line is controlled primarily by the tailings solid content at deposition. The red line (waste rock skeleton deformation line) represents the

point at which a continuous, load-bearing skeleton of waste rock is formed, and deformation is governed by the waste rock skeleton. The position of this line is controlled primarily by the maximum void ratio of the waste rock skeleton. Once the blend has crossed both lines, deformation is governed by a coupled process involving both skeleton deformation and consolidation. A more in-depth description of the construction of the chart is given in Section 2.7.1.

2.7.1 Construction of the material property boundary chart

The material boundary chart is constructed based on the following assumptions:

- Tailings are fully saturated;
- Blends are said to be in a “uncompacted state”, unless one of these conditions is met:
 - a) Waste rock skeleton void ratio exceeds the maximum (i.e. a continuous waste rock skeleton is formed), or
 - b) The blend is fully saturated.

Blends in an uncompacted state are considered rock-dominated if condition (a) is met first and fines-dominated if condition (b) is met first;

- For blends in a uncompacted state, *compaction* is the dominant volume change process. Compression is due to the removal of air voids. Tailings will remain at constant void ratio (i.e. consolidation does not occur until all air voids are removed); and
- The model does not consider the mixing of waste rock water or fines with tailings. It is recommended for use with typical run-of-mine waste rock which is fairly dry

($w_r < 5\%$). It is not recommended for waste rocks containing high moisture contents or high fines contents.

The “just-filled” mix ratio (R_{opt}) may be defined as the mix ratio at which all voids in the waste rock skeleton, at its maximum porosity, are filled with saturated tailings at their discharge moisture content. The “just-filled” mix ratio is synonymous with the optimum mix ratio described by Wickland, Wilson et al. (2006) for “paste rock” blends. The “just-filled” mix ratio is a function of minimum waste rock porosity (n_{rmax}), moisture content of the rock (w_r) and tailings (w_t) and specific gravity of solids for the rock (G_{sr}) and tailings (G_{st}). The *just-filled line* forms the theoretical boundary between rock- and fines-dominated uncompacted blends. The critical mix ratio may be calculated as follows:

$$R_{opt} = \frac{(1 - n_{rmax})G_{sr}}{(n_{rmax} - w_r(1 - n_{rmax})G_{sr})\left(1 - \frac{w_t G_{st}}{1 + w_t G_{st}}\right)G_{st}} \quad (2-16)$$

The *tailings consolidation line* may be defined by the expression:

$$\rho_d = \frac{1 + \frac{1}{R}}{w_r + \frac{w_t}{R} + \frac{1}{G_{sr}} + \frac{1}{R G_{st}}} \quad (2-17)$$

The *waste rock skeleton deformation line* may be defined by the expression:

$$\rho_d = (1 - n_{rmax})G_{sr} \left(1 + \frac{1}{R}\right) \quad (2-18)$$

Input parameters used to generate Figure 2-10 are given in Table 2-1.

Table 2-1: Input parameters for Figure 2-10

Parameter	Value
Specific gravity of rock solids (G_{sr})	2.73
Specific gravity of tailings solids (G_{st})	2.76
Maximum waste rock skeleton porosity (n_{rmax})	45%
Waste rock moisture content (w_r)	2.1%
Tailings moisture content (w_t)	19.3%

2.8 Summary and conclusions

The co-disposal of waste rock and filtered tailings is an emerging technology which has advantages over traditional methods of mine waste disposal. Filtered tailings “dry stacking” is becoming an increasingly widely used alternative to traditional slurry tailings. The addition of waste rock to a filtered tailings stack has the potential to improve the stability of the deposit, possibly allowing for rapid stacking without compaction and allowing for the dry stacking to be economical at the biggest mines.

Work by previous researchers, focusing primarily on blends of waste rock and paste tailings, has shown that the geotechnical behaviour of a blend is governed by particle packing configuration and that the configuration can be predicted from the mix ratio. However, the established theory is not applicable in the case of filtered tailings and waste rock blends which are placed loose and compacted under self weight. This paper presents an extended theoretical model to predict the structure and behaviour of blends of waste rock and tailings, based upon mix ratio and density. It is based upon the co-

disposal mix design theory developed by Wickland, Wilson et al. (2006) but is extended to consider the case of loosely placed materials and to consider the effect of volume change on structural configuration.

A methodology for the application of ternary diagrams to characterise blends of waste rock and tailings blends is presented. These diagrams provide a useful method for quickly evaluating the properties of a blend of a given mix ratio and tailings solids content, and may assist in high-level tailings planning and design.

A conceptual model has been developed to describe the behaviour of filtered tailings and waste rock blends, based upon the particle packing arrangement of the tailings. It is postulated that the geotechnical behaviour of blends, and primary mechanism of volume change, is governed by particle configuration. The model may be used to predict the structure and behaviour of the blend, based on the mix ratio and density. The verification of this model through experimental studies is required.

References

- Åberg, B. (1992). "Void ratio of noncohesive soils and similar materials." Journal of geotechnical engineering **118**(9): 1315-1334.
- AMEC. (2008). "Rosemont Copper Company Filtered Tailings Dry Stacks Current State of Practice Final Report." from <https://www.rosemonteis.us/files/technical-reports/012312.pdf>.
- Amoah, N. (2019). Large-Scale Tailings Filtration and Dry Stacking at Karara Magnetite Iron Ore Operation. Tailings and Mine Waste 2019, Vancouver, Canada.
- ASTM (2016). ASTM D4254-16 Standard Test Methods for Minimum Index Density and Unit Weight of Soils and Calculation of Relative Density.
- Bolton, M. D. (1986). "The strength and dilatancy of sands." Géotechnique **36**(1): 65-78.
- Brawner, C. and J. Argall, GA (1978). Concepts and experience for subsurface storage of tailings. Proceedings of the 2nd International Tailings Symposium, Tailings Disposal Today, Denver, Colo.
- Bussiere, B. (2007). "Colloquium 2004: Hydrogeotechnical properties of hard rock tailings from metal mines and emerging geoenvironmental disposal approaches." Canadian Geotechnical Journal **44**(9): 1019-1052.
- Butikofer, D., B. Erickson, A. Marsh, R. Friedel, L. Murray and M. J. Piggot (2017). Filtered Tailings Disposal Case History: Operation and Design Considerations Part II. Tailings and Mine Waste 2017. Banff, AB.
- Charles, M. and R. Charles (1971). The use of heavy media in the pipeline transport of particulate solids. Advances in Solid-Liquid Flow in Pipes and its Application, Elsevier: 187-197.
- COSIA (2012). Technical Guide for Fluid Fine Tailings Management.
- Crystal, C. and C. Hore (2018). Filter-Pressed Dry Stacking: Design Considerstions Based on Practial Experience. Tailings and Mine Waste 2018. Keystone, CO.
- Davies, M. P. and S. Rice (2001). "An alternative to conventional tailings management—"dry stack" filtered tailings." Proceeding of Tailings and Mine Waste'01: 411-420.
- Green, P. (1981). "De-watering coal refuse." Coal Age **86**: 145-157.
- Jewell, R. J. and A. B. Fourie (2006). Paste and thickened tailings: A guide, Australian Centre for Geomechanics, The University of Western Australia.

Lara, J., E. Pornillos and H. Muñoz (2013). Geotechnical-geochemical and operational considerations for the application of dry stacking tailings deposits–state-of-the-art. Proceedings of the 16th International Seminar on Paste and Thickened Tailings, Belo Horizonte, Brazil, June 17–20.

Latham, J.-P., A. Munjiza and Y. Lu (2002). "On the prediction of void porosity and packing of rock particulates." Powder Technology **125**(1): 10-27.

Morgenstern, N., S. Vick and D. Van Zyl (2015). "Report on Mount Polley tailings storage facility breach." Report of independent expert engineering investigation and review panel. Prepared on behalf of the Government of British Columbia and the Williams Lake and Soda Creek Indian Bands.

Morgenstern, N., S. Vick and B. Watts (2016). Fundão Tailings Dam Review Panel Report on the Immediate Causes of the Failure of the Fundão Dam.

Newman, L., K. Arnold and D. Wittwer (2010). Dry stack tailings design for the Rosemont Copper project. International Conference on Tailings & Mine Waste. Tailings and Mine Waste.

Peronius, N. and T. Sweeting (1985). "On the correlation of minimum porosity with particle size distribution." Powder technology **42**(2): 113-121.

Robertson, P., L. de Melo, D. Williams and G. Wilson (2019). Report of The Expert Panel on the Technical Causes of the Failure of Feijão Dam 1.

Robertson, P. K., A. V. da Fonseca, B. Ulrich and J. Coffin (2017). "Characterization of unsaturated mine waste: a case history." Canadian Geotechnical Journal **54**(12): 1752-1761.

Rousé, P. C., R. J. Fannin and D. A. Shuttle (2008). "Influence of roundness on the void ratio and strength of uniform sand." Géotechnique **58**(3): 227-231.

Tsirel, S. (1997). "Methods of granular and fragmented material packing density calculation." International Journal of Rock Mechanics and Mining Sciences **34**(2): 263-273.

Vick, S. G. (1990). Planning, design, and analysis of tailings dams, BiTech.

Wang, C., D. Harbottle, Q. Liu and Z. Xu (2014). "Current state of fine mineral tailings treatment: A critical review on theory and practice." Minerals Engineering **58**: 113-131.

Wickland, B. and S. Longo (2017). Mine waste case examples of stacked tailings and co-disposal. Tailings and Mine Waste '17. Banff, Alberta, Canada.

Wickland, B. E. and G. W. Wilson (2005). "Self-weight consolidation of mixtures of mine waste rock and tailings." Canadian Geotechnical Journal **42**(2): 327-339.

Wickland, B. E., G. W. Wilson and D. Wijewickreme (2010). "Hydraulic conductivity and consolidation response of mixtures of mine waste rock and tailings." Canadian Geotechnical Journal **47**(4): 472-485.

Wickland, B. E., G. W. Wilson, D. Wijewickreme and B. Klein (2006). "Design and evaluation of mixtures of mine waste rock and tailings." Canadian Geotechnical Journal **43**(9): 928-945.

Williams, D. (1997). Effectiveness of co-disposing coal washery wastes. Proceedings of the 4th International Conference on Tailings and Mine Waste.

Williams, M., K. Seddon, T. Fitton, A. Fourie, R. Jewell, P. Slatter and A. Paterson (2008). Surface disposal of Paste and Thickened Tailings—A brief history and current confronting issues. 11th Int. Seminar on Paste and Thickened Tailings.

Youd, T. (1973). Factors controlling maximum and minimum densities of sands. Evaluation of relative density and its role in geotechnical projects involving cohesionless soils. American Society for Testing and Materials STP 523. Philadelphia, PA: 98-112.

Yu, A. and N. Standish (1993). "A study of the packing of particles with a mixture size distribution." Powder Technology **76**(2): 113-124.

3 A NOVEL METHOD OF SIMULATING “DRY STACKED” TAILINGS DEPOSITION USING CRL TESTS

3.1 Introduction

Almost all mines produce fluid tailings as a by-product from the mineral extraction process. Conventionally, these tailings are stored behind dams usually constructed from the tailings themselves (Vick 1990). These structures can present a challenge for reclamation and closure, and are a long-term risk and liability. As large, high-profile failures continue to occur, tailings dams are increasingly being seen as unacceptable by many stakeholders (Morgenstern, Vick et al. 2015, Morgenstern, Vick et al. 2016). To address this problem, an increasing trend in the industry is the deposition of tailings in self-supporting “dry stacks”, typically using pressure filtration to rapidly dewater the tailings before stacking (Davies and Rice 2001). The geotechnical performance of filtered tailings may also be improved by addition of rock to the deposit (Bareither, Gorakhki et al. 2018). Addition of rock to a filtered tailings deposit has the potential to allow for rapid stacking of un-compacted dry stacks, which may make dry stacking economical at large scale. Since these deposits are not impounded by dams, the pore pressure at the base of the stack is critical to stability. There is a need to predict the build-up and dissipation of excess pore pressures so that stable stacks can be designed.

Problems of this nature in conventional tailings deposits would typically be handled using the classic one-dimensional consolidation theories developed by Terzaghi (1936) or Gibson (1958). Gibson’s solution has been shown to give reasonable results in calculating

excess pressures generated during slurried tailings deposition (Mittal and Morgenstern 1976) or during the placement of underground backfills (Fahey, Helinski et al. 2010). However, both of these approaches require the measurement or an assumption of the co-efficient consolidation (c_v), which is most commonly determined using a classic incremental loading consolidation test and a curve-fitting procedure (Olson 1986, ASTM 2011). Alternatively, various types of stress- or strain-controlled continuous loading tests may be used to estimate the consolidation parameters (von Fay and Cotton 1986, Znidarčić, Schiffman et al. 1986, Davison and Atkinson 1990).

There are a number of drawbacks to this approach. Both of the classic theories assume a constant value of c_v , which is clearly not the case in reality. Whilst Terzaghi's theory has proven itself surprisingly robust in the case of natural clays (Schiffman and Gibson 1964), the case of mine tailings is more complex. There is no consensus in the literature regarding void ratio – c_v relationships for different types of mine tailings (Mittal and Morgenstern 1976, Blight and Steffen 1979, Vick 1990). Furthermore, incremental load tests are time-consuming; tests can typically last several days. In the case of filtered tailings, the collection of undisturbed samples for conventional oedometer testing is not feasible and samples must be reconstituted and saturated in a laboratory, which may not best represent field conditions.

Loosely placed stacks of filtered tailings and waste rock have a complex structure, which consists of dense lumps of filtered tailings, large air voids and rock particles. Compression behaviour of these blends is governed by a combination of compaction and unsaturated consolidation processes. The structure and compression behaviour of filtered tailings and

waste rock blends is described in Chapter 2. There is currently no theoretical model that can adequately predict the behaviour of these materials. This chapter presents an experimental approach that can be used to simulate the behaviour of a loosely placed dry stack, and predict the development of pore pressure build up, using an experimental approach that simulates field conditions

It has been shown that controlled rate of loading (CRL) tests can be used to simulate tailings deposition (Shokouhi and Williams 2015, Shokouhi and Williams 2017, He et al. 2017). Bareither, Gorakhki et al. (2018) investigated the compression behaviour of unsaturated filtered tailings and waste rock blends, termed “Geowaste”, at mix ratios of 0.4 : 1 and 1 : 1 rock : tailings using a constant strain rate test up to 1630 kPa (representing a stack depth of approximately 75 m). The objective was to assess the build-up of pore pressure and to estimate profiles of pore pressure, stress and unit weight within a full scale “Geowaste” deposit. The general findings were that adding rock reduces or eliminates pore pressure development; no positive pore pressure was reported for the 1:1 blend at a strain rate of 3 mm/hr. However, it is not clear how this strain rate relates to the rate of stacking in the field. Both previous studies have used a constant load rate to simulate a constant rate of deposition. This is questionable, since in reality the drainage path length in the field increases as tailings are deposited, causing the rate of dissipation of excess pore pressure to reduce with respect to time. The method presented here attempts to take account of this by the application of an incrementally increasing load rate in the laboratory.

The objective of the testing was to investigate the compression behaviour of rapidly placed “dry stacks” of blended filtered tailings and waste rock. In particular, there was a focus on the pore pressure response and density under self-weight consolidation for a given mix ratio, stack height and rate of rise.

3.2 Method

A new test method that enables the placement of tailings stacks to be simulated quickly and easily, using CRL tests, is presented in this section.

The test methodology was developed to replicate field conditions as closely as possible, by coupling compaction and consolidation in the same test using a cell capable of large strains. The samples are placed in the cell at their natural blended moisture contents in a loose and unsaturated state. Vertical stress is applied at the top of the sample, and the drainage of air and water is allowed from the top of the sample only. The sample initially undergoes compaction. Upon development of positive pore pressure, the sample undergoes a coupled compaction-consolidation process. Upon saturation, the sample undergoes a purely consolidation process.

3.2.1 *Equipment*

The cell used in this study was a slurry consolidometer, custom built to the specifications of the University of Queensland by Wille Geotechnik of Germany. The cell has an internal diameter of 150 mm and is capable of accommodating samples up to 300 mm high. An axial load is applied via a 10 kN high precision electromechanical load frame. It is equipped with two load cells, one located on the loading piston that measures the applied load and one located at the base of the sample. The vertical displacement of the loading

ram is measured via an LVDT; this is used to measure the settlement of the sample. The device is fully computer controlled, and any sequence of load steps and load rates may be applied. The device is shown in Figure 3-2 and shown schematically in Figure 3-1. Figure 3-3 shows the placement of a sample in the cell.

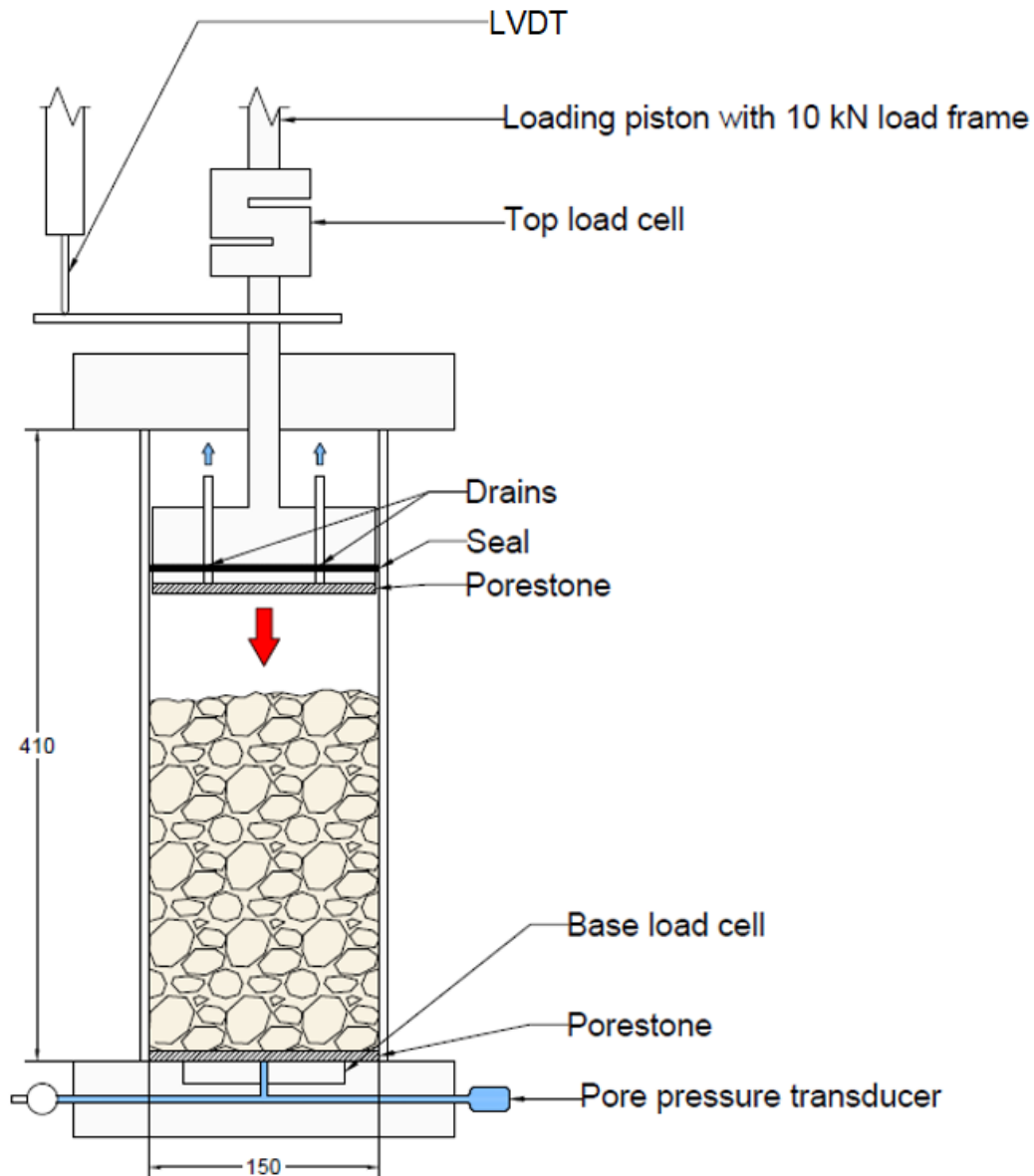


Figure 3-1: Slurry consolidometer schematic (dimensions in mm)

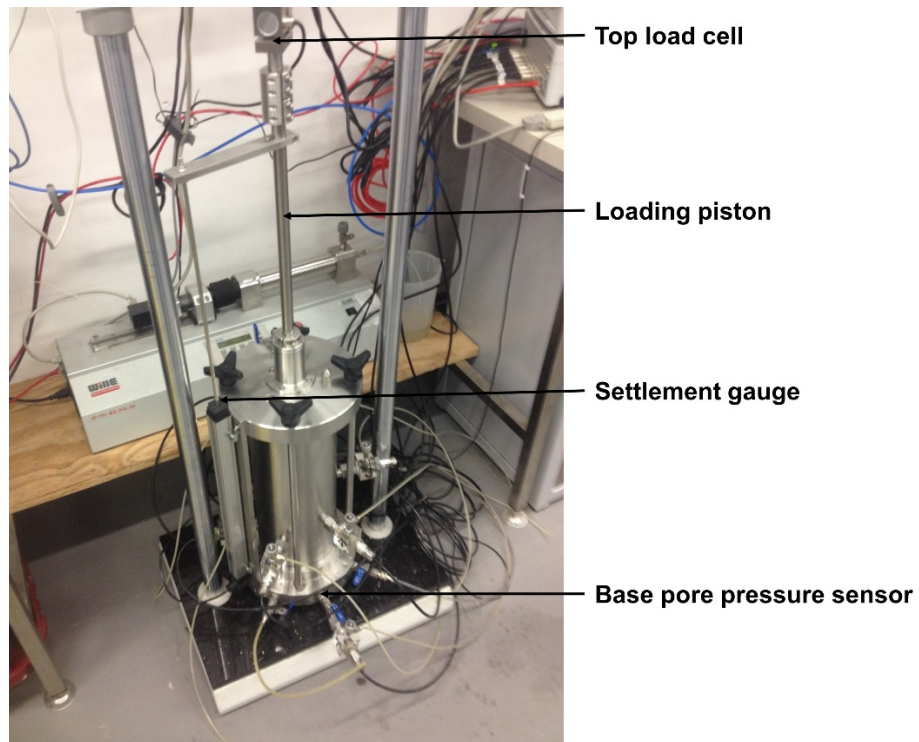


Figure 3-2: Slurry consolidometer



Figure 3-3: Placement of filtered tailings sample in slurry consolidometer

3.2.2 *Theoretical approach*

The theory upon which the testing method is based is presented in this section. Two cases are considered. The first case considers when tailings are placed rapidly in a single lift, where it is shown that consolidation time can be scaled by varying the length of the drainage path. A similar approach is widely used in the geotechnical centrifuge modelling of consolidation and seepage processes (Taylor 1995, Butterfield 2000). This principle is then applied to the second case, which applies this principle to the more complex problem of the slow deposition of tailings at a constant rate. It is shown how loading rates which may be applied in the laboratory to simulate field deposition at a constant rate can be calculated.

Case 1 – Rapid Deposition

In many cases, dry-stacked tailings are placed rapidly in a single lift, whereupon the stacker is then moved. In these cases, the time required to place the stack is short compared to the time which the stack will rest before subsequent loading, and the problem may be simplified by assuming that the load rate is effectively instantaneous.

Unlike traditional tailings deposition, “dry stacked” tailings are placed at high solids contents, so it is reasonable to assume that strains due to consolidation settlement are small. In practice, it is difficult to incorporate drains at the base of the stack into the design. Therefore, it is conservative to assume single drainage from the top of the stack for design purposes, although base drainage will inevitably occur to some extent in reality.

This analysis considers the development and dissipation of excess pore pressure at the base of the stack. It is based on an assumption of saturated conditions, and considers

positive pore pressure only. Although the materials are initially placed in the unsaturated condition, it is assumed that they will behave as a saturated material after compaction and upon the onset of positive pore pressure development.

The solution to Terzaghi's differential equation of consolidation for excess pore pressure at the base of a half-closed layer (u_b), assuming that initial excess pressure (u_i) is constant throughout the layer, is (Terzaghi 1943):

$$\frac{u_b}{u_i} = \sum_{m=0}^{m=\infty} \frac{2}{M} (\sin M) \exp(-M^2 T_v) \quad (3-1)$$

Where:

$$M = \frac{\pi}{2} (2m + 1)$$

$$T_v = \frac{c_v t}{d^2}$$

Where t is the time since the load was applied and d is the length of the longest drainage path. It is noted that implicit in Equation 3-1 are the assumption that strains are small and that the hydraulic conductivity (k) is constant throughout the process.

Given that the degree of dissipation of excess pore pressure (u_b/u_i) in a homogenous material is a function of t / d^2 , it is possible to "scale time" by varying the drainage path length in the laboratory. The dimensionless "time scaling factor" may be defined as follows:

$$\text{Time scaling factor } (T_s) = \frac{T}{t} = \frac{h^2}{d^2} \quad (3-2)$$

Where t = simulated field time, T = actual laboratory time, d = equivalent field drainage path length and h = laboratory drainage path length.

A full derivation of Equation 3.2 is given in Appendix A.

If single drainage is assumed, d may be considered equivalent to the height of the stack in the field, and h may be considered equivalent to the height of the sample in the laboratory. The equivalent field drainage path length may be calculated as follows:

$$d = \frac{\sigma}{\gamma} \quad (3-3)$$

Where σ is the vertical stress applied to the sample, and γ is the unit weight of the material. A worked example of this case is given in Appendix A.

Case 2 – Slow rate of deposition

It may be useful to consider the case of a stack rising gradually at a given rate of rise. Tailings deposition may be simulated in the laboratory by the application of a gradually increasing load, where the sample represents an element at the base of the stack. However, when considering the dissipation of excess pore pressure, the constant rate of rise cannot be simulated by the application of a constant rate of loading. In the field, the drainage path length increases as the stack rises, so consequently the rate of dissipation of excess pore pressure slows down as the load increases. Therefore, to simulate this problem in the laboratory, the load must be applied at a gradually increasing rate.

The problem may be approximated by dividing the test into a series of load steps and applying a constant rate of loading for each step. The load rate for each step may be calculated using a similar approach to that given in Case 1. For the case of a constant rate of rise and assuming single drainage, stack height (d) may be expressed as follows:

$$d = mt \quad (3-4)$$

Where t = simulated “field” time and m is the rate of rise to be simulated.

The “field” time of a given load step may therefore be given as follows:

$$t = \frac{\Delta d}{m} \quad (3-5)$$

Where Δd is the change in stack height throughout the step. The “laboratory time” (T) of the step can then readily be calculated using Equation 3-2. The loading rate ($\Delta\sigma / \Delta T$) for the step can then easily be calculated. A worked example is given in Appendix A.

3.2.3 *Materials*

The materials used in this study are filtered gold tailings and waste rock collected between February and May 2016 from Penasquito Mine, an 110,000 t/day open pit gold and silver mine in Zacatecas, Mexico, operated by Newmont Goldcorp. Waste rock was collected from inside a waste rock dump at the mine. The mine currently deposits tailings as slurry in an impoundment behind a dam constructed from cycloned sand and rockfill (Malgesini, Aubone et al. 2017) but is evaluating a change in tailings technology to co-disposed waste rock and filtered tailings. Filtered tailings were generated using a pilot scale filter plant located at the mine. Further details of material sampling are given in Section 3.4.

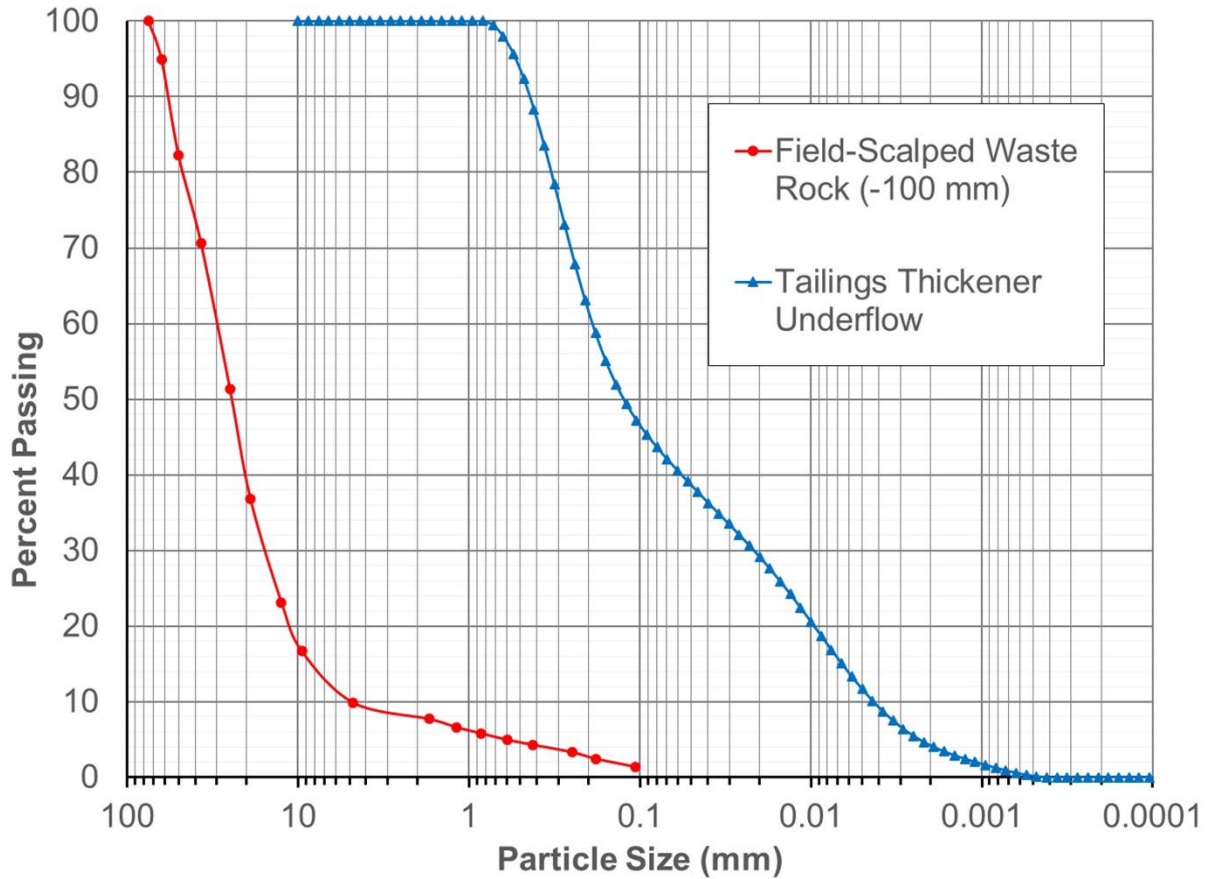
3.2.3.1 *Basic characterisation*

The geotechnical index properties of the filtered tailings and waste rock are given in Table 3-1.

Table 3-1: Index properties

Property	Filtered tailings	Waste rock
Specific gravity of solids G_s	2.76	2.73
Gravimetric moisture content w (%)	19.3	2.1
Liquid limit (%)	20	Non-plastic
Plastic limit (%)	17	Non-plastic
Plasticity index (%)	3	Non-plastic

The particle size distribution of the field-scalped waste rock was carried out using the dry sieving method. The particle size distribution of the thickener underflow was carried out using laser diffraction at the Penasquito Mine. It is assumed that the thickener underflow will not have a significantly different particle size distribution to the filtered tailings. The particle size distributions are shown in Figure 4-8.



the tests presented in this paper is limited to 19 mm, which gives a ratio of approximately 1 : 8.

The objective of the blending procedure was to combine the waste rock and filtered tailings into a perfectly mixed, homogenous material. Whilst it is recognised that this is unlikely to be representative of field conditions, perfect blending was targeted to produce good quality, repeatable results at the laboratory scale. Materials were blended using a Hobart food mixer, shown in Figure 3-5 and Figure 3-6.



Figure 3-5: Blending apparatus



Figure 3-6: Preparation of blend

Calculated particle size distributions of blended materials are given in Figure 3-7.

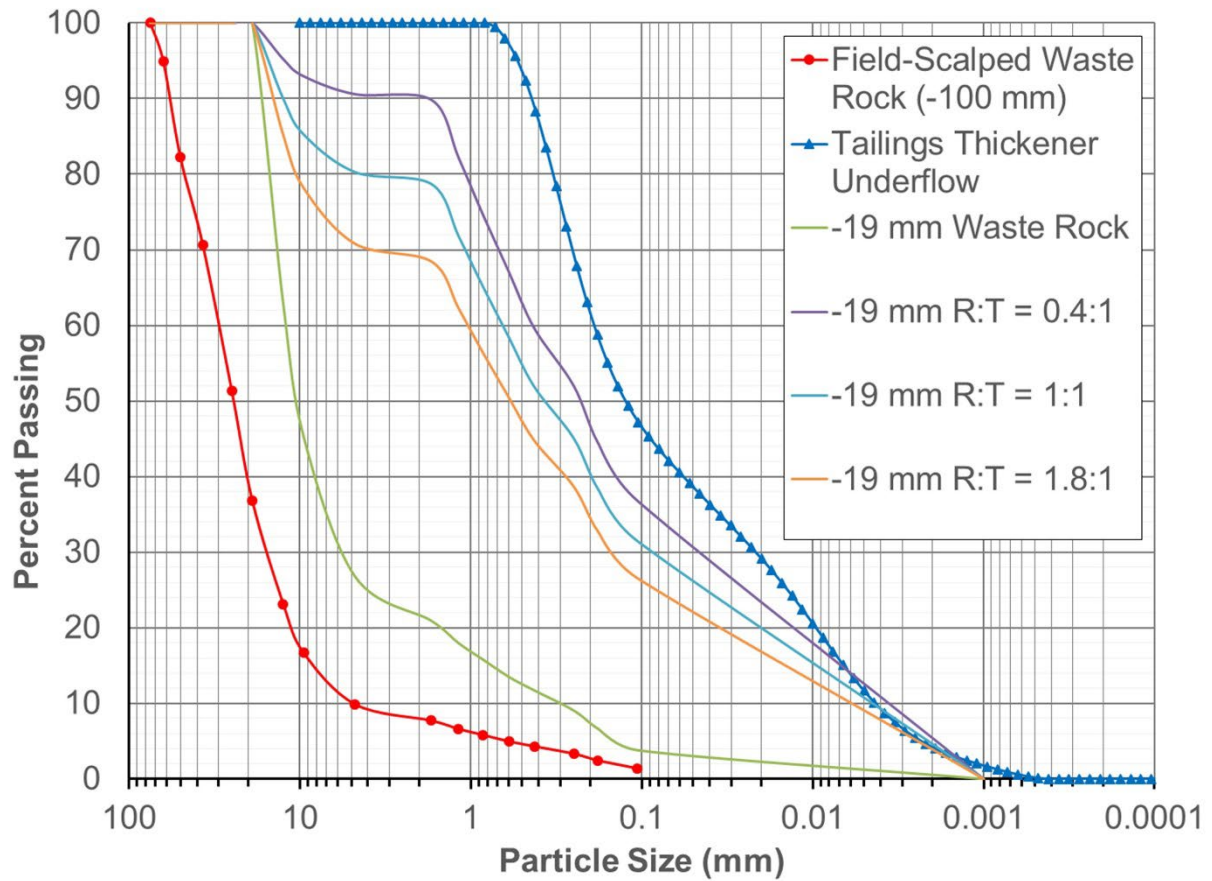


Figure 3-7: Particle size distributions for blended materials

3.2.4 Summary of tests performed

Tests were performed in two series, based upon the two theoretical approaches described in the preceding section:

- Series 1 – Rapid deposition
- Series 2 – Slow rate of deposition

Each series is described below:

Series 1 – Rapid deposition

Due to constraints regarding access to equipment, it was only possible to carry out rapid deposition tests on filtered tailings alone.

The primary objective of these tests was to show the validity of the theoretical approach. This is demonstrated by varying the sample height and, consequently, varying the time scaling factor. It was hypothesised that excess pore pressure will be observed to dissipate faster in the thinner sample due to the decreased drainage path length, but when the dissipation curves are plotted using simulated “field time” calculated using the respective time scaling factors, they will appear the same. The tests are summarised in Table 3-2.

Table 3-2: Summary of tests performed in series 1 (rapid deposition)

Test	Material	Initial sample height (mm)	Vertical stress (kPa)	Load rate (kPa / minute)	Time scaling factor T_s
1-1	Filtered tailings	100	350	1000	1.03×10^{-5}
1-2	Filtered tailings	30	262	10,000	9.29×10^{-7}

The sample height between tests was varied by a factor of 3; this gives an approximate change of 1 order of magnitude in the time scaling factor. Lower vertical stresses were used for the thinner sample; this was to ensure that the distribution of vertical stress throughout the sample was approximately equal in each case, given that longer samples have higher wall friction losses.

This test series is also useful for predicting the pore pressure response and density of a filtered tailings deposit placed rapidly in a single lift.

Series 2 – Slow rate of deposition

Slow rate of deposition tests were carried out on filtered tailings alone and on filtered tailings and waste rock blends at a range of mix ratios.

The objectives were to simulate the deposition of the blends at a slow constant rate and to investigate the effect that the addition of rock has on the pore pressure response and density of a filtered tailings stack.

Three tests were performed: one on pure filtered tailings and two further tests on waste rock – filtered tailings blends at mix ratios of 1:1 and 1.8:1 rock to tailings by dry mass. The sample preparation and blending procedure is described in Section 3.4. The tests performed are summarised in Table 3-3.

Table 3-3: Summary of tests performed in series 2 (slow deposition)

Test	Dry mix ratio (rock : FT) (before scalping)	Dry mix ratio (rock : FT) (after scalping)	Initial sample height (mm)	Peak vertical stress (kPa)
2-1	Filtered tailings	Filtered tailings	239	560
2-2	1	0.37	252	560
2-3	1.8	0.66	256	560

It was found that significant compaction occurred before excess pore pressure developed. To reduce overall test time, a seating load of 100 kPa was applied at a faster rate to remove the majority of macro-scale air voids from the sample. Thereafter, the load was applied in 10 subsequent steps with an incrementally increasing rate, calculated using the method described in Section 3.2.2. Load steps were calculated based upon the sample height after compaction (i.e. the height of the sample after 100 kPa was reached, as opposed to the initial height of the sample). The load rates were determined to simulate a constant rate of rise of approximately 2 m per month. Load steps for each test are given in Table 3-4.

Table 3-4: Test series 2 load steps and load rates

Load step (kPa)	Load rates for each step (kPa / minute)		
	Test 2-1	Test 2-2	Test 2-3
100	5.0	5.0	5.0
146	1.4	1.3	1.4
192	2.7	2.4	2.6
238	4.3	3.9	4.2
284	6.5	5.7	5.7
330	8.8	7.2	8.3
376	10.5	10.8	10.5
422	14.1	12.3	14.1
468	18.9	15.6	17.5
514	22.9	17.7	20.1
560	27.5	22.2	24.1

3.3 Results

3.3.1 Test series 1

Gravimetric moisture contents were measured at the start and end of the test, enabling the calculation of moisture and density properties given in Table 3-5.

Table 3-5: Initial and final moisture content and density properties for test series 1

Test	Test duration (hours)	Initial			Final		
		w (%)	S_r (%)	ρ_{bulk} (g/cm ³)	w (%)	S_r (%)	ρ_{bulk} (g/cm ³)
Test 1-1	1.8	18.8	51.0	1.62	19.5	90.7	2.07
Test 1-2	1.2	18.8	55.5	1.69	19.8	79.2	1.95

The low initial degree of saturation can be attributed to large-scale air voids between saturated “lumps” of filter cake deposited in a loose state. The higher initial density observed in the thinner samples is probably due to a greater degree of compaction during placement. Although it is difficult to draw conclusions regarding the final conditions due to the fact that the sample heights and test times were not the same, the lower final density in the thinner samples can probably be attributed to the lower stress applied to the top of the sample.

The results of each test are plotted in Figure 3-8 and Figure 3-9. The red line shows the vertical stress applied to the sample as measured at the load cell on the loading piston. The green line shows the vertical stress as measured at the base of the cell. The difference between the red and green lines represents friction losses, mainly wall friction. The blue line shows the pore pressure measured at the base of the sample. The dashed line shows settlement, plotted on a secondary axis.

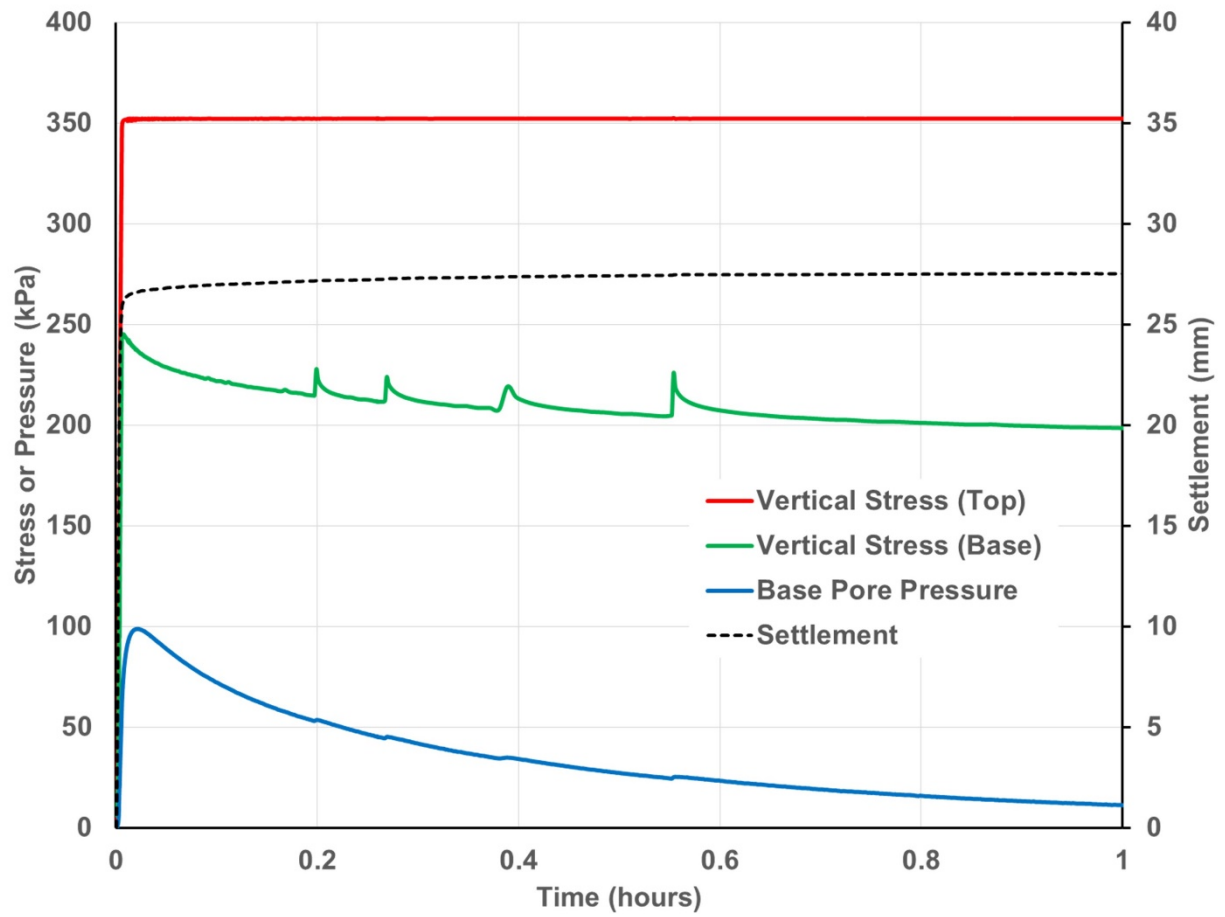


Figure 3-8: Test 1-1 – Initial sample height 100 mm

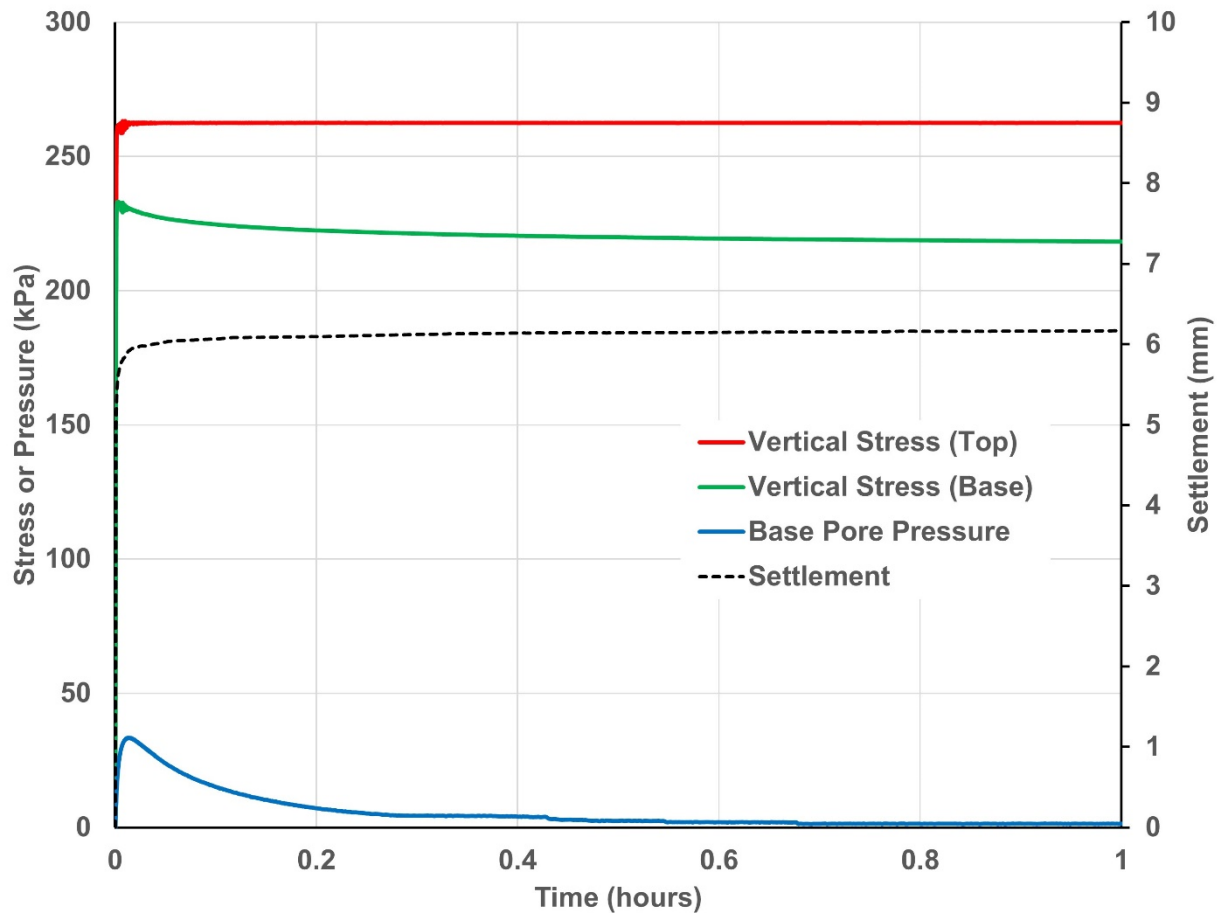


Figure 3-9: Test 1-2 – Initial sample height 30 mm

Initially, there is very large settlement before excess pore pressures develop, due to the removal of large-scale air voids. The thicker sample was observed to develop higher excess pore pressure than the thinner sample. This can be explained by the “lag time” effect; due to the unsaturated nature of the sample, there is likely to be a “lag time” in the measurement of excess pore pressure at the base. Thus, it is probable that peak pore pressures have already dissipated before they can be measured by the sensors. This would imply that the measured peak pore pressure is lower than the true peak pore pressure.

Using the approach given in Section 3.2.2, these curves may be plotted against a “field time” axis, by using a time scaling factor, T_s . Time scaling factors were determined from equations 4.2 and 4.3 based on the average stress ($\bar{\sigma}$), assuming a linear distribution of vertical stress throughout the height of the sample, as given below:

$$\bar{\sigma} = \frac{\sigma_{top} + \sigma_{base}}{2} \quad (3-6)$$

In theory, the pore pressure curves for the two tests should collapse onto approximately the same line when plotted onto a “field time” axis. Figure 3-10 shows the base pore pressure curves for the two different sample heights, plotted on a “field time” axis.

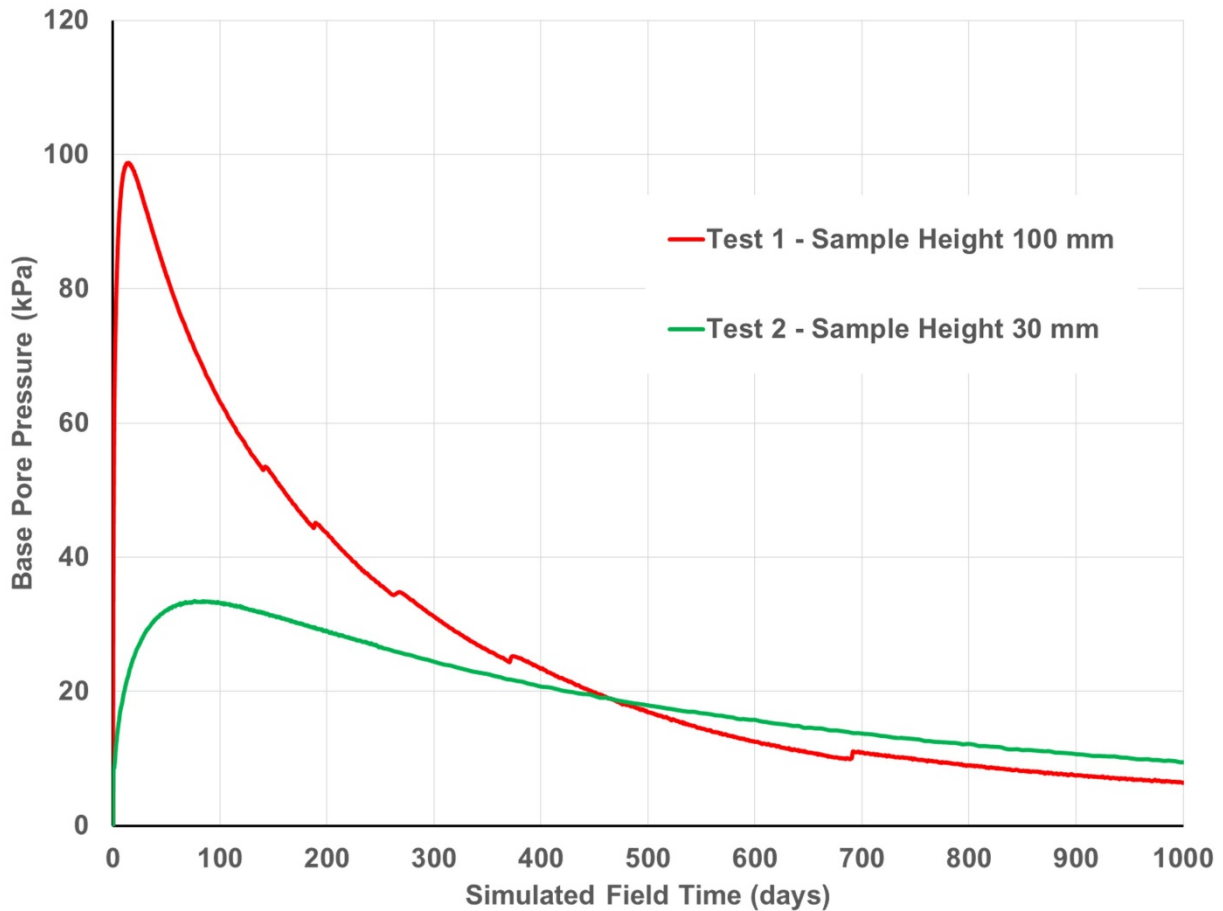


Figure 3-10: Base pore pressure against simulated field time for samples with different initial height

The results are encouraging in a general way, especially with regard to the ends of the curves. One problem is that the true peak excess pore pressure cannot be determined, due to the “lag” effect discussed above. This effect will be more prevalent in the thinner sample since the peak pore pressure will dissipate more rapidly. Consequently, it should be expected that a lower peak pore pressure will be observed in the thinner sample. There may also be significant scale effects, due to the fact the material is not homogeneous in nature and has a distinct “lump” structure.

Since the stresses on the samples are slightly different, it may be useful to plot the curves in a figure using normalised pore pressure, defined as follows:

$$\text{Normalised base pore pressure} = \frac{\text{Base pore pressure}}{\text{Peak base stress}} \quad (3-7)$$

Figure 3-11 shows curves of the base pressure normalised with respect to peak base stress for the two sample heights, plotted on a “field time” axis.

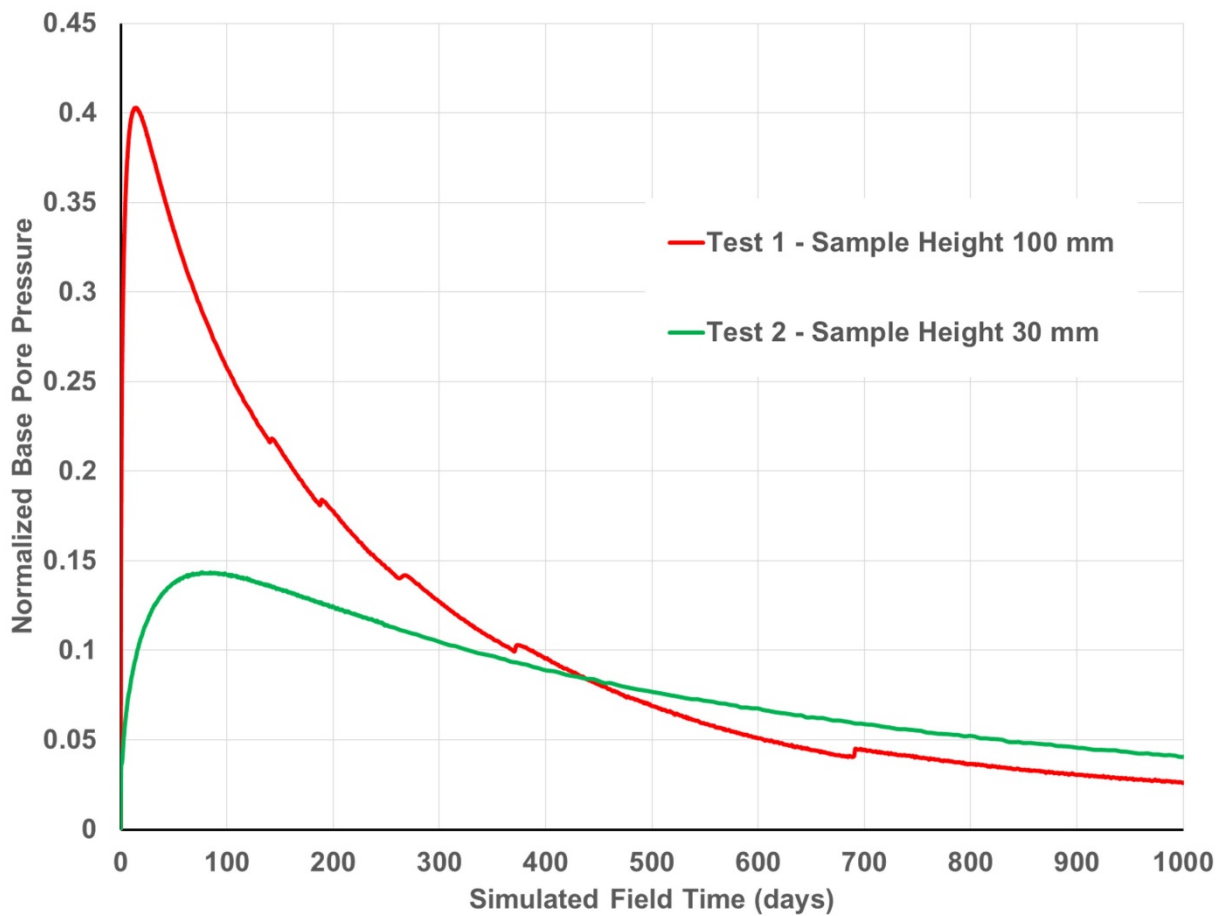


Figure 3-11: Normalised base pore pressure against simulated field time for samples with different initial height

3.3.2 Test series 2

The tests were carried out at an incrementally increasing load rate intended to simulate a rate of rise of 2 m/year. The samples were loaded up to a peak stress of 560 kPa. For the tests described here, this gives a peak stress measured at the base of the cell of approximately 250 kPa, which equates to a final stack height of approximately 14 m. After the peak load was reached, the load was maintained and the dissipation of excess pore pressure was monitored. The tests performed are summarised in Section 3.2.4. The moisture content, degree of saturation and density at the start and end of each test are given in Table 3-6.

Table 3-6: Initial and final moisture content and density properties for test series 2

Test	Test duration (hours)	Initial			Final		
		w (%)	S_r (%)	ρ_{bulk} (g/cm³)	w (%)	S_r (%)	ρ_{bulk} (g/cm³)
Test 2-1 – Pure FT	5	20.1	39.5	1.38	19.5	94.9	2.10
Test 2-2 – R=0.37	5	15.2	25.7	1.31	15.3	91.1	2.17
Test 2-3 – R=0.66	5	12.4	27.6	1.33	13.7	89.7	2.20

The results of each test are shown in Figure 3-12, Figure 3-13 and Figure 3-14.

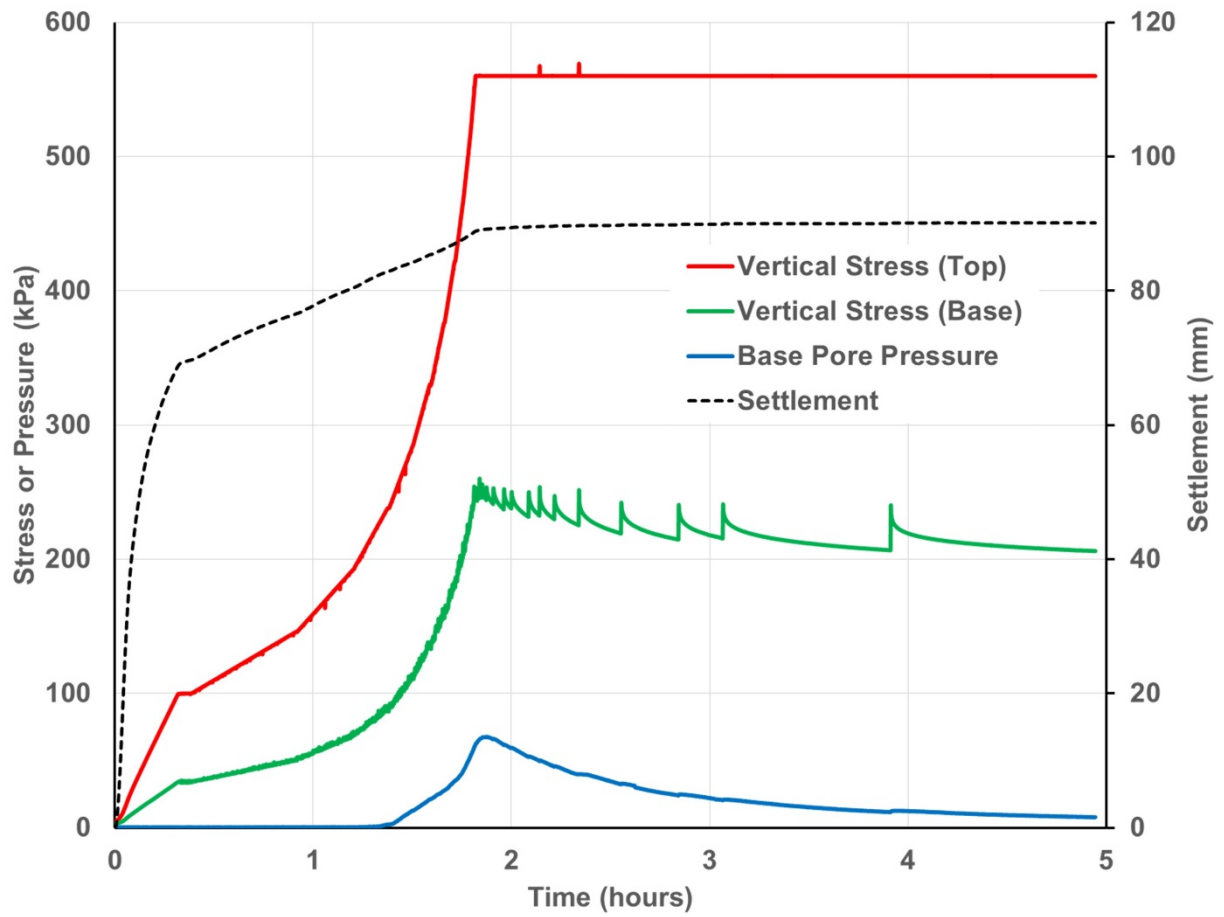


Figure 3-12: Test 2-1 – Filtered tailings

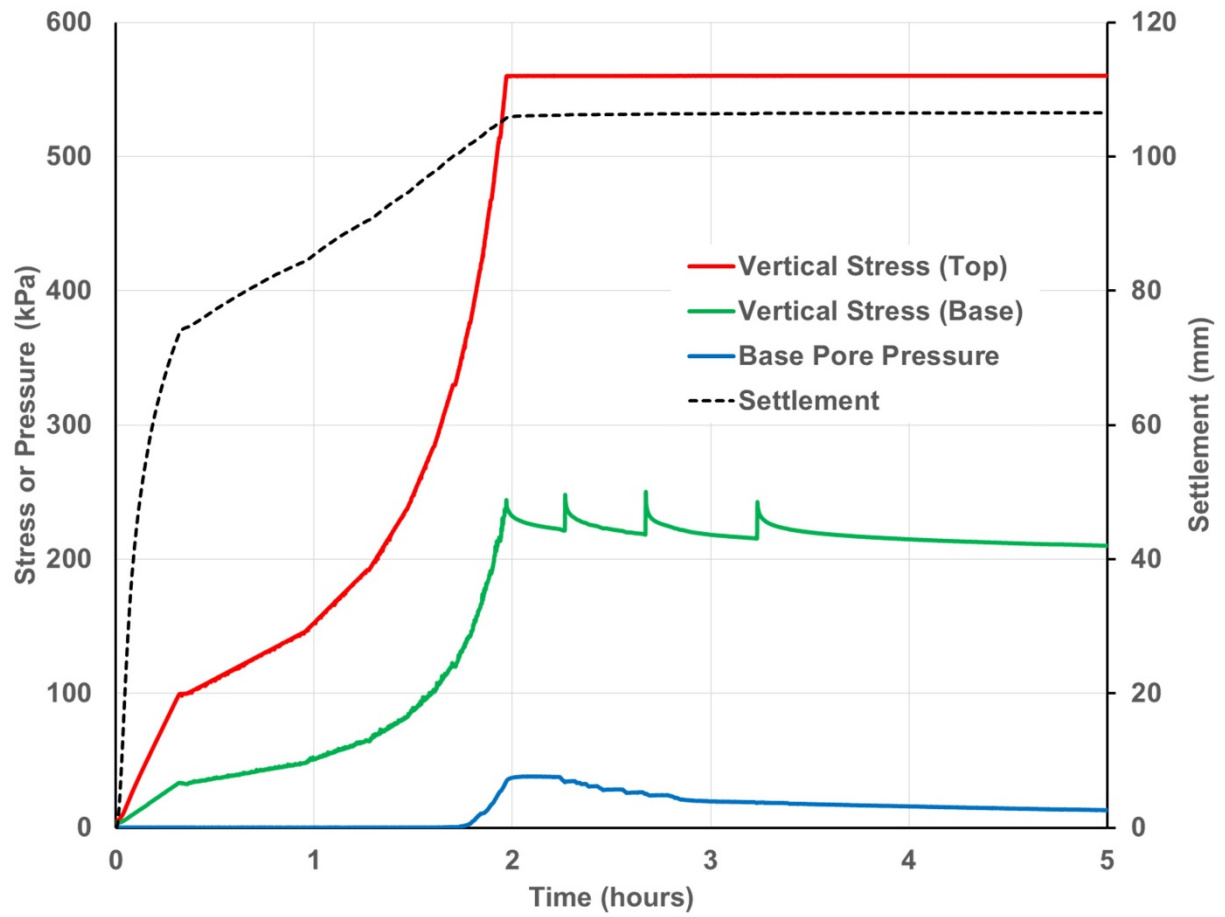


Figure 3-13: Test 2-1 – $R = 1$ Blend

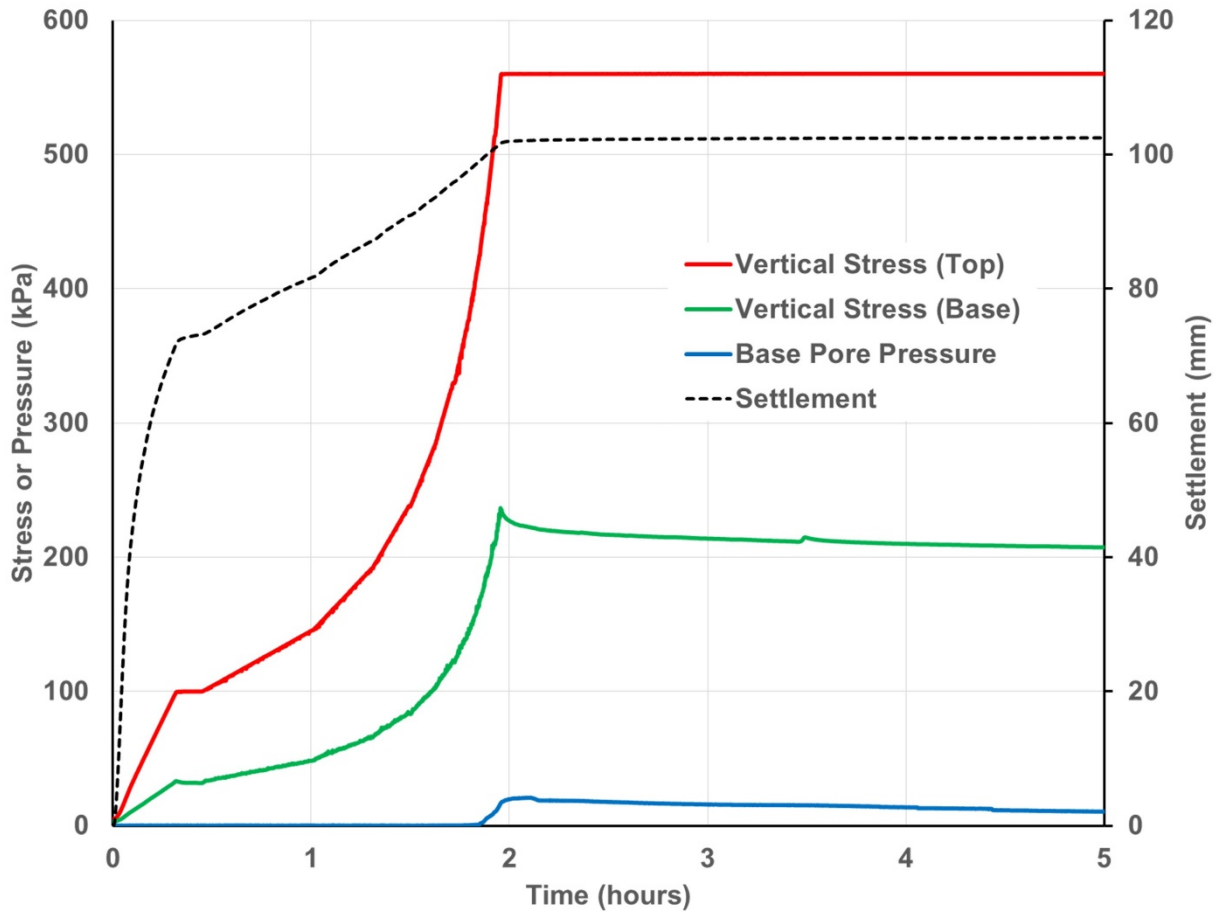


Figure 3-14: Test 2-1 – $R = 1.8$ Blend

The results show that the addition of a small amount of rock to the filtered tailings significantly reduces the build-up of excess pore pressure. The addition of rock also appears to slightly increase the wall friction. The results can then be plotted on a “field time” axis, using time-scaling factors determined using Equation 3.2, shown in Figure 3-15, Figure 3-16 and Figure 3-17.

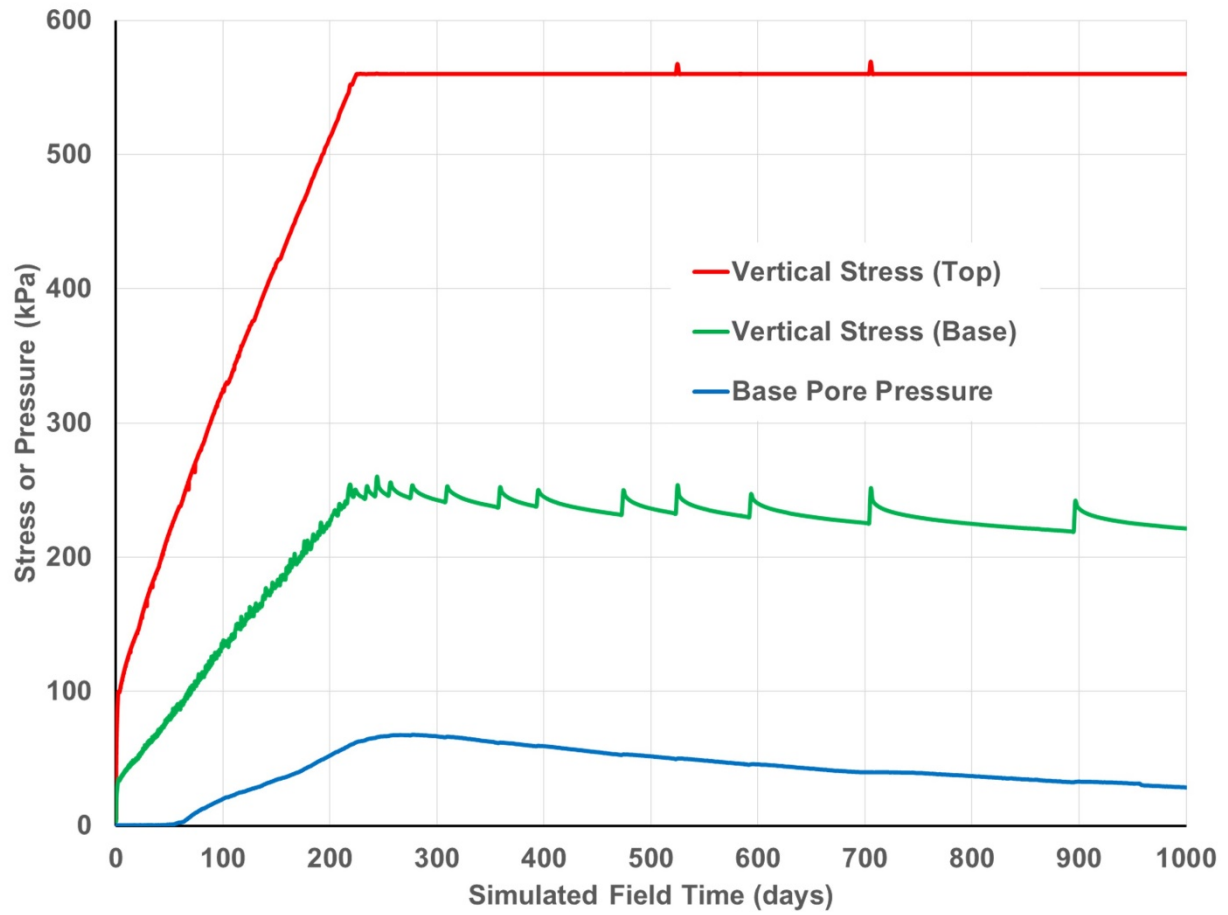


Figure 3-15: Test 2-1 – Filtered tailings (plotted on simulated field time axis)

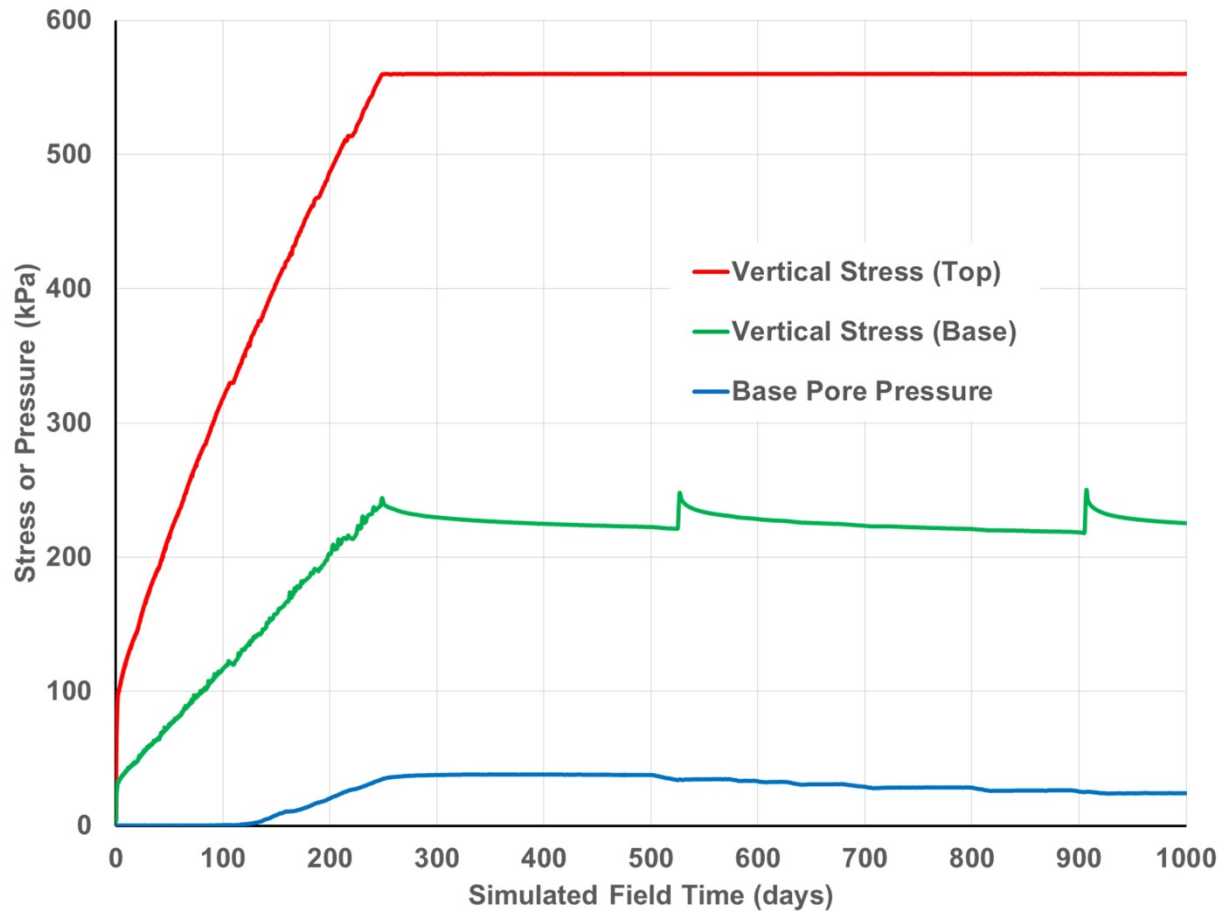


Figure 3-16: Test 2-1 – $R = 1$ blend (plotted on simulated field time axis)

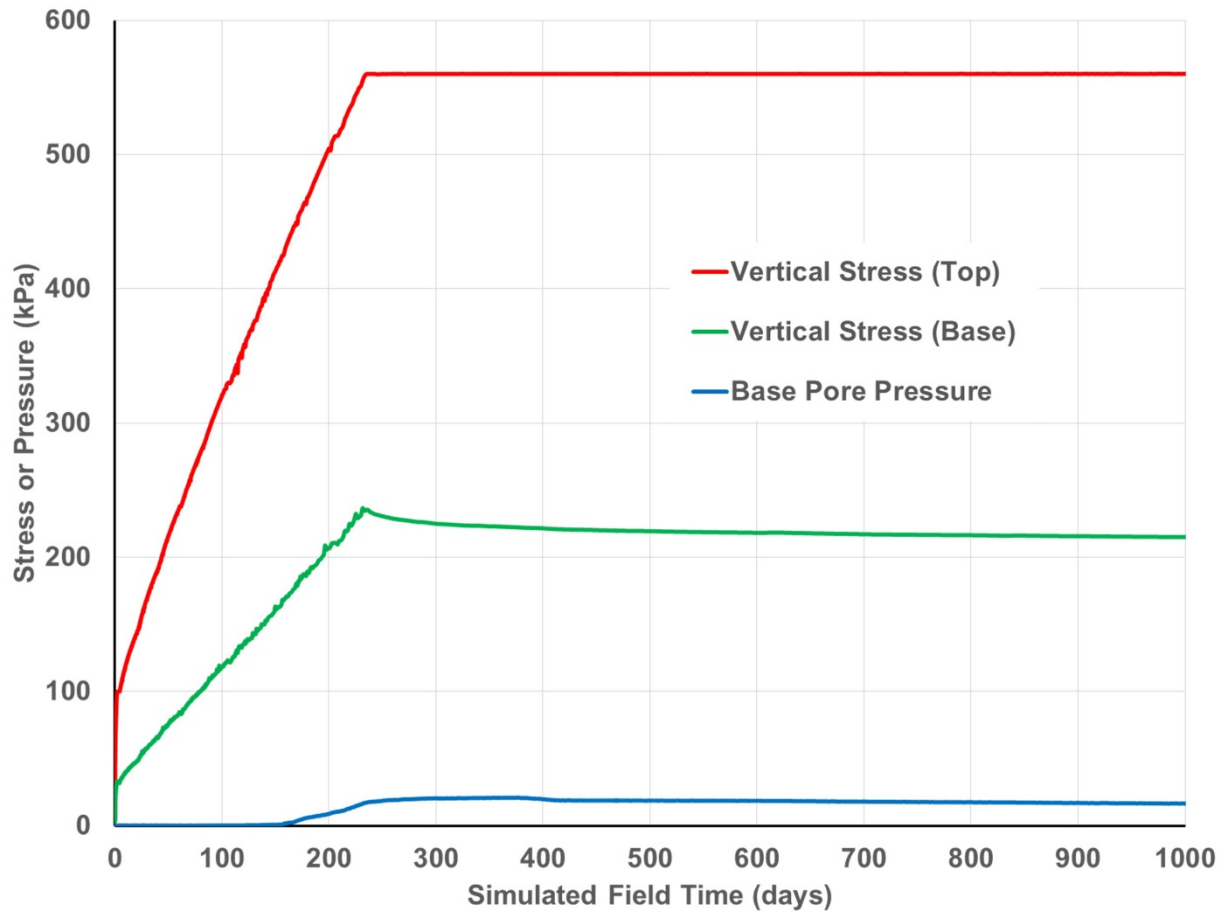


Figure 3-17: Test 2-3 – $R = 1.8$ blend (plotted on simulated field time axis)

It can be seen that the stress increase becomes linear with respect to “field time”, representing a simulated constant rate of rise of approximately 2 m/month. Note that in these examples, the stack height is calculated based on average stress (Equation 3.6), not top stress. Thus, the loading rates for each step were calculated based on the estimated base stress for that step. This explains the slight curvature evident in the top stress line when plotted on a “field time” axis. Non-linearity in the base stress line may be caused by a change in the height of the sample after initial compaction or by errors in the estimation of the base stress for each load step. However, the base stress line appears to be linear in all cases, which suggests that the assumptions used are reasonable.

3.4 Analysis and discussion

A new method of simulating tailings deposition in the laboratory has been presented, using a controlled rate of loading, which is incrementally increased to account for the increasing drainage path length in the field as the tailings stack rises. To validate this method, filtered tailings samples of a range of heights were loaded rapidly in a single step, and the dissipation of excess pore pressure was measured. The difference in the drainage path length between the lab and field was then used to scale time, based on the classic Terzaghi consolidation theory. The results presented in Figure 3-11 appear to show that the method is a reasonable approximation; however, there is clearly a need for more testing on a wider range of materials to validate the method. The second series of tests demonstrated that the same time scaling method can be used to simulate a constant field deposition rate by the application of an incrementally increasing load rate.

The pore pressure response, density and container wall effects are discussed in the following sections.

3.4.1 *Pore pressure response*

The second series of tests demonstrates how the method presented in this paper can be used to evaluate the stability of a range of stack designs, given a constant rate of deposition. The results suggest that the addition of even a relatively small amount of waste rock significantly increases the rate of dissipation of excess pore pressure. The pore pressure response normalised with respect to peak base stress (Equation 3.7) is shown in Figure 3-18 and plotted on a simulated field time axis in Figure 3-19.

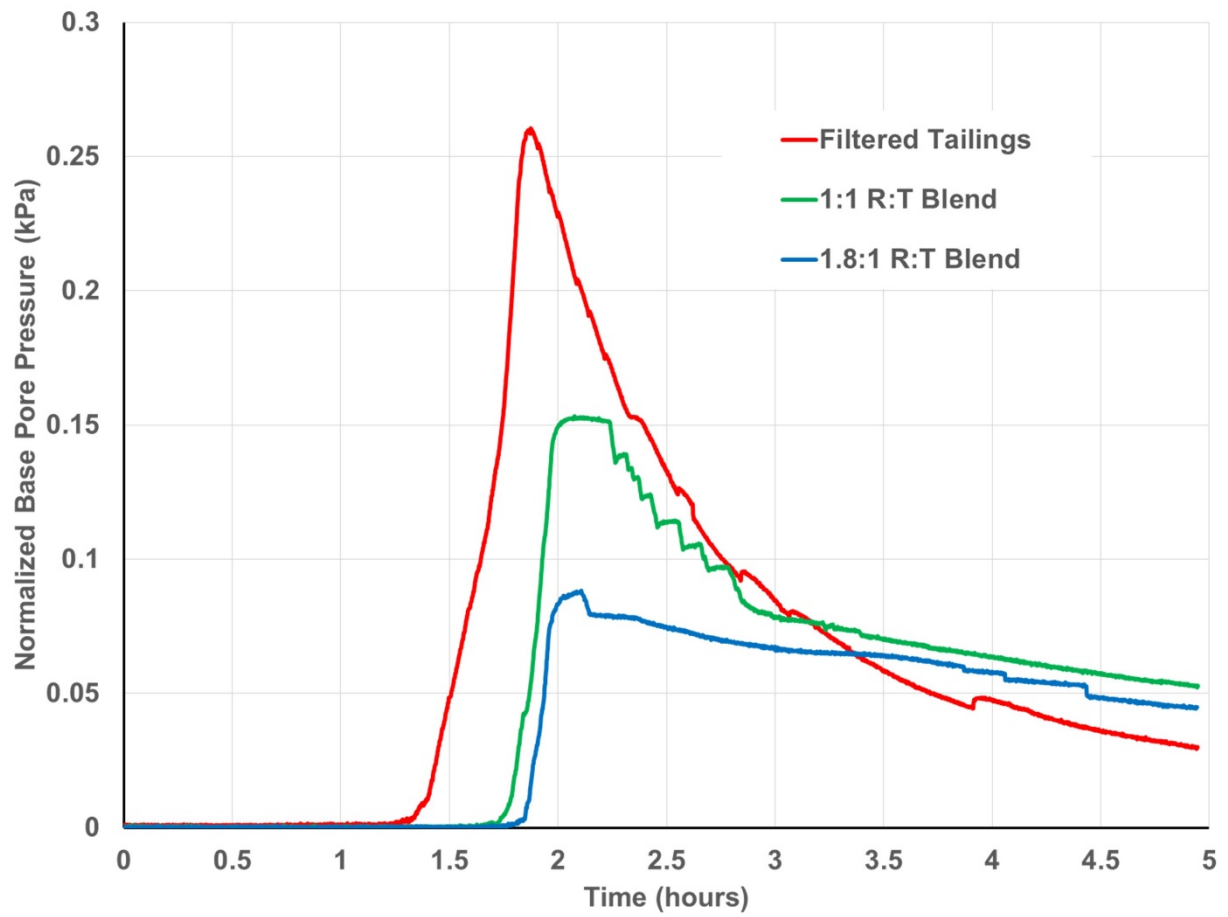


Figure 3-18: Normalised base pore pressure against time

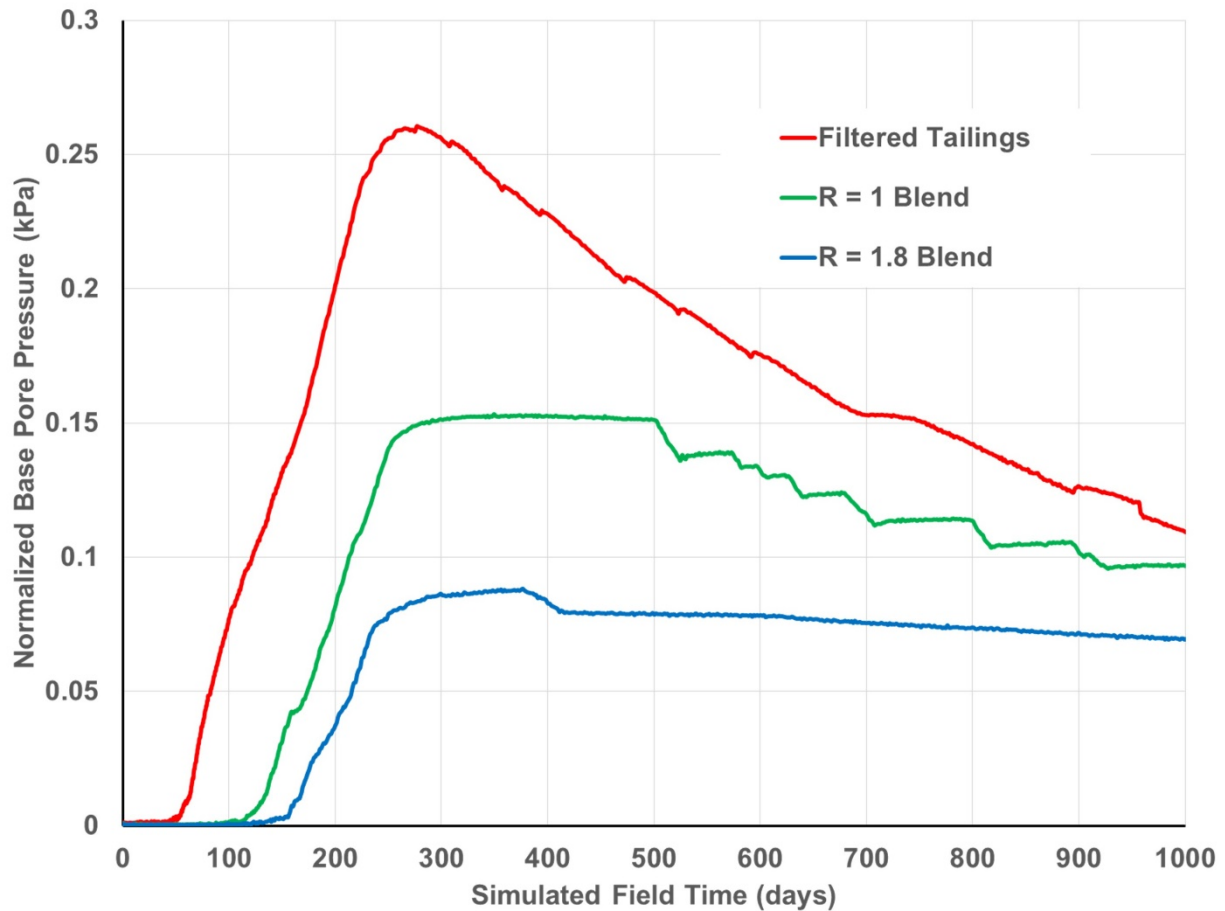


Figure 3-19: Normalised base pore pressure against simulated field time

Both of the mix ratios used in this study could be said to be in the “floating” configuration (Wickland, Wilson et al. 2006), consisting of discontinuous waste rock particles in a continuous matrix of fine tailings. However, the materials used in his study are complex and heterogeneous in nature, consisting of dense, saturated filter cake “lumps”, rock particles and air voids. The introduction of rock reduces the overall degree of saturation and probably creates preferential flow paths between filter cake lumps.

One of the principle differences between the tailings stack and the sample in the consolidation cell which is worthy of further examination is the distribution of vertical

stress throughout the sample. Figure 3-20 (a) shows the distribution of vertical stress in a tailings stack, whereas Figure 3-20 (b) shows a typical vertical stress distribution in the slurry consolidometer cell. Point A in Figure 3-20 (b) represents the stress measured on the loading piston. Point B represents the stress measured at the base of the sample.

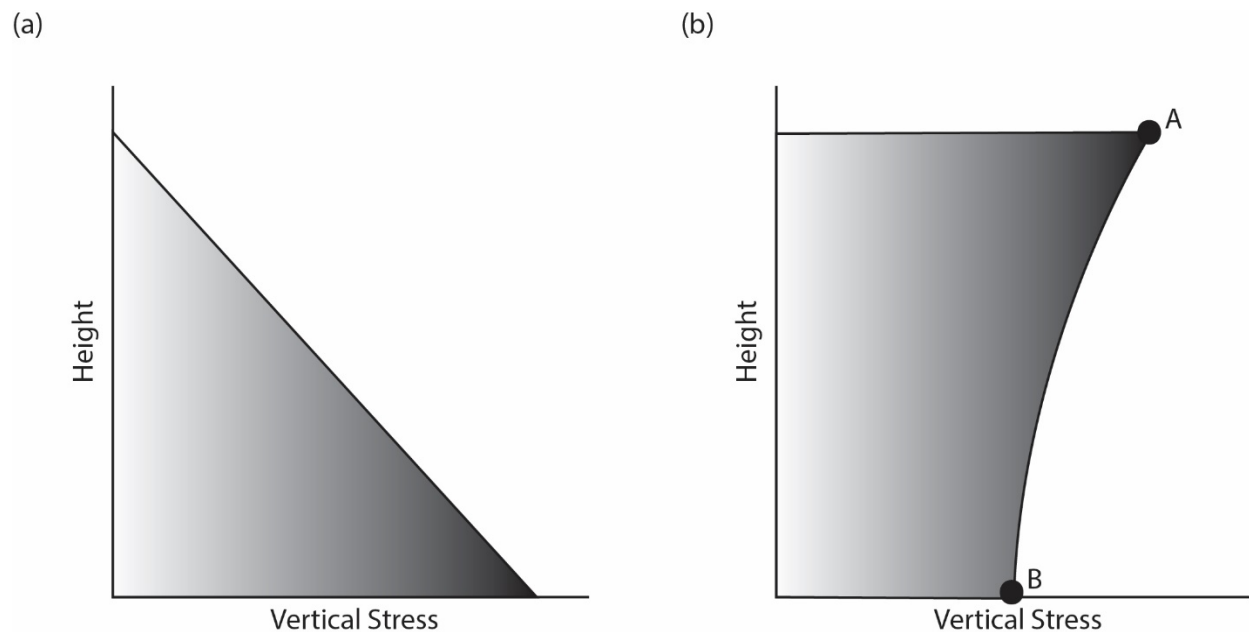


Figure 3-20: Typical vertical total stress distributions in (a) Tailings stack, and (b) Slurry consolidometer cell

Clearly then, a soil element at the base of the slurry consolidometer may be considered to represent a soil element at base of the stack, but the stress distribution throughout entire sample does not represent the distribution throughout the entire stack (as it would in a centrifugal model for example). Thus, the soil along length of the drainage path in the cell will be at a different state of stress than the soil along the drainage path in the field. In general, permeability might reasonably be expected to decrease with increased

confining stress, so the results given here are likely to be conservative. Given this difference in stress distribution, it follows that there is also a difference in excess pore pressure distribution. Although there is no difference in the overall hydraulic gradient along the full length of the drainage path, there will be localised differences, including negative hydraulic gradients indicating downward flow. Whilst this is likely to have an influence on the results, a rigorous analysis of this effect would require numerical modelling. The difference between points A and B on Figure 3-20 may be described as “wall friction”. The wall friction is not constant throughout the test; as excess pore pressure dissipates, effective stress develops and the wall friction increases. Wall friction is due to the shearing of the sample under compressive stress. Wall friction is discussed in detail in Section 3.4.4.

3.4.2 *Density*

Figure 3-21 shows the relationship between the global void ratio (e) and average vertical stress.

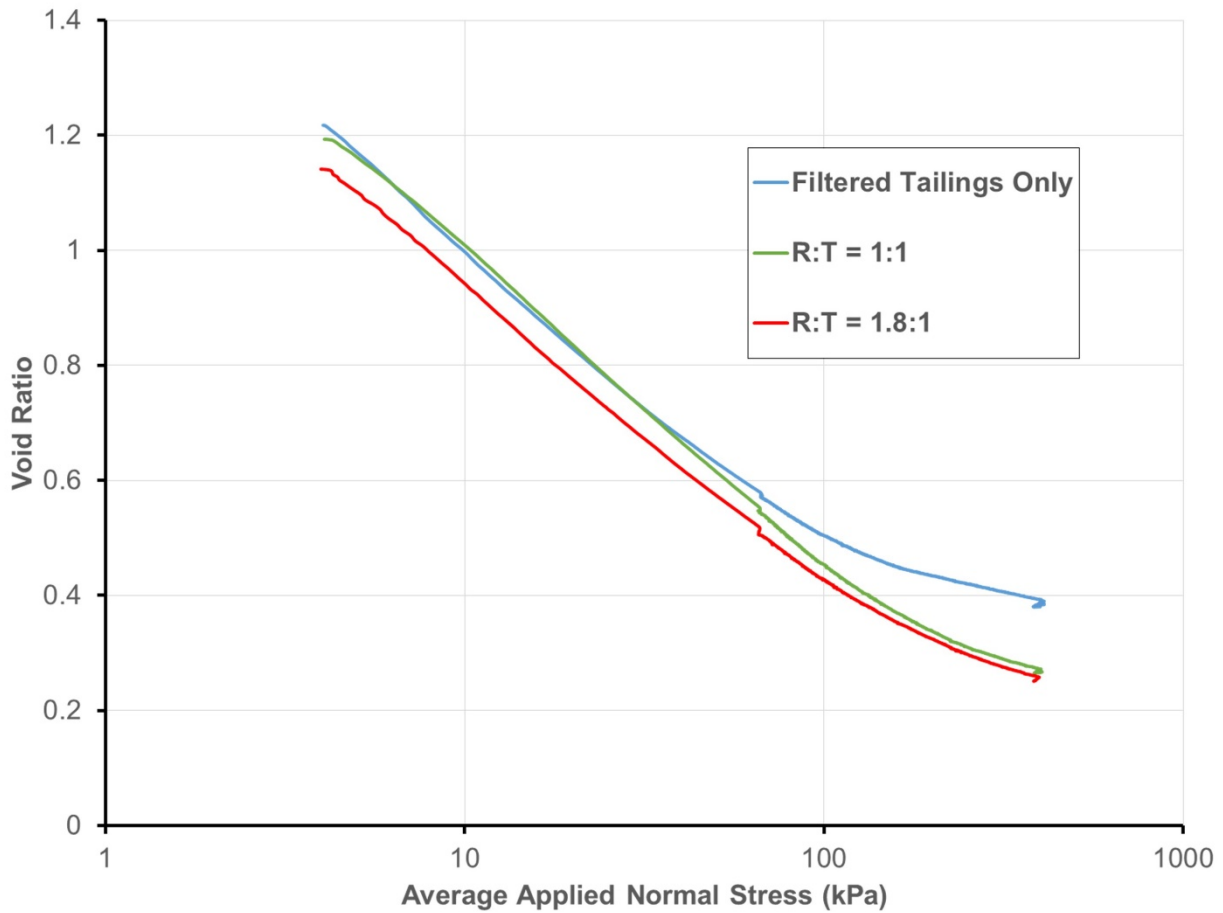


Figure 3-21: Void ratio – average normal stress relationship

It can be seen that the addition of rock increases the overall density of the stack. A distinct reduction in compressibility is evident at higher stresses.

3.4.3 Blend structure and configuration

This section discusses the results of the slurry consolidometer testing within the framework of the blend structure and consolidation theory presented in Section 2.7. Given that the mix ratio is known and the dry density at any point in the test can be calculated, it is possible to use the theory to predict the structural configuration of the blend at any

given time. Figure 3-22 shows the tests from series 2 plotted on the property boundary chart described in Section 2.7.

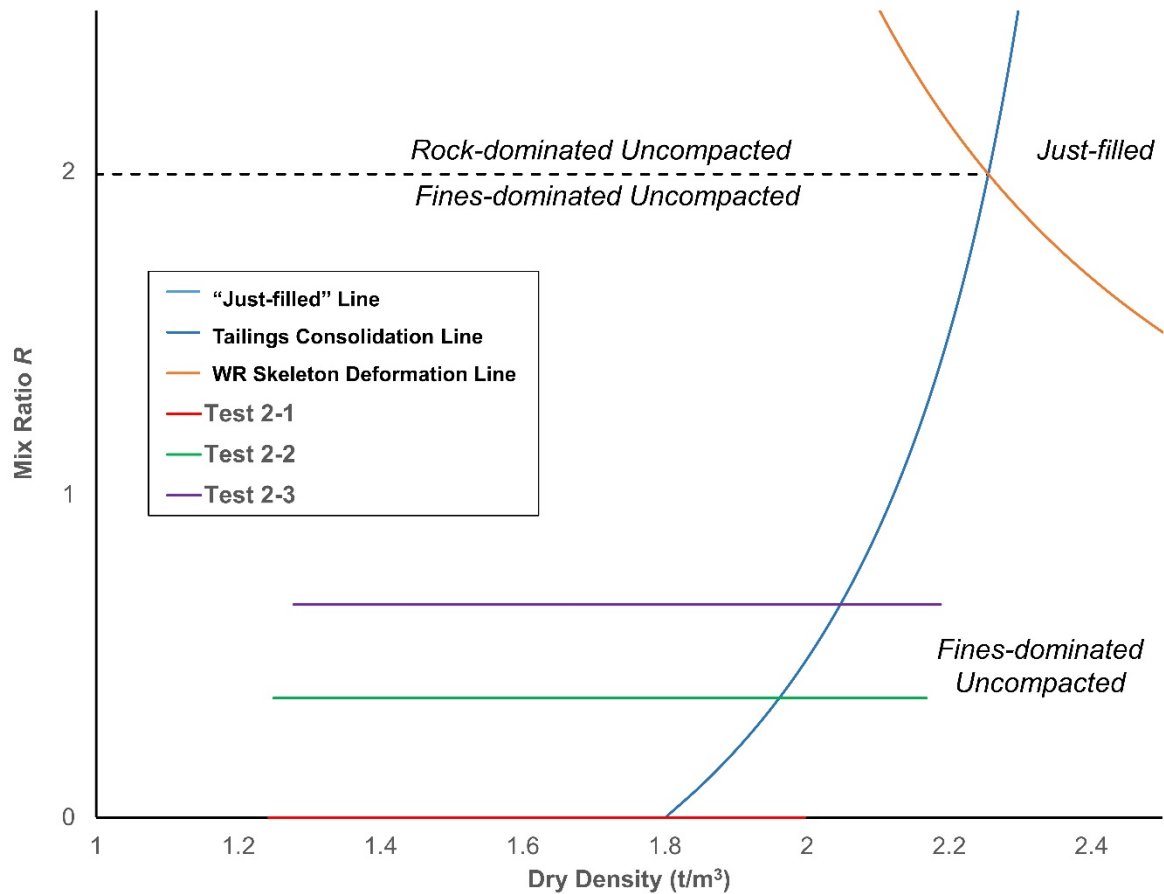


Figure 3-22: Slurry consolidometer tests plotted on property boundary chart

Figure 3-22 shows that the samples are all in the fines-dominated region. Initially, the samples may be described as fines-dominated uncompacted, with compaction being the governing volume change mechanism. The blue line represents the point when the blend becomes fully saturated, and consolidation is the governing volume change mechanism.

Figure 3-23, Figure 3-24 and Figure 3-25 show applied stress, base stress and pore pressure response plotted against dry density for the three tests. The plots are annotated with the “tailings consolidation line”.

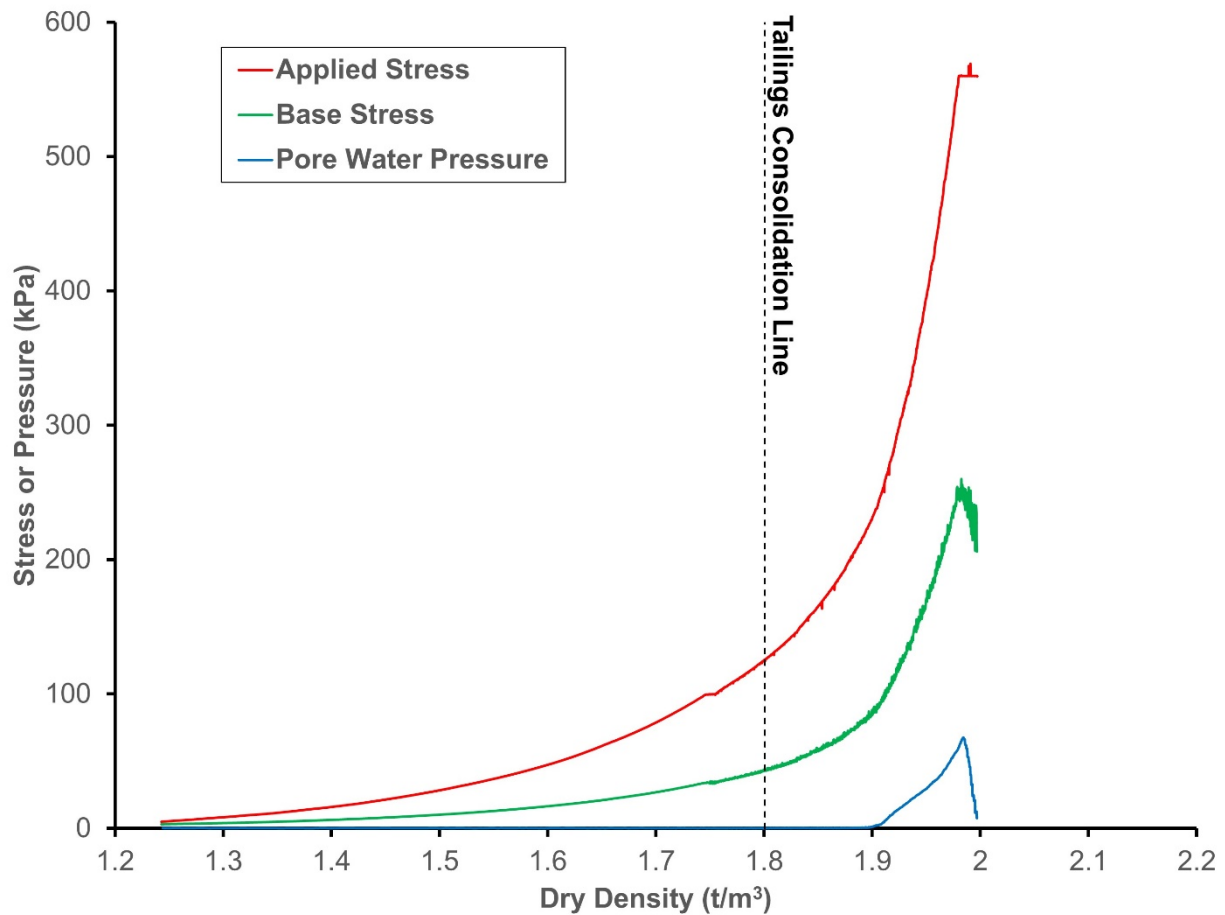


Figure 3-23: Test 2-1 (Pure FT) dry density – applied stress and pore water pressure plot

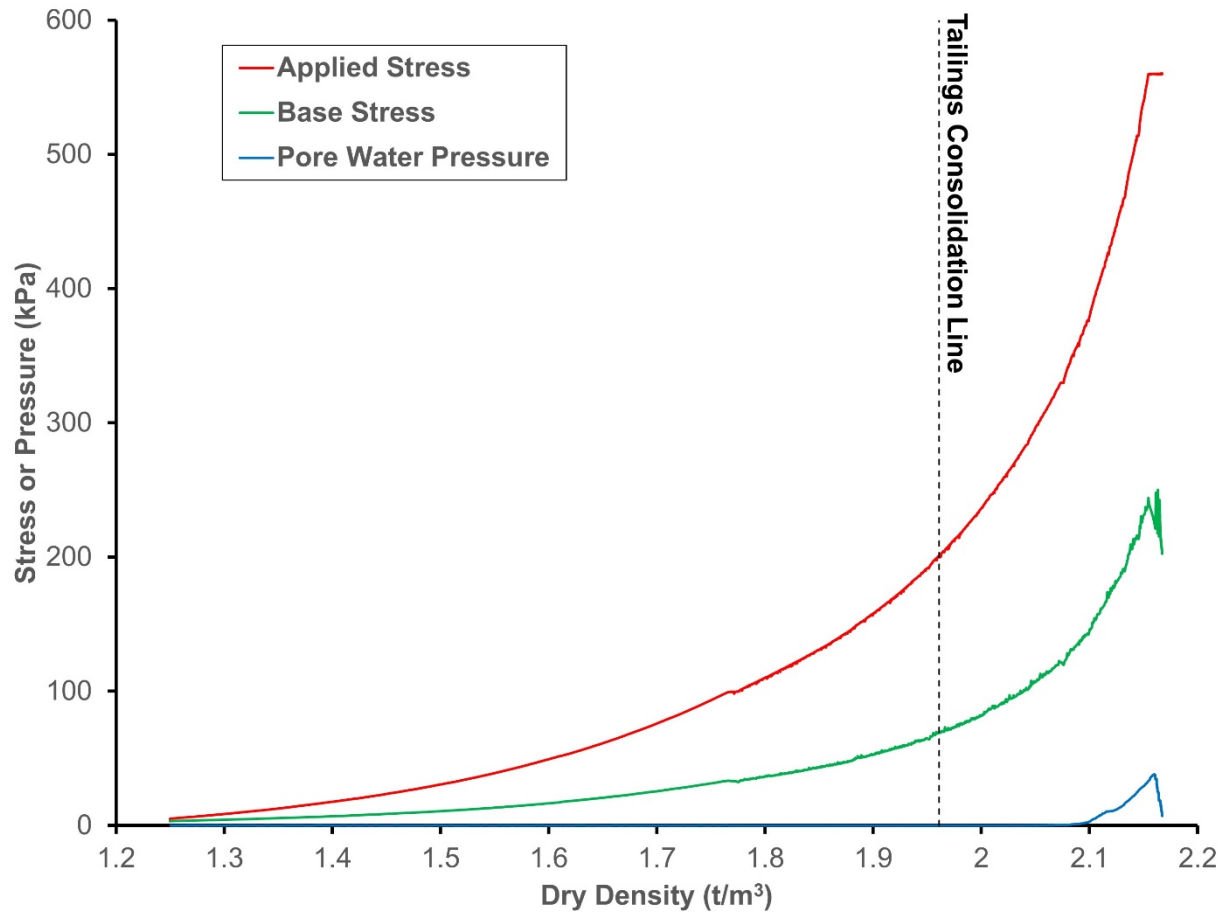


Figure 3-24: Test 2-2 ($R = 1$ blend) dry density – applied stress and pore water pressure plot

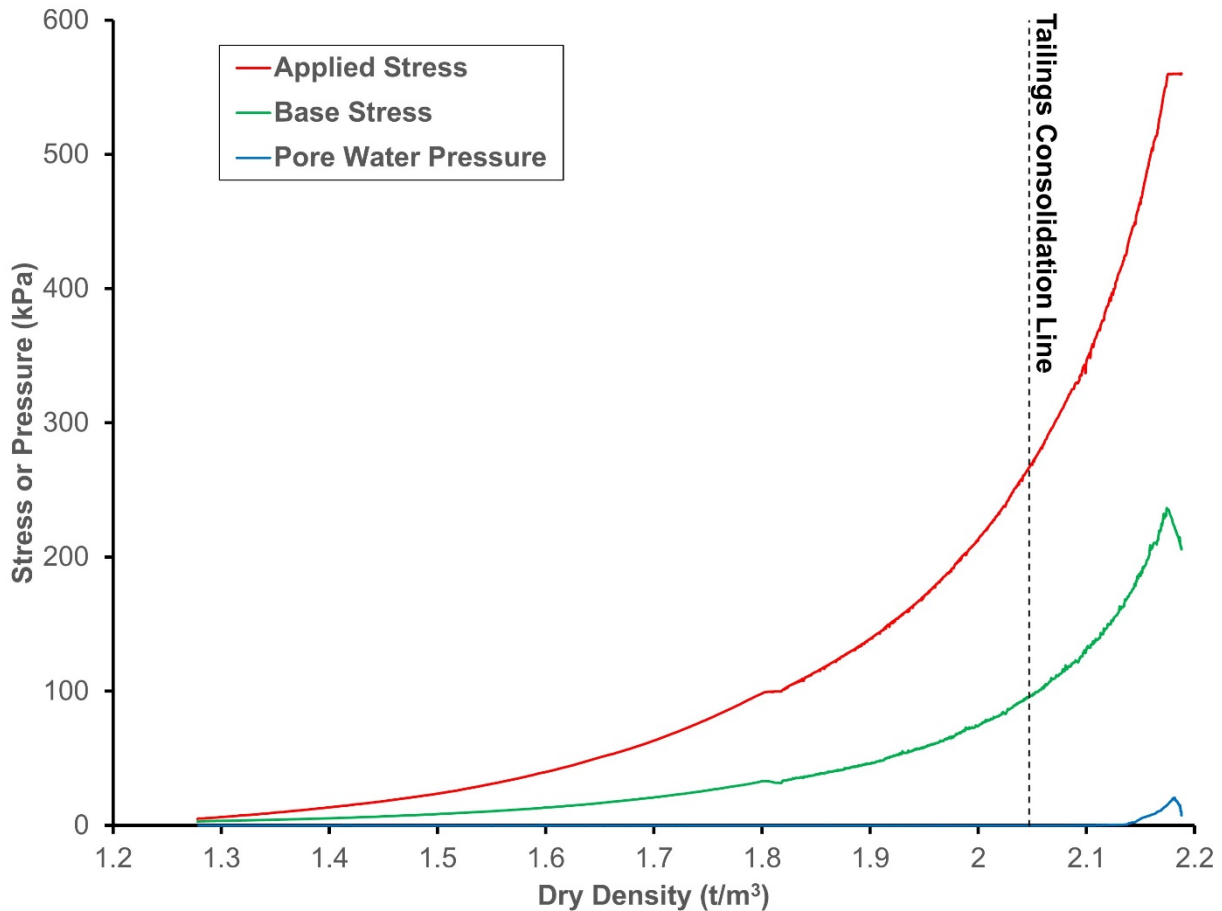


Figure 3-25: Test 2-2 ($R = 1.8$ blend) dry density – applied stress and pore water pressure plot

Based on the theory presented in Section 2.7, it might be expected that the onset of positive pore pressures would coincide with the crossing of the “tailings consolidation line”. In all cases, the pore pressures are observed to develop at a significantly higher density than predicted by the theory. Two explanations are proposed for this. First, the load rate may be such that excess pore pressures are being dissipated before they can be measured and recorded by the sensor. Second, due to the stiff nature of the filtered tailings cakes, there is likely to be some generation of excess pore pressure, and subsequent drainage of water, whilst air voids are still present in the sample. The conceptual model assumes that the moisture content of the tailings does not change until

the blend becomes fully saturated. Due to the drainage of tailings water prior to reaching full saturation, air voids may still be present in the blend after it crosses the tailings consolidation line. The presence of air voids explains the lag time in the measurement of positive porewater pressures. An inspection of the applied stress and base stress curves supports this view; there is no distinctly evident change in the compressibility of the material that occurs when it crosses the tailings consolidation line, rather a gradual transition.

Figure 3-26, Figure 3-27 and Figure 3-28 illustrate this by plotting dry density against the average vertical stress using a logarithmic scale.

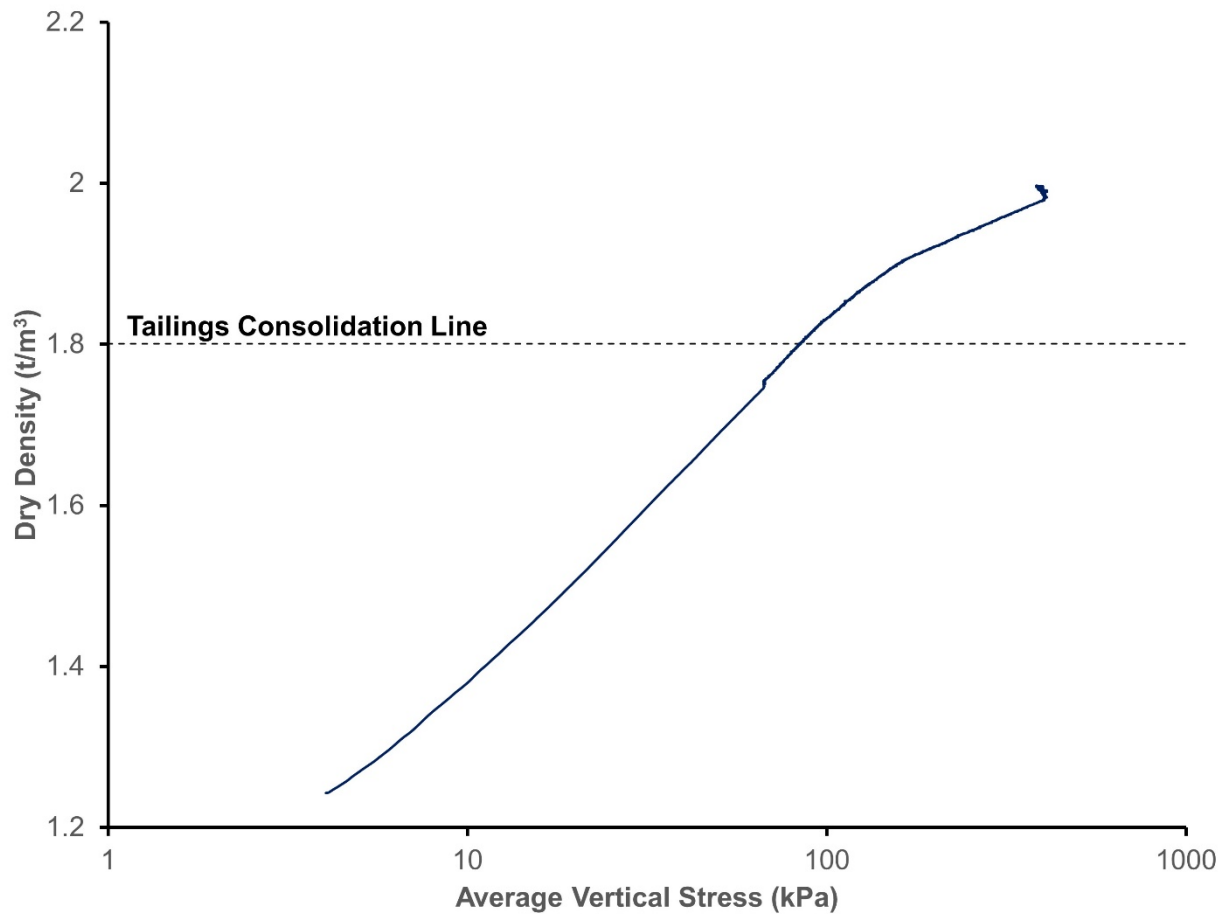


Figure 3-26: Test 2-1 (Filtered tailings) average vertical stress – dry density plot

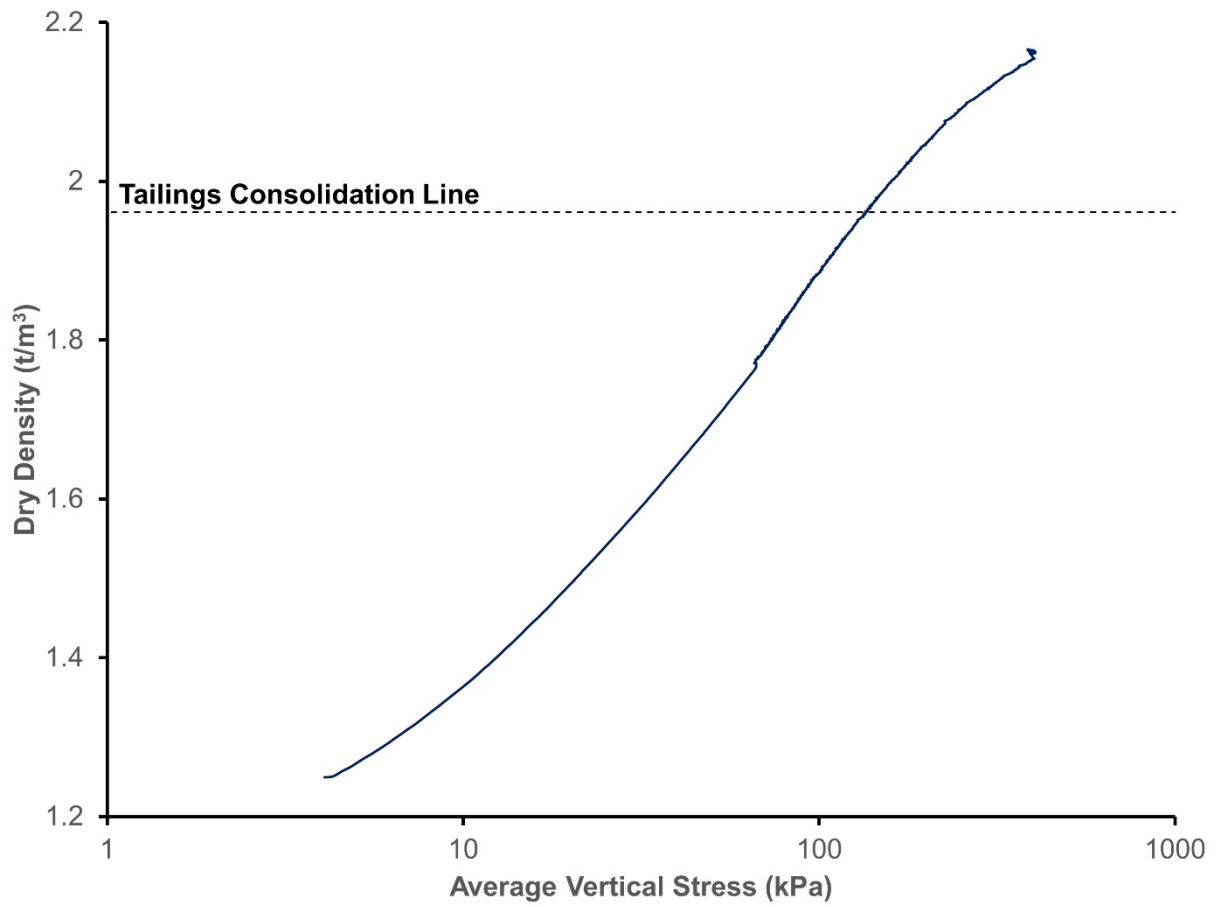


Figure 3-27: Test 2-2 ($R = 1$ blend) average vertical stress – dry density plot

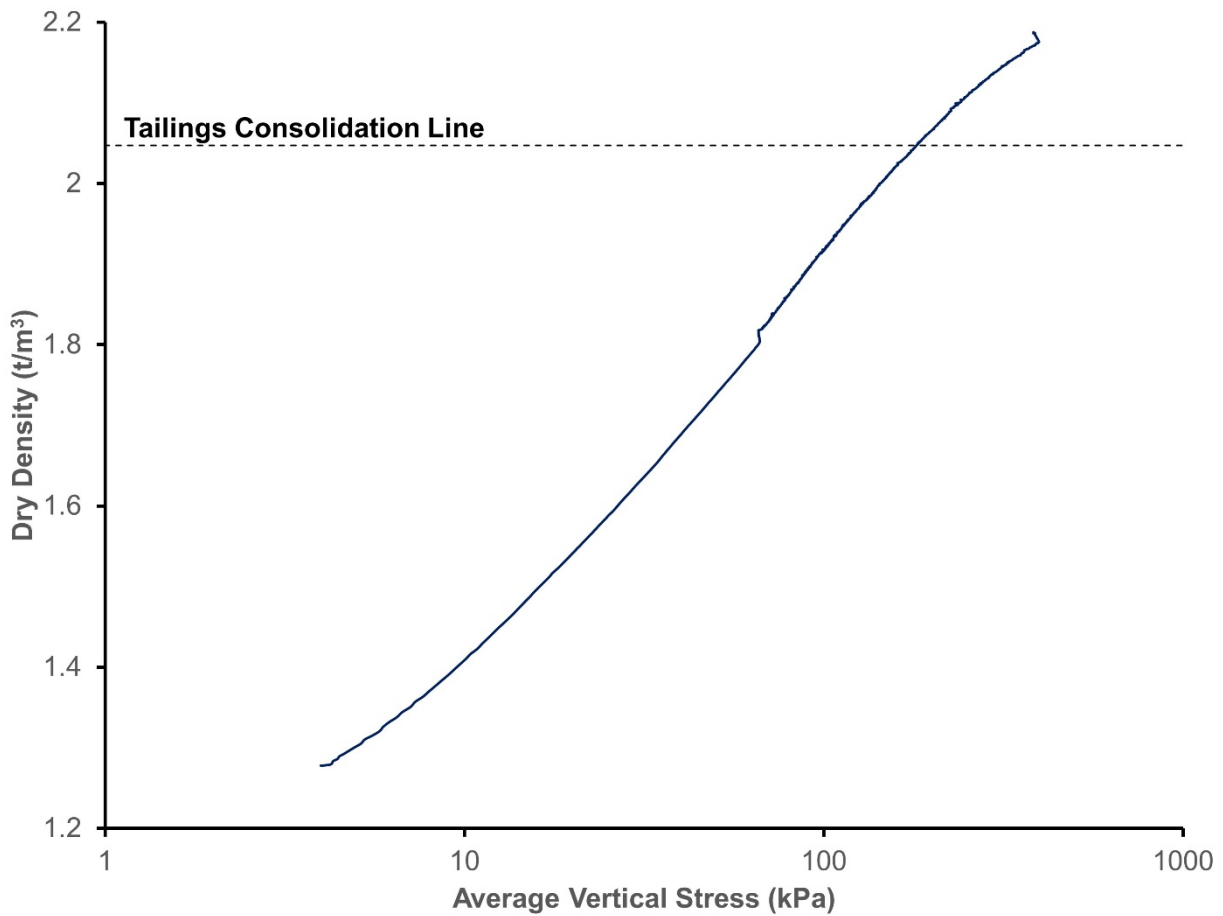


Figure 3-28: Test 2-3 ($R = 1.8$ blend) average vertical stress – dry density plot

It can be seen that as expected there is a change in compressibility that occurs when the blend transitions from an “uncompacted” state (compaction dominated) to a “compacted” state (consolidation dominated). However, the results show a gradual, rather than a distinct transition. The change in compressibility appears more distinct at lower mix ratios, i.e. blends containing more rock appear to be more compressible. It should be noted that the results presented here do not represent samples where excess pore pressures have fully drained. Blends with higher rock content may appear to be more compressible because the excess pore pressure has dissipated faster.

3.4.4 Container wall effects

The use of two load cells, one on the loading piston and one at the base of the cell, was successful in evaluating the amount of lateral friction caused by the cell wall. This was found to be significant; in the filtered tailings tests, stress recorded at the base of the cell was as little as 37% of the applied stress. The wall friction is due to the lateral force caused by the shearing of the sample and due to the fact that the applied stress is not equally distributed throughout the top of the sample. The wall friction losses recorded in the slurry consolidometer tests are given in Table 3-7.

Table 3-7: Wall friction losses in slurry consolidometer tests

Test	Material	Initial Sample Height (mm)	Maximum Applied Stress (kPa)	Maximum Wall Friction Loss^(a) (%)
1-1	Filtered tailings	100	350	43
1-2	Filtered tailings	30	262	18
2-1	Filtered tailings	239	560	63
2-2	1:1 Rock : Filtered tailings blend	252	560	63
2-3	1.8:1 Rock : Filtered tailings blend	256	560	63

(a) Defined as (Applied stress - Minimum base stress) / Applied stress

Generally, higher wall friction was observed for stronger, stiffer samples and for longer samples that had more area in contact with the wall. The wall friction was observed to increase throughout the test, as excess pore pressure dissipated and effective stress

develops. The wall frictions reported in Table 3-7 are the maxima and in all cases represent the end of the test. If the tests were allowed to continue, the wall friction would likely increase as pore pressure continued to dissipate.

Most established consolidation tests, such as the classic oedometer test (ASTM D2435), the Rowe and Barden (1966) cell, or the large strain consolidation apparatus developed by Suthaker and Scott (1996), which is widely used for oil sands tailings, do not have the capability to quantify wall friction loss. In oedometer tests, this problem is minimised by using a low sample height relative to the diameter. The recommended ratios include 5:2 diameter : height (ASTM D2325) and 3 : 1 to 4 : 1 (Lambe and Whitman 1969). By way of comparison, the tests presented in this thesis to simulate the stacking of filtered tailings blends have a diameter : height ratio of approximately 3 : 5. A ratio up to 1 : 1 may be preferred for samples containing large particles, because it allows for the maximisation of the largest allowable particle size. Nevertheless, even a 30 mm sample of filtered tailings, with a diameter : height ratio of 5 : 1, was observed to have a friction loss of approximately 18%.

Other methods for the mitigation of wall friction effects that have been demonstrated in the oedometer testing of rockfills include the use of floating ring oedometers (Parkin and Adikari 1981) or use of “anti-friction” liners or lubricants (Marsal 1973, Oldecop and Alonso 2017). Other methods that have been used to account for the effects of friction in the interpretation of results include ring jacking tests (Penman and Charles 1976) and sophisticated cells that allow the measurement of lateral stress directly. This is typically achieved by the use of strain gauges on the cell, where a compromise must be struck

between having a sufficiently stiff ring to reasonably satisfy the assumption of zero lateral strain and allowing enough deflection to allow for a reasonably accurate measurement of lateral stress (Oldecop and Alonso 2017).

3.4.4.1 Estimation of wall friction using arching theory

Soil arching models, first developed to model arching in grain silos (Jansen 1895) and backfilled trenches (Marston 1930, Terzaghi 1943) may be used to predict the vertical stress at the base of the cell. Such models are widely used in the analysis of backfilled mine stopes (Pirapakaran and Sivakugan 2007, Singh, Shukla and Sivakugan 2011, Ting, Shukla and Sivakugan 2011). Vertical stress (σ_v) at a depth (z) can be calculated (Grabinsky, M., p.c. 2021):

$$\sigma_v(z) = \sigma_{vmax} \left(1 - \exp \left(-\frac{z}{R_h} K \tan \varphi \right) \right) + q \exp \left(-\frac{z}{R_h} K \tan \varphi \right) \quad (3-8)$$

Where:

$$\sigma_{vmax} = \frac{\gamma R_h - c}{K \tan \varphi}$$

R_h is the hydraulic radius, defined:

$$R_h = \frac{A}{P} \quad (3-9)$$

Where A is the area of the sample and P is the perimeter of the sample. q is the surcharge pressure imposed on the top of the sample, which in this case may be considered equivalent to the vertical stress applied via the loading piston, and K is the co-efficient of horizontal earth pressure. In practice the co-efficient of horizontal earth

pressure is likely to fall within the limiting cases of the at-rest earth pressure (K_0) and the active state (K_a), defined (Rankine 1857):

$$K_a = \frac{1 - \sin \phi}{1 + \sin \phi} \quad K_0 = 1 - \sin \phi \quad (3-10)$$

Equation 3-8 may be used to predict the base stress during the slurry consolidometer for both the at-rest and active cases, as shown in Figure 3-29, Figure 3-30 and Figure 3-31. Friction angles of 35° for the filtered tailings alone and 40° for the blended materials were used to compute the base stress, derived from the direct shear tests presented in Chapter 4.

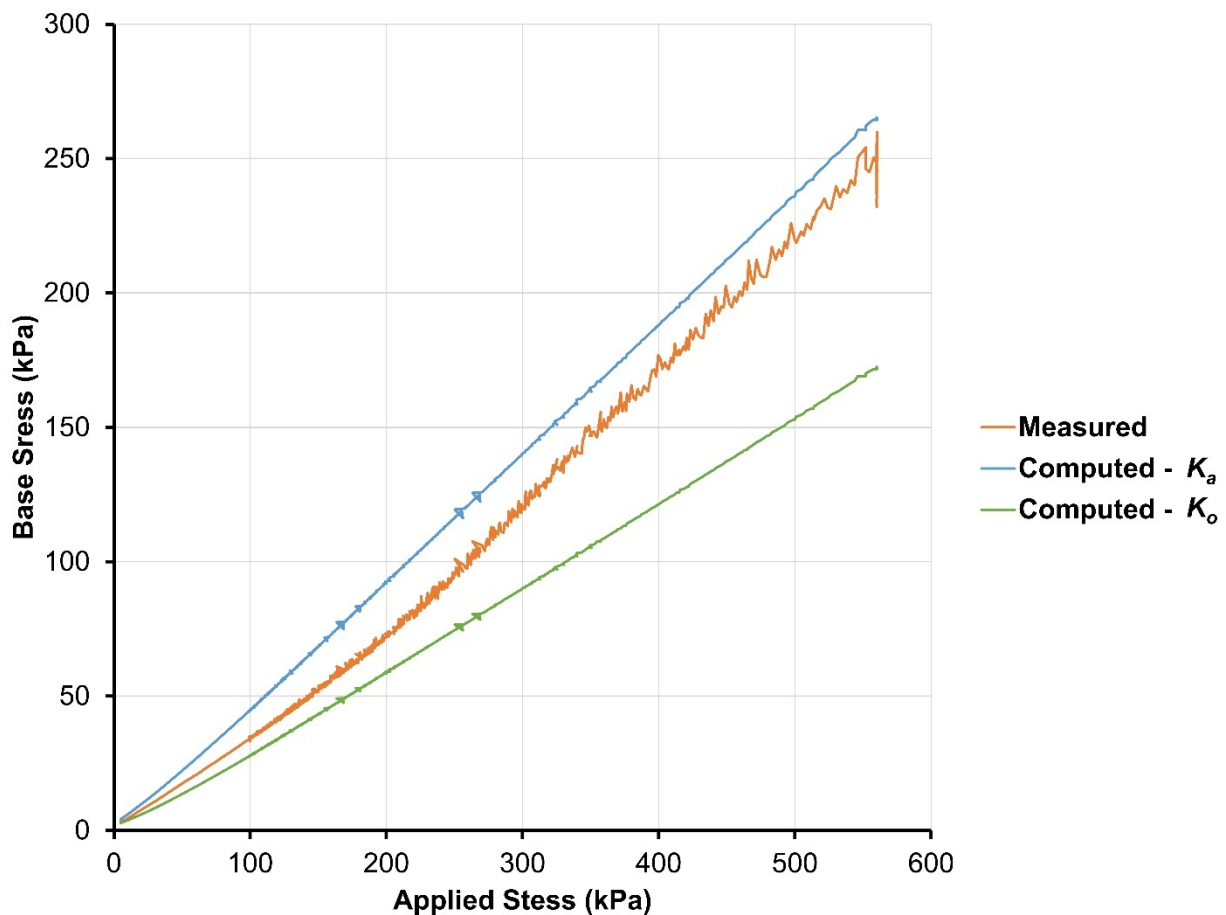


Figure 3-29: Measured and computed base stress for test 2-1 (pure tailings)

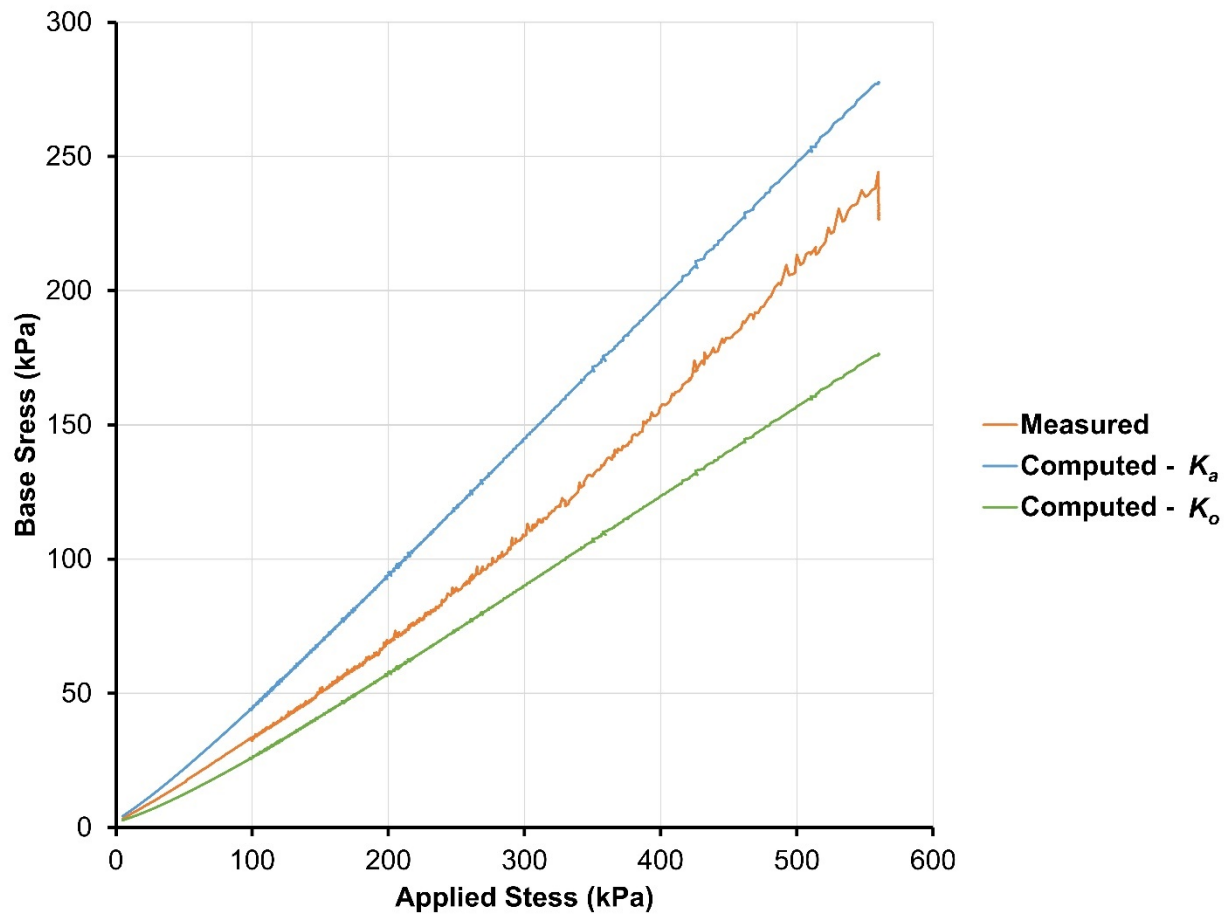


Figure 3-30: Measured and computed base stress for test 2-2 (1R:1T blend)

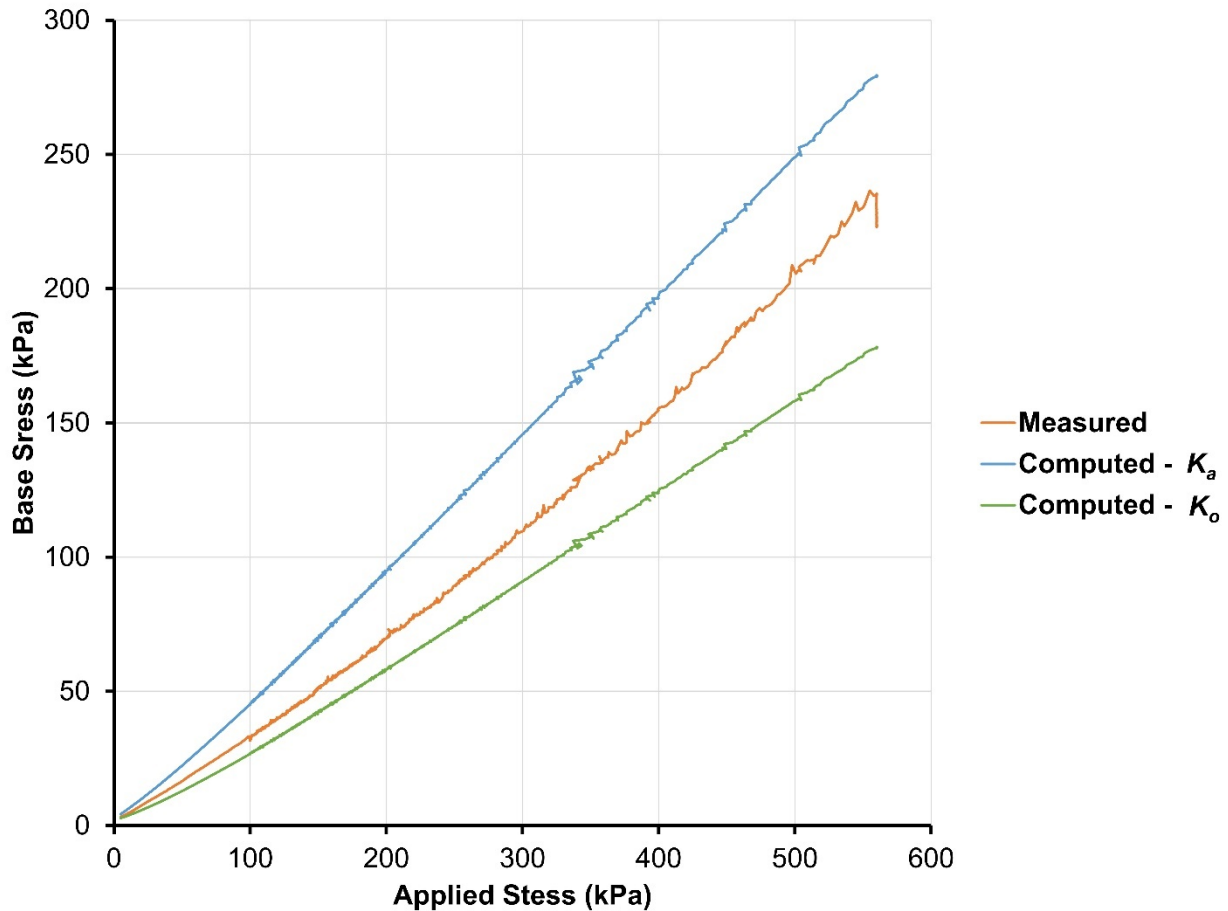


Figure 3-31: Measured and computed base stress for test 2-2 (1.8R:1T blend)

It can be seen that, as expected, the measured base stress falls in between the computed base stress considering at-rest and active states. In all cases, the curve starts closer to the at-rest state and trend toward the active state with increasing applied vertical stress. This behaviour is observed to be much more prevalent in the filtered tailings alone than in the blended materials, and the blend with higher rock content appears closer to the at-rest state. This could be because the wall friction effects in the consolidometer cell do not reflect the same frictional behaviour in the direct shear test. In addition, the samples with higher rock content generally display more dilation during shearing. Under “rigid” sidewall

constraints, this would result in higher stress generated normal to the sidewall (i.e. the dilation effect implies a higher instantaneous friction angle.

In summary, the stress state of the sample in the slurry consolidometer test is complex and varies throughout the sample. Significant friction losses were observed during the tests. The use of two loads cells, at the top and the base of the cell, is a simple and effective means for the quantification of the wall friction losses.

In further testing, the modification of the experimental method is recommended to reduce the influence of wall friction on the test. The most simple and robust way to achieve this by minimising the ratio of sample height to diameter. Other methods involving physical modifications to the apparatus may be considered, such as the use of lubricants or liners on the cell wall.

A simple method based upon soil arching models is presented which provides a useful means to quickly and easily predict the base pressure in the cell. This was shown to give generally good results for the tests presented in this thesis. However it is not considered to be a substitute for the use of a base load cell.

3.4.5 Other issues identified with the slurry consolidometer test

Several other issues were identified with the experimental method during the course of the research, namely, that the test does not allow for the accurate determination of basic mass – volume properties during the test. Three causes are identified for this:

1. The calculation of the sample volume requires a knowledge of sample height, which is calculated from the initial height and settlement. Settlement can be measured accurately via the LVDT. However an accurate measurement of the

initial sample height is difficult. This leads to inaccuracy in the calculation of sample volume.

2. Whilst bulk density can be measured directly, other properties such as the void ratio and dry density must be calculated based upon moisture content, which is obtained from a sub-sample at the beginning of the test. Variability in moisture content throughout the sample due to inconsistent mixing or natural heterogeneity in particle structure (variations in rock particle size of the sub-sample, for example) can cause an inaccurate calculation of initial moisture content. This can cause the inaccurate measurement of the void ratio, dry density and degree of saturation.
3. Water is allowed to drain from the top of the sample during the test. However, the experimental apparatus does not allow for the quantity of this water to be measured. Consequently, there is no way of knowing the moisture content and degree of saturation. It is possible to assume that the drainage does not occur until 100% saturation is reached and thus calculate the degree of saturation. However, this approach did not produce meaningful results. An unacceptable degree of error is likely to arise due to the drying out of the sample, generation of positive pore pressures and drainage by consolidation before the sample is saturated or errors in measurement of initial moisture content.

The rectification of these issues would require modification of the apparatus.

3.5 Further discussion and conclusions

Compression of unsaturated, “dry stacked” tailings, or blended waste rock and tailings, is a complex and multi-faceted process which is inherently difficult to model. Firstly,

compaction is the dominant process. Compaction is a complex process which is generally governed by initial moisture content, due to lubrication of the particles by water, suction pressures and other factors. In geotechnical practice, the compaction behaviour of a soil is determined by an experimental method such as the classic Proctor test; there is no generalised numerical soil behaviour model currently in use that can describe compaction. Following compaction, the volume change of the blend is also controlled by unsaturated and saturated consolidation once excess pore pressure develops.

The complexity of the system is increased further by the natural heterogeneity of these materials. Upon deposition, a blend may consist of intact, dense lumps of saturated filter cakes, large air voids, coarse or fine waste rock particles and loose tailings fines. Thus, it is likely that all three processes discussed above may be occurring concurrently at different points in a sample, with drainage paths occurring in multiple directions. Whilst it is recognised that development of a generalised theory or numerical model that could predict the compression behaviour of these materials based on measurable parameters would be a valuable contribution, such a model would extremely complex and unlikely to be successfully applied in practice.

On the contrary, the approach taken in this research is an experimental one. An innovative testing method to simulate tailings deposition and to predict the development of pore pressure at the base of the stack for a given rate of rise has been developed, using controlled rate of loading compression tests. This test provides a relatively quick and inexpensive method of evaluating the potential performance of any combination of dry stacked, blended mine wastes.

The compression tests presented in this paper were undertaken on filtered gold tailings and on blended filtered tailings and waste rock at a range of mix ratios. It is demonstrated that the addition of waste rock to filtered tailings reduces the build-up of pore pressure when loaded in compression with an incrementally increasing load. This suggests that the co-disposal of filtered tailings with rock will reduce the build-up of pore pressure during stacking, improving stability and allowing more rapid deposition, or deposition in higher lifts.

References

- ASTM (2011). D2435/D2435M-11 Standard Test Methods for One-Dimensional Consolidation Properties of Soils Using Incremental Loading, ASTM International.
- Bareither, C. A., J. Gorakhki, J. Scalia and M. Jacobs (2018). Compression Behaviour of Filtered Tailings and Waste Rock Mixtures: Geowaste. Tailings and Mine Waste 2018. Keystone, CO.
- Blight, G. and O. Steffen (1979). "Geotechnics of Gold Mine Waste Disposal, Current Geotechnical Practice in Mine Waste Disposal." Geotech. Eng. Div., American Society of Civil Engineers.
- Butterfield, R. (2000). "SCALE-MODELLING OF FLUID FLOW IN GEOTECHNICAL CENTRIFUGES." Soils and Foundations **40**(6): 39-45.
- Davies, M. P. and S. Rice (2001). "An alternative to conventional tailings management—"dry stack" filtered tailings." Proceeding of Tailings and Mine Waste'01: 411-420.
- Davison, L. R. and J. H. Atkinson (1990). "Continuous loading oedometer testing of soils." Quarterly Journal of Engineering Geology and Hydrogeology **23**(4): 347-355.
- Fahey, M., M. Helinski and A. Fourie (2010). "Consolidation in accreting sediments: Gibson's solution applied to backfilling of mine stopes." Géotechnique **60**(11): 877-882.
- Gibson, R. E. (1958). "The Progress of Consolidation in a Clay Layer Increasing in Thickness with Time." Géotechnique **8**(4): 171-182.
- He, W., Williams, D. and Shokouhi, A (2017). Numerical study of slurry consolidometer tests taking into account wall friction. Computers and Geotechnics **91**: 39-47
- Janssen, H. A. (1895). Versuche uber getreidedruck in silozellen. Z. Ver. Dtsch. Ing., **39**(35), 1045-1049.
- Lambe, T. W. and R. V. Whitman (1969). Soil Mechanics. New York, John Wiley and Sons.
- Malgesini, M., L. Aubone, R. Hunsaker and W. Boyd (2017). Tailings and Mine Waste 2017. Keystone, CO.
- Marachi, N. D. (1969). "Strength and Deformation. Characteristics of Rockfill Materials." Report No. TE-69-5 to State of California Department of Water Resources.
- Marsal, R. J. (1973). Embankment dam engineering : casagrande volume. A. Casagrande, R. C. Hirschfeld, S. J. Poulos and G. E. Bertram. New York :, Wiley.

Marston, A. (1930). The theory of external loads on closed conduits in the light of the latest experiments. In *Highway research board proceedings* (Vol. 9).

Mittal, H. K. and N. R. Morgenstern (1976). "Seepage control in tailings dams." Canadian Geotechnical Journal **13**(3): 277-293.

Morgenstern, N., S. Vick and D. Van Zyl (2015). "Report on Mount Polley tailings storage facility breach." Report of independent expert engineering investigation and review panel. Prepared on behalf of the Government of British Columbia and the Williams Lake and Soda Creek Indian Bands.

Morgerstern, N., S. Vick and B. Watts (2016). Fundão Tailings Dam Review Panel Report on the Immediate Causes of the Failure of the Fundão Dam.

Oldecop, L. and E. Alonso (2017). "Measurement of Lateral Stress and Friction in Rockfill Oedometer Tests Enabling the Analysis of the Experimental Results in the p' - q Space." Geotechnical Testing Journal **40**(5): 822-832.

Olson, R. (1986). State of the Art: Consolidation Testing. STP34606S Consolidation of Soils: Testing and Evaluation. R. Yong and F. Townsend. West Conshocken, PA, ASTM International: 7-70.

Parkin, A. and G. Adikari (1981). Rockfill deformation from large-scale tests. Proceedings of the 10th International Conference Soil Mechanical and Foundations Engineering Stockholm.

Parkin, A. K. (1991). Through and Overflow Rockfill Dams. Advances in Rockfill Structures. E. M. das Neves. Dordrecht, Springer Netherlands: 571-592.

Penman, A. and J. Charles (1976). "The quality and suitability of rockfill used in dam construction. Dams and embankments, Practical Studies from the BRE." London: The Construction Press **6**: 72-85.

Pirapakaran, K., & Sivakugan, N. (2007). Arching within hydraulic fill stopes. Geotechnical and Geological Engineering, 25(1), 25-35

Rowe, P. W. and L. Barden (1966). "A New Consolidation Cell." Géotechnique **16**(2): 162-170.

Schiffman, R. L. and R. E. Gibson (1964). "Consolidation of non-homogeneous clay layers." Journal of the Soil Mechanics and Foundations Division ASCE **5**(90): 1-30.

Shokouhi, A. and D. J. Williams (2015). Settling and consolidation behaviour of coal tailings slurry under continuous loading. Tailings and Mine Waste 2015. Vancouver, BC.

Shokouhi, A. and D. J Williams (2017). Volume change behaviour of mixtures of coarse coal reject and tailings. *Mining Technology*, 126:3, 163-176

Singh, S., Shukla, S. K., & Sivakugan, N. (2011). Arching in inclined and vertical mine stopes. Geotechnical and Geological Engineering, 29(5), 685-693.

Taylor, R. N. (1995). Geotechnical Centrifuge Technology, Taylor & Francis.

Terzaghi, K. (1943). Theoretical soil mechanics, J. Wiley and Sons, inc.

Ting, C. H., Shukla, S. K., & Sivakugan, N. (2011). Arching in soils applied to inclined mine stopes. International Journal of Geomechanics, 11(1), 29-35.

Terzaghi, K. and O. K. Fröhlich (1936). Theorie der Setzung von Tonschichten: eine Einführung in die analytische Tonmechanik, Franz Deuticke.

Vick, S. G. (1990). Planning, design, and analysis of tailings dams, BiTech.

von Fay, K. and C. Cotton (1986). Constant-Rate-of-Loading (CRL) Consolidation Test. STP34618S Consolidation of Soils: Testing and Evaluation, ASTM International.

Wickland, B. E., G. W. Wilson, D. Wijewickreme and B. Klein (2006). "Design and evaluation of mixtures of mine waste rock and tailings." Canadian Geotechnical Journal **43**(9): 928-945.

Znidarčić, D., R. L. Schiffman, V. Pane, P. Croce, H. Y. Ko and H. W. Olsen (1986). "The theory of one-dimensional consolidation of saturated clays: part V, constant rate of deformation testing and analysis." Géotechnique **36**(2): 227-237.

4 THE SHEAR STRENGTH OF FILTERED TAILINGS AND WASTE ROCK BLENDS

4.1 Introduction

Almost all mines produce fluid tailings as a by-product from the mineral extraction process. Conventionally, these fluid tailings are stored behind dams, which are usually constructed from the tailings themselves (Vick 1990). These structures can present a challenge for reclamation and closure, and are a long-term risk and liability. As large, high-profile failures continue to occur (Morgenstern, Vick et al. 2015, Morgenstern, Vick et al. 2016, Robertson, de Melo et al. 2019), tailings dams are increasingly being seen as unacceptable by many stakeholders. To address this problem, an increasing trend in the industry is the deposition of tailings in self-supporting “dry stacks”, typically using pressure or vacuum filtration to rapidly de-water the tailings before stacking. Another technology that is gaining traction in dry-stacking is the co-disposal of waste rock and tailings. Both approaches have now seen practical application (Habte and Bocking 2017, Wickland and Longo 2017). Combining these techniques offers an attractive solution for mine waste management. The addition of waste rock to a filtered tailings stack may improve stability, as well as reduce overall waste volumes. Since the stacks are self-supporting and not impounded by dams, the shear strength of the blend is an important design parameter. Whilst several researchers have investigated the geotechnical properties of waste rock and fine tailings blends, there is very limited work in this field relating to filtered tailings. The objective of the study presented herein was to investigate the shear strength of waste

rock and filtered tailings blends, specifically the relationship between strength and mix ratio.

4.2 Background

Co-disposal is certainly not a new idea and has been applied in many forms over the years, including in underground backfills (Brawner and Argall 1978), in the Canadian oil sands (Lord and Isaac 1989) and in the pumped co-disposal of coal wastes (Williams 1997). Wickland (2006) introduced the concept of blending waste rock and tailings to create a new, engineered material with favorable properties, termed “paste rock”. At an optimum mix ratio, the void spaces in the waste rock skeleton are “just filled” with fine tailings, giving a blend that combines the high strength and low compressibility of the rock with the low permeability and water retention properties of the tailings. Subsequently, several researchers have investigated the shear strength of “paste rock”-style blends. Khalili, Wijewickreme et al. (2010) investigated the monotonic and cyclic (Wijewickreme, Khalili et al. 2010) shear response of “Paste Rock”. A series of tri-axial tests were undertaken on “Paste Rock” blends at the optimum mix ratio. The shear strength was found generally to be the same as waste rock alone. Jehring and Bareither (2016) carried out tri-axial tests on blends of crushed gravel and four different tailings types. The project was focused on cover design; consequently, the maximum confining stress used was 40 kPa. Blends were prepared at mix ratios close to the optimum. Similar to the previous study, it was found that that friction angles measured for the blends were almost as high as those measured for rock alone.

Borja Castillo (2019) investigated the undrained strength behaviour and critical state analysis of blended filtered tailings and waste rock, termed “Geowaste”, at a single mix ratio of 1.2 : 1 rock to tailings by dry mass. A series of 38 mm diameter triaxial tests was undertaken on tailings samples, and 150 mm diameter tri-axial tests were undertaken on blended samples. The blended samples showed strain-hardening, contractive behaviour below 500 kPa confining stress, and dilative behaviour at 500 kPa. The undrained strength of the blends was found to be comparable to tailings alone at confining stresses of 50 kPa and 100 kPa. At a confining stress of 500 kPa, the blended materials were significantly stronger. It was shown that the critical state line for tailings alone is equivalent to the critical state line for the blended materials when an equivalent tailings void ratio (e_t^*) is used to represent the fines fraction using the approach given by Thevanayagam (2007) and a fitting parameter is used.

None of these previous studies comprehensively investigated the shear strength of blends with mix ratios significantly below optimum, i.e. blends in the “floating” condition, that consist of discontinuous waste rock particles supported by a continuous tailings matrix. It was generally supposed that these blends would have a strength similar to the tailings themselves. With the emergence of filtered tailing – waste rock blends, where a waste rock “skeleton” is no longer a necessity for a self-supporting stack, there is a clear need to revisit this question. In the mainstream geotechnical literature, “floating” rock particles have been generally shown to improve the stability of slopes (Iannacchione and Vallejo 2000). Hamade and Bareither (2018) carried out tri-axial testing on mixtures of synthetic waste rock and tailings at the full range of mix ratios. Friction angles were reported to increase with increasing rock content. With increasing rock content, shear

behaviour transitioned from a contractive to a dilative response. Due to constraints in equipment size, a maximum particle size of 25 mm was used for tri-axial testing.

4.3 Objective

The objectives of the investigation were to test the hypothesis that adding rock to a filtered tailings stack would increase the shear strength and to investigate the relationship between the mix ratio and shear strength. Particular focus was given to blends in the “floating” condition, as this was identified as a knowledge gap.

4.4 Materials

The materials used in this study are filtered gold tailings and waste rock. This section contains details of the field programme where the samples were collected and basic geotechnical characterisation of the materials.

4.4.1 Sampling

The filtered tailings and waste rock used in the study were collected between February and May 2016 from Penasquito Mine, an 110,000 t/day open pit gold and silver mine in Zacatecas, Mexico, operated by Newmont Goldcorp. Waste rock was collected from inside a waste rock dump at the mine. The mine currently deposits tailings as slurry in an impoundment behind a dam constructed from cycloned sand and rockfill (Malgesini, Aubone et al. 2017) but is evaluating a change in tailings technology to co-disposed waste rock and filtered tailings. Filtered tailings were generated using a pilot scale filter plant located at the mine.

This section contains details of the sampling of the materials. Waste rock and filtered tailings are dealt with in turn in the following sections.

4.4.1.1 Waste rock

The objective of this part of the study was to sample rock that was best representative of the material that would be used in a commercial-scale co-disposal project involving the blending of waste rock and tailings. Obtaining a representative sample of run-of-mine waste rock is inherently challenging; particle sizes may vary from fines to large boulders, making the determination of the full particle size distribution difficult due to the very large sample size and large equipment required. Furthermore, waste rock is prone to segregation when it is dumped (Hawley and Cunning 2017), so the material at any given point in the dump is unlikely to represent the material as a whole.

In a co-disposal project, the method of blending, typically using conveyors, limits the maximum permissible particle size. Waste rock used for this study was selected from a waste rock dump that had been previously crushed and transported by conveyor. A sampling site was selected in a location where a cut had been made into the dump to collect material for construction purposes. To minimise the influence of segregation during dumping, an excavator was used to select material from a range of different locations (Figure 4-1). The material was mixed using the excavator before being transferred to a loader. The material was mixed again by the loader (Figure 4-2 and Figure 4-3). The material was then screened by hand, and particles larger than 100 mm were removed (Figure 4-4).



Figure 4-1 Waste rock sampling



Figure 4-2 Waste rock sampling



Figure 4-3 Waste rock sampling



Figure 4-4 Waste rock sampling

4.4.1.2 Tailings

Whole tailings were filtered using a pilot-scale filter plant located at the mine. Flocculant was added to the tailings, and they were thickened to approximately 55% solids. The thickened tailings were then de-watered using pressure filtration, with the pressure provided by the feed pump. The pilot plant is shown schematically in Figure 4-5, Figure 4-6 and Figure 4-7. The feed pump operated at 225 psi (1551 kPa), and the residence time in the filter press was typically 2 minutes.

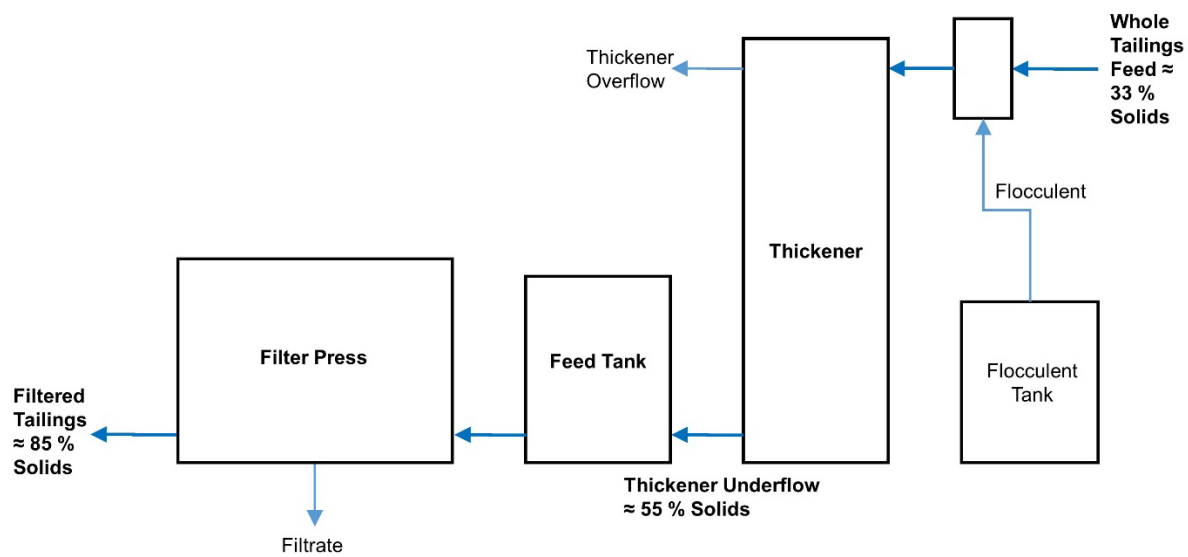


Figure 4-5 Pilot-scale filter plant schematic

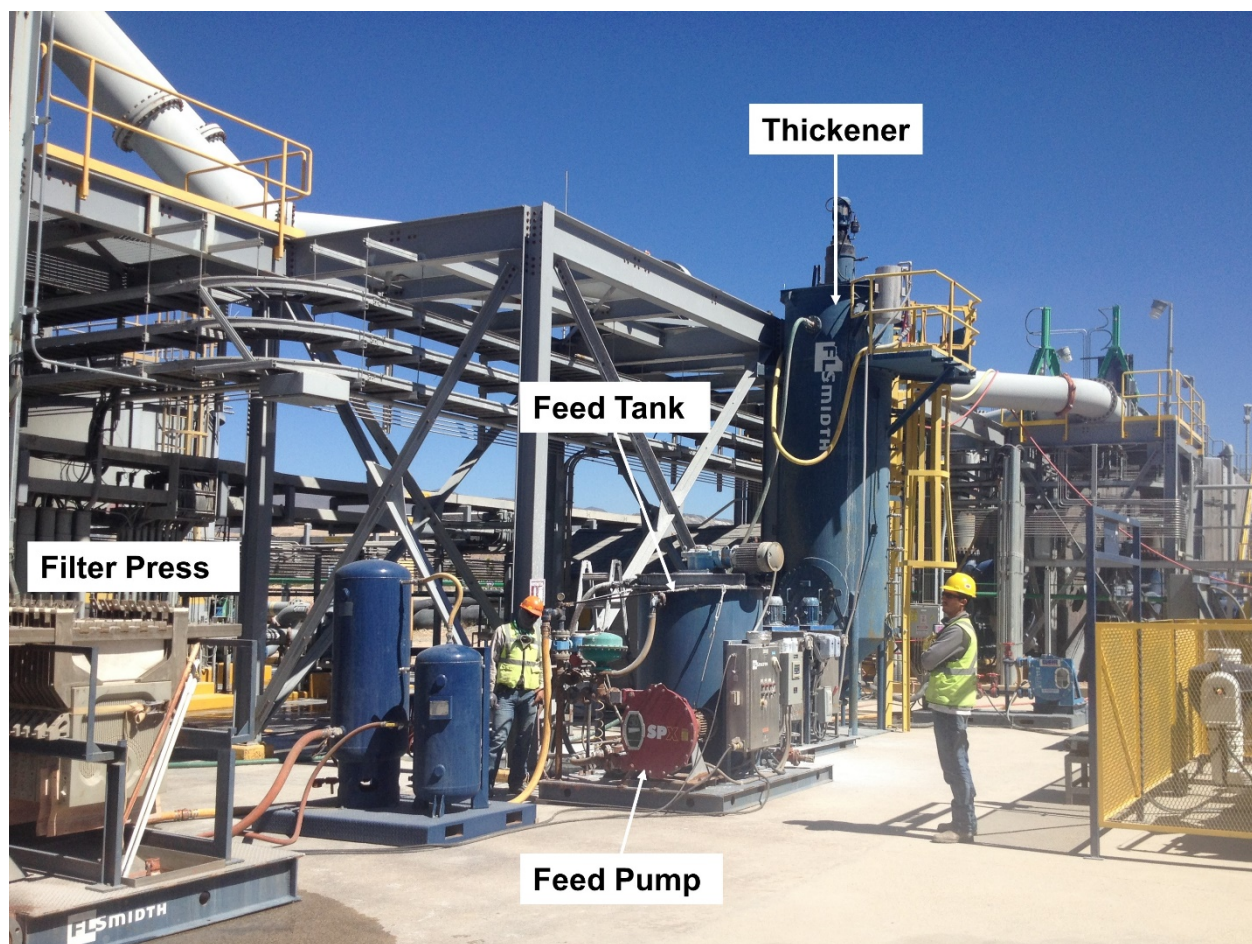


Figure 4-6: Pilot-scale filter plant



Figure 4-7: Filter press

4.4.2 Basic characterisation

The geotechnical index properties are given in this section.

4.4.2.1 Moisture content

The gravimetric moisture content of the filter cakes was measured at regular intervals during sampling. Average gravimetric moisture contents are given in Table 4-1.

Table 4-1 Gravimetric moisture content of waste rock and filtered tailings

Material	w (%)
Filtered tailings	19.29
Waste rock	2.10

4.4.2.2 Atterberg limits

Atterberg limits for the filtered tailings are given in Table 4-2.

Table 4-2: Atterberg limits for filtered tailings

Property	Value (%)
Liquid limit	20
Plastic limit	17
Plasticity index	3

4.4.2.3 Particle size distribution

The measurement of the particle size distribution of the field-scalped waste rock was carried out using the dry sieving method. The particle size distribution of the thickener underflow was carried out using laser diffraction at Penasquito Mine. It is assumed that the thickener underflow will not have a significantly different particle size distribution to the filtered tailings. The particle size distributions are shown in Figure 4-8.

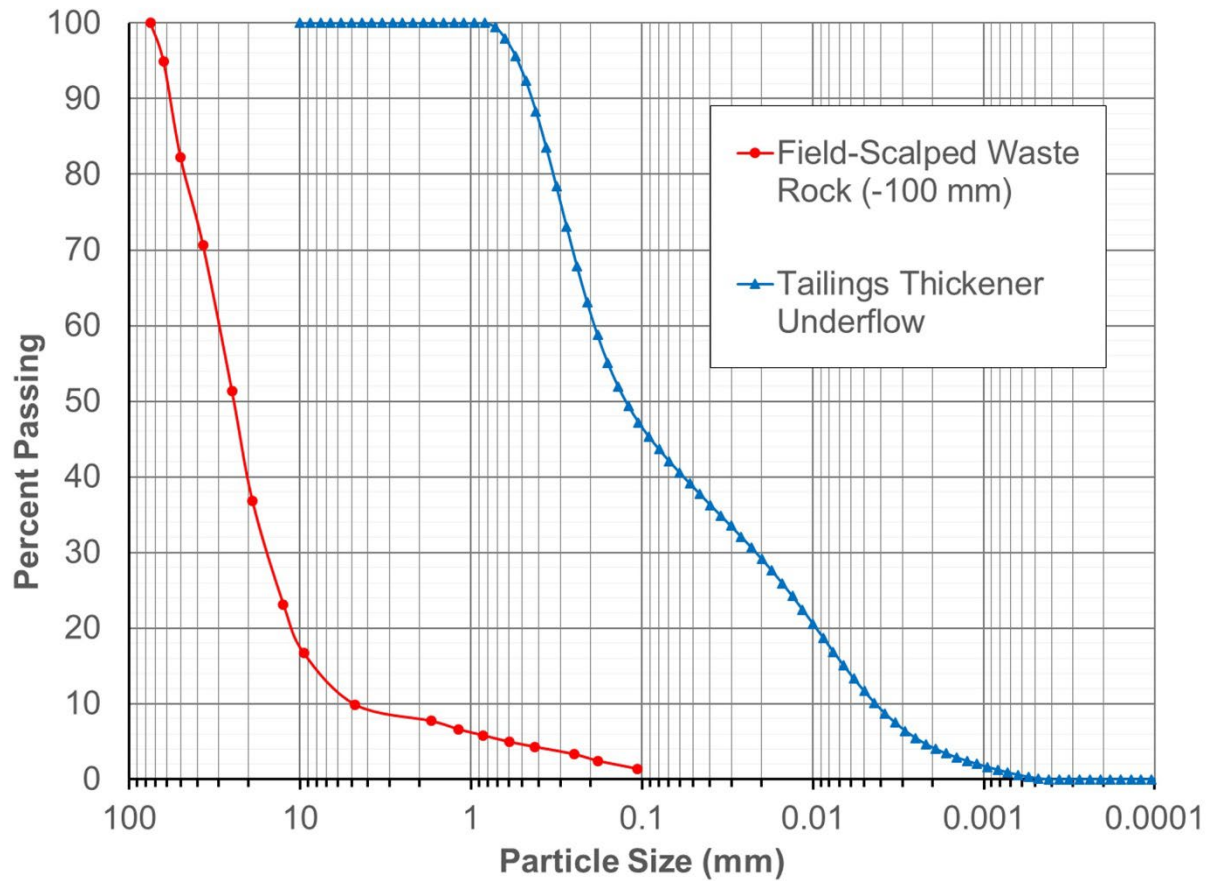


Figure 4-8: Particle size distribution

4.4.2.4 Specific gravity of solids

The specific gravity of solids were measured using a helium pycnometer. The results are given in Table 4-3.

Table 4-3 Specific gravity of soil solids for waste rock and filtered tailings

Material	G_s
Filtered tailings	2.756
Waste rock	2.726

4.4.2.5 Soil-water characteristic curve

To assist in evaluation of the influence of matric suction on the results, the soil water characteristic curve (SWCC) for the filtered tailings was measured. The SWCC was determined using the axis translation method (Fredlund and Rahardjo 1993) up to a maximum matric suction of 500 kPa using a Tempe cell, on a reconstituted tailings sample prepared to a void ratio of 0.56. A curve fit was performed using the Fredlund and Xing (1994) equation. The SWCC is shown in Figure 4-9 and curve fitting parameters are given in Table 4-4.

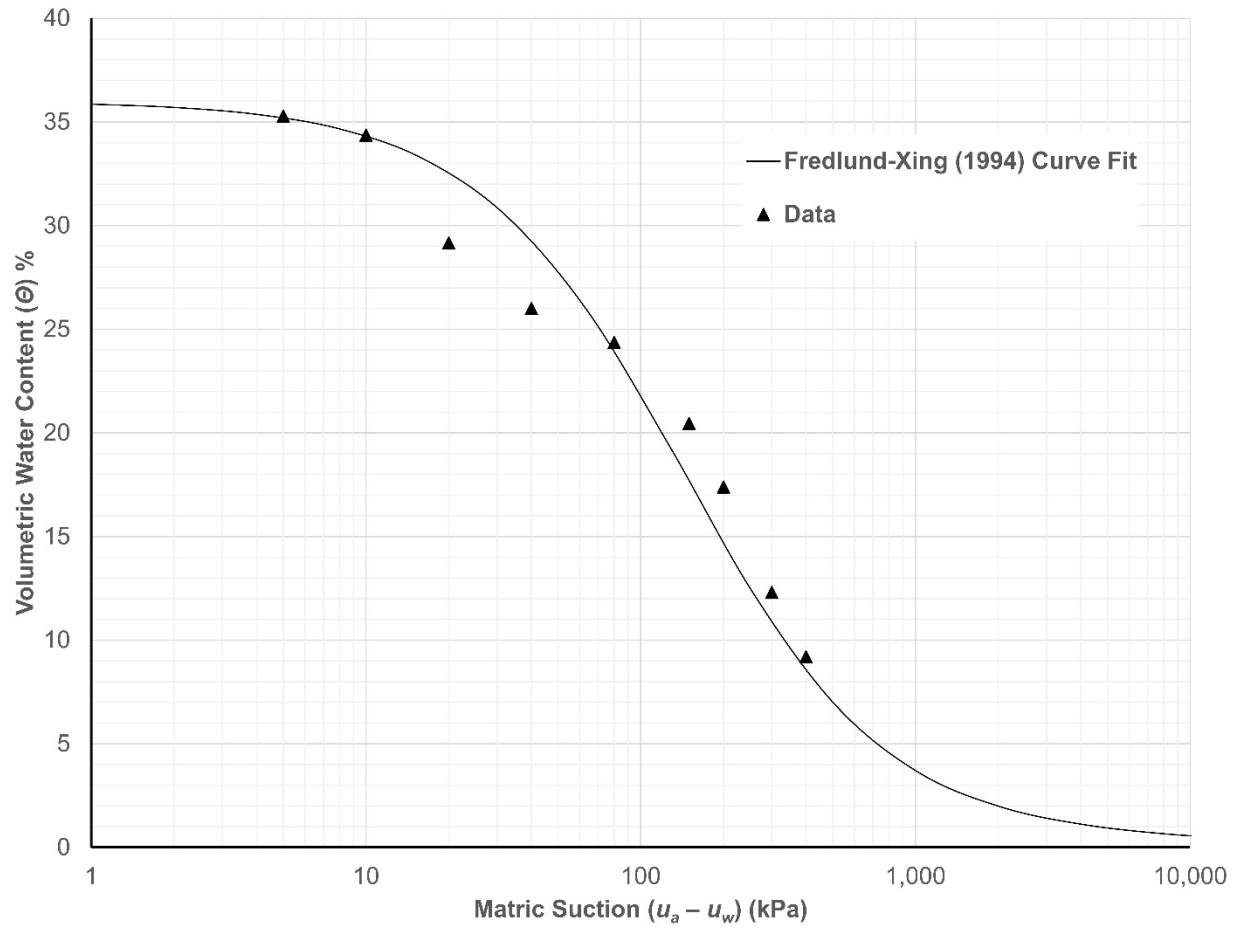


Figure 4-9: Soil water characteristic curve for filtered tailings

Table 4-4: Fredlund – Xing curve fitting parameters

Parameter	Value
a	150
n	1.1
m	2.6
ψ_r (kPa)	10,000
θ_s	0.36

4.4.3 Sample preparation and blending

4.4.3.1 Particle scalping

Due to the constraints imposed by the size of the equipment, blends were screened such that particles above a minimum size were removed. The choice of maximum particle size was critical. Given that the largest particles have the potential to significantly affect the results, it was necessary to pick the largest possible size that would produce repeatable results without excessive scale-effects.

The direct shear box is one of the oldest and most well-established methods of shear strength measurement in geotechnical practice; however, whilst several researchers have investigated scale effects and recommended minimum box dimensions, there is little consensus in the literature or standards. Roscoe (1970) reports that the width of the shear band is somewhere around $10D_{50}$. This finding has been generally backed up by other researchers who have studied the direct shear test in more detail; a good summary is given by Cerato and Lutenecker (2006). In addition to ensuring that the height of the box accommodates the full shear band width, the box must also be long enough to allow full shear band propagation and to minimise end effects. Scarpelli and Wood (1982) recommend a minimum box length of $100D_{50}$; Stone and Wood (1992) recommend $176D_{50}$. ASTM 3080-90 (2006) recommends minimum H/D_{max} and W/D_{max} ratios of 6. The maximum recommended particle size for the shear box dimensions used in this test are summarised in Table 4-5.

Table 4-5: Maximum recommended particle size parameters for a 300 x 300 x 200 mm direct shear test

Study / Standard	Parameter (mm)	
	D_{50}	D_{max}
Roscoe (1970)	20	-
Scarpelli and Wood (1982)	3	-
Stone and Wood (1992)	1.7	-
ASTM (2006)	-	33

For the purposes of comparison, D_{50} and D_{max} parameters for the blends tested are given in Table 4-6.

Table 4-6: D_{50} and D_{max} parameters for blends tested

Mix Ratio (R)	Parameter (mm)	
	D_{50}	D_{max}
Tailings	0.12	0.8
0.4	0.22	37
1	0.75	37
1.8	1.6	37
Waste rock	18	37

A maximum particle size of 37 mm was selected because it was the closest standard sieve size to the ASTM recommendation of 33 mm. It can be seen that all of the blends

meet the maximum D_{50} recommended by Roscoe (1970) to account for the width of the shear band. The blended materials also meet the maximum D_{50} recommended by other authors to minimise end effects. Consequently, the selection of 37 mm as the maximum particle size was considered to be valid because the strength of the blended materials was the primary focus of the study.

4.4.3.2 Effective mix ratios

The removal of large rock particles alters the mix ratio of a blend. Effective mix ratios for the blends above are given in Table 4-7.

Table 4-7: Effective (after scalping) mix ratios for blends produced

Maximum particle size (mm)	Dry mix ratio (<i>R</i>)	Effective dry mix ratio	Predicted moisture content (%)	Measured moisture content (%)
37	0.4	0.28	15.5	15.9
	1	0.71	12.2	13.8
	1.8	1.27	9.7	12.3
	1	0.37	14.6	15.2
	1.8	0.66	12.5	14.2

It should be noted that the scalped blends are generally wetter than predicted, and this effect increases with increasing rock content. This may be because the majority of the water in the waste rock is contained in the finer fraction.

4.4.3.3 Particle size distributions of blended materials

The calculated particle size distributions of the blended materials are given in Figure 4-10.

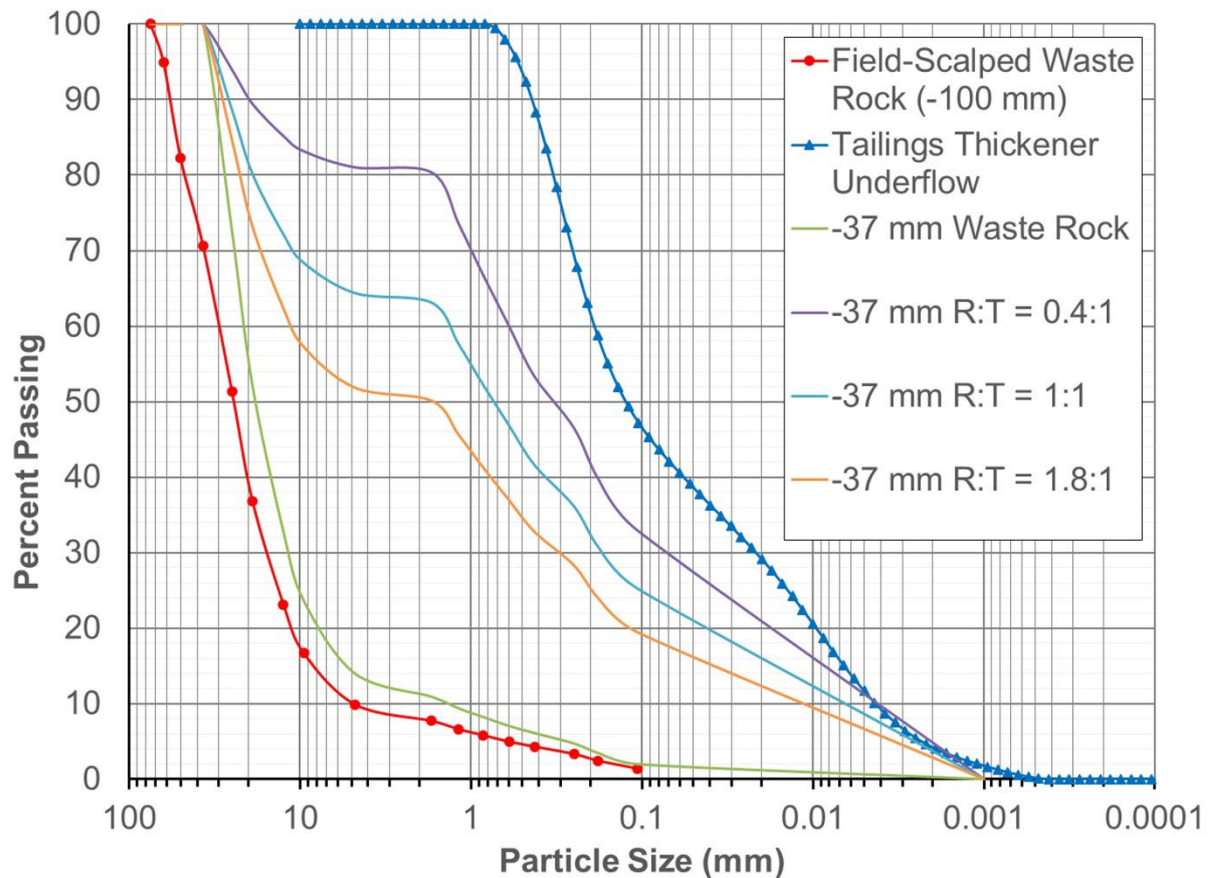


Figure 4-10: Particle size distributions for blended materials scalped to 37 mm

4.4.3.4 Blending procedure

The objective of the blending procedure was to combine the waste rock and filtered tailings into a perfectly mixed, homogenous material. Whilst it is recognised that this is unlikely to be representative of field conditions, perfect blending was targeted to produce good quality, repeatable results at the laboratory scale.

Blending of the materials was carried out at the University of Alberta. To minimise drying out during transit, the materials were placed in sealed pails immediately upon collection at the site. However, to account for any evaporative losses that did occur, samples were taken of the materials upon arrival, and distilled water was added during the blending process to bring the materials' moisture content up to the values recorded during sample collection, given in Table 4-1.

The materials were blended using a concrete mixer. The blending apparatus is shown in Figure 4-11. A blend with a mix ratio of 1 is shown in Figure 4-12.



Figure 4-11: Blending apparatus



Figure 4-12: 1:1 rock to tailings blend scalped to 37 mm

4.5 Method

The direct shear test is widely used in geotechnical practice for the determination of the shear strength parameters of granular materials (ASTM D3080). An advantage of this test is that the shear box can readily be scaled up to permit testing on large grained materials. The selection of a test method that allows the largest possible particle size is critical; it has been shown that the removal of large particles can significantly affect the shear strength parameters measured in the direct shear test (Xu, Williams et al. 2017). Large scale shear boxes up to 300 x 300 mm are widely available and have been used for measuring the shear strength of rockfills, coarse aggregates and geomembranes (Bauer and Zhao 1993, Alfaro, Miura et al. 1995, Yu, Ji et al. 2006).

Large-scale direct shear tests were carried out at the University of Queensland using a shear box manufactured by Wille Geotechnik. The box dimensions were 300 x 300 x 205 mm. Tests were carried out on filtered tailings alone, waste rock alone and on mix ratios of 0.4, 1 and 1.8. All materials were scalped to -37 mm, as described above. Each material was tested at vertical confining stresses of 250, 500 and 1000 kPa. Confining stresses were applied in one load step at a rate of 100 kPa/minute, using an electromechanical loading piston. The materials were tested at the blended water contents. The samples were sheared out at a strain rate of 0.1 mm/minute to ensure fully drained conditions. The shear force was measured throughout the test using a load cell. The vertical deformation was measured throughout the consolidation and shearing phases of the test using four linear variable differential transformers (LVDTs) mounted on the corners of the box. The reading of all four settlement gauges was averaged, and this is recorded as settlement. Figure 4-13 shows the filling of the shear box containing a sample with a mix ratio of 0.4.



Figure 4-13: Large scale direct shear box containing an $R = 0.4$ sample

The moisture content was taken prior to filling and after shearing. The total mass of material placed in each test was recorded, and the initial sample height was measured, enabling the calculation of density and phase relationships at initial and final conditions. Figure 4-14 shows the collection of moisture samples from the sheared material. To assess particle breakage effects, the particle size distributions were taken after shearing the waste rock samples, using the sieve method.



Figure 4-14: Collection of moisture sample from sheared material

4.6 Results

4.6.1 Summary

The peak shear stress measured during each test is given in Table 4-1 and shown in Figure 4-15. Figure 4-15 is annotated with lines representing friction angles of 35, 40 and 45 degrees.

Table 4-8: Peak shear stress

Normal Stress (kPa)	Peak shear stress (kPa)				
	Filtered tailings	R = 0.4 blend	R = 1 blend	R = 1.8 blend	Waste rock (-37 mm)
250	171.2	212.2	230.9	223.6	292.6
500	351.7	393.2	439.1	442.7	554.3
1000	712.1	805.5	851.3	850.5	797.4

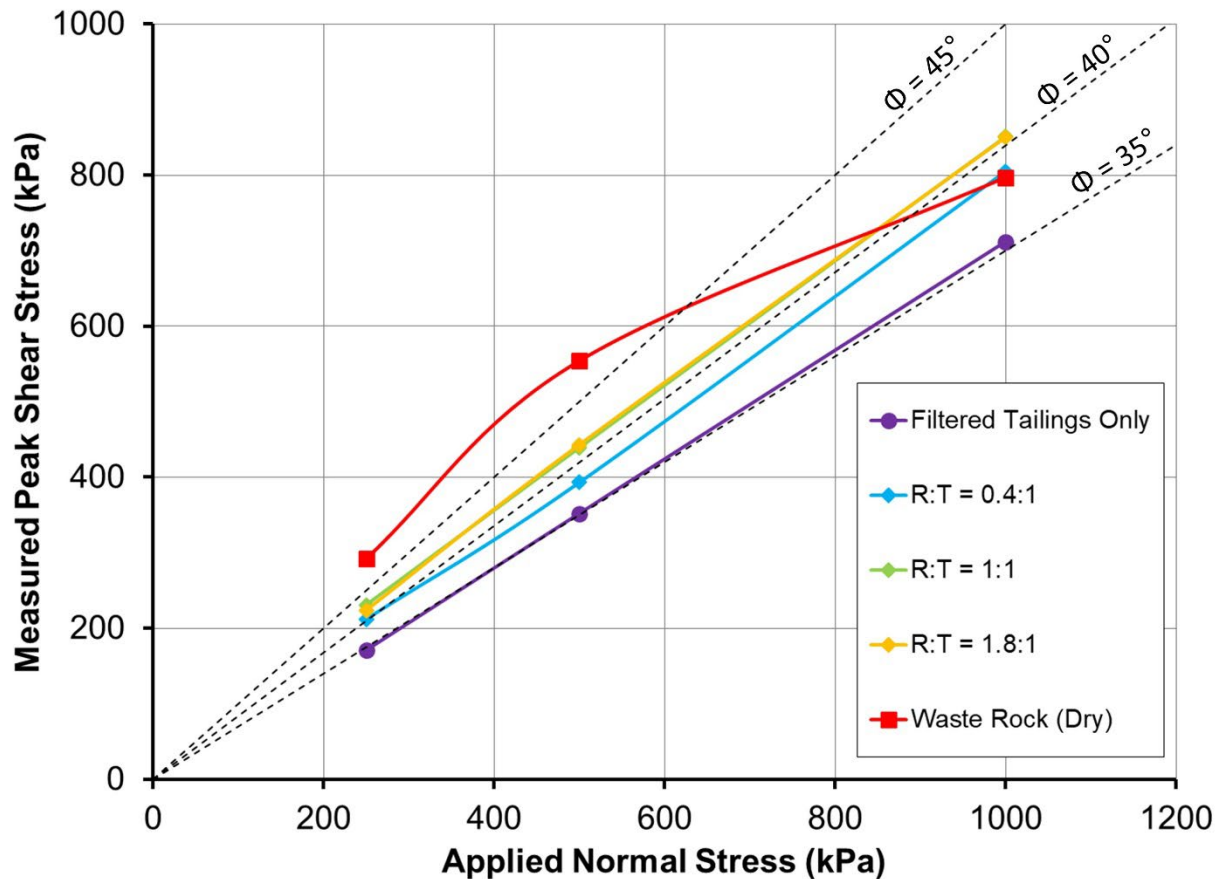


Figure 4-15: Shear box test results summary

In general terms, the results show that the addition of rock to filtered tailings results in increased shear strength; waste rock and filtered tailings blends are always stronger than tailings alone. The shear strength appears to increase with higher rock content up to a limiting value of around 1:1. At a confining stress of 1 MPa, blended materials are stronger than rock alone. Calculated friction angles based upon linear regression are presented in Table 4-9.

Table 4-9: Friction angles

Material	ϕ' (°)
Filtered tailings	36
0.4:1 R:T blend	39
1:1 R:T blend	40
1.8:1 R:T blend	40
Waste rock	33

4.6.2 Shear stress – strain behaviour

Figure 4-16, Figure 4-17 and Figure 4-18 show the shear stress and vertical settlement plotted against horizontal displacement for all tests at confining stresses of 250, 500 and 1000 kPa, respectively. The shear stress is represented by the solid lines, and settlement is represented by the dashed lines and is plotted on the secondary axis. Due to the fact that there was some variation in the heights of the samples at the start of shearing, settlement is presented in terms of % strain as opposed to absolute values. This allows better comparison of the magnitude of settlement between different mix ratios. As

indicated on the charts, during the tests on the $R = 1.8$ sample at 250 and 500 kPa, the vertical confining stress was briefly interrupted during the test due to mechanical issues. This is not believed to have had significant impact on the results.

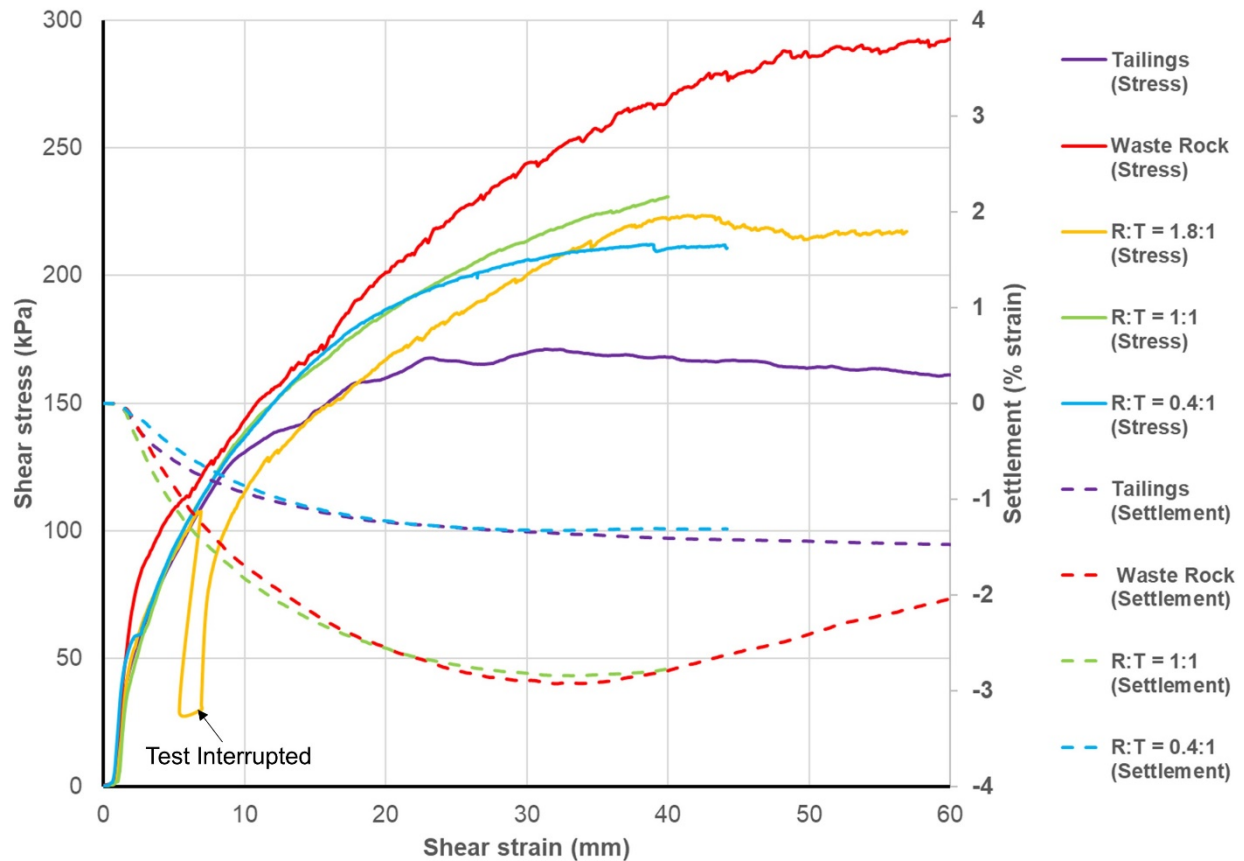


Figure 4-16: Direct shear test results at 250 kPa confining stress

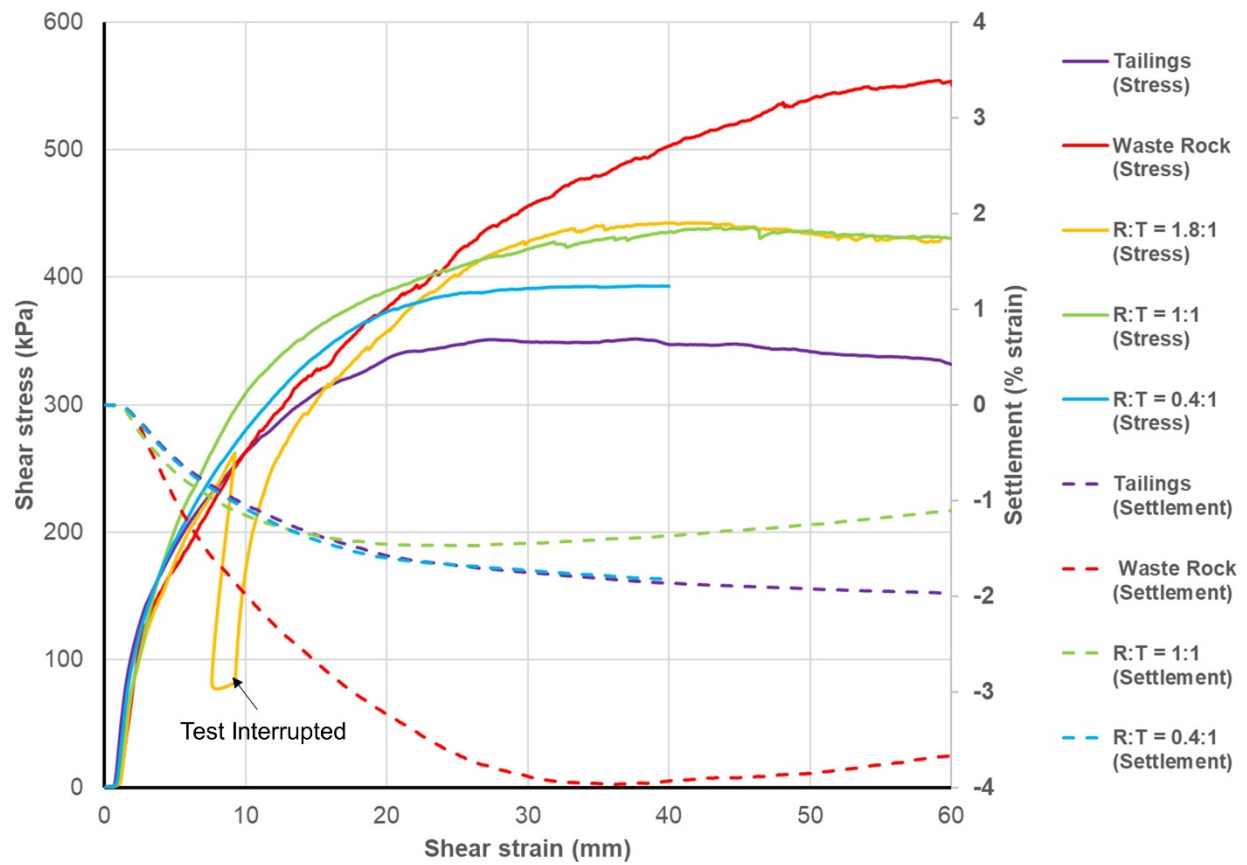


Figure 4-17: Direct shear test results at 500 kPa confining stress

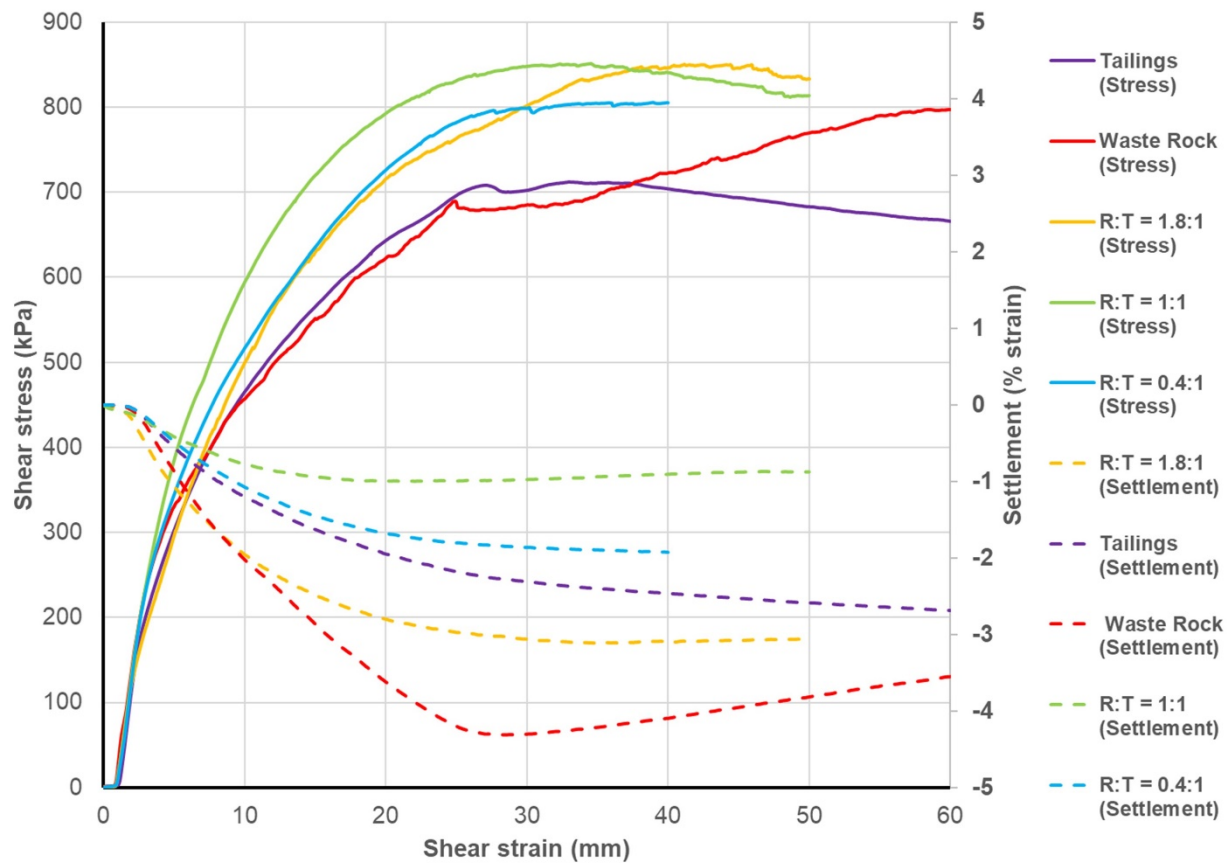


Figure 4-18: Direct shear test results at 1000 kPa confining stress

All materials showed net contractive behaviour over the range of stresses tested. However, blends with higher rock content show a phase transition point where maximum settlement is reached, with dilative behaviour after. This suggests that the blends with higher rock content have some dilation potential which could potentially reduce excess pore pressure during undrained shearing. Waste rock generally shows greater settlement during shearing than tailings alone or blended material. There appears to be no discernable correlation between the mix ratio and magnitude of settlement. Samples with higher rock content appear to reach failure at higher strains. There appears to be an interruption in the stress – strain curve for the pure rock test at a normal stress of 1000

kPa which occurs at approximately 25 mm shear strain; this may explain the lower than expected peak shear stress recorded for this test.

4.6.3 Moisture content and density

The moisture content and density parameters are given in Table 4-10 for samples prior to consolidation, samples post consolidation but prior to shearing, and samples after shearing. The gravimetric moisture contents were measured from sub-samples taken during filling and from the shear plane, as shown in Figure 4-14. The void ratio, dry density and degree of saturation were calculated, based upon the total mass of the sample at the start of the test and sample dimensions. Due to an error in the laboratory, the final moisture content for the $R = 0.4$ sample at 250 kPa was not recorded.

Table 4-10: Moisture content and density of direct shear samples

Mix ratio	Confining stress (kPa)	Pre-consolidation				Consolidated pre-shearing		Post shearing			
		e	w (%)	ρ_d (g/cm ³)	S_r (%)	e	ρ_d (g/cm ³)	e	w (%)	ρ_d (g/cm ³)	S_r (%)
R=0.4	250	0.83	16.0	1.49	52.8	0.79	1.52	0.39	~	1.96	~
	500	0.83	16.4	1.50	54.1	0.56	1.75	0.53	15.5	1.79	80.3
	1000	0.65	15.5	1.66	65.4	0.41	1.94	0.37	14.0	1.99	102
R=1	250	0.63	13.4	1.67	57.5	0.46	1.87	0.42	12.7	1.92	82.0
	500	0.46	15.0	1.87	89.8	0.35	2.02	0.33	12.1	2.05	98.7
	1000	0.60	13.1	1.70	59.4	0.58	1.73	0.56	11.0	1.75	54.0
R=1.8	250	0.56	11.3	1.75	55.4	0.45	1.88	0.41	10.9	1.94	72.9
	500	0.66	12.7	1.64	52.7	0.41	1.93	0.38	10.1	1.97	72.1
	1000	0.73	12.9	1.58	48.3	0.38	1.98	0.32	10.6	2.07	89.5
Pure Rock	250	0.89	~	1.44	~	0.77	1.54	0.73	~	1.54	~
	500	0.77	~	1.54	~	0.60	1.70	0.55	~	1.70	~
	1000	0.92	~	1.42	~	0.59	1.72	0.53	~	1.72	~
Pure Tails	250	0.76	18.4	1.56	66.5	0.56	1.75	0.53	12.4	1.56	64.1
	500	0.68	19.0	1.62	75.9	0.47	1.86	0.43	16.6	1.62	104
	1000	0.72	17.3	1.58	65.4	0.44	1.90	0.39	14.8	1.58	102

The results show some variability in the samples. In particular, the R=1 sample consolidated to 500 kPa has an unusually high dry density. This is believed to be due to the higher moisture content of that sample, which was more favourable for compaction. It is not clear what caused the variability in moisture content in the samples. Possible explanations include the re-distribution of moisture during transit (for example, flow of moisture under gravity to the bottom of a bucket) or incomplete mixing. Errors in the calculation of density could also occur if the moisture content was not representative of the whole sample.

4.6.4 Particle size distributions

The particle size distributions of the sheared waste rock samples are given in Figure 4-19.

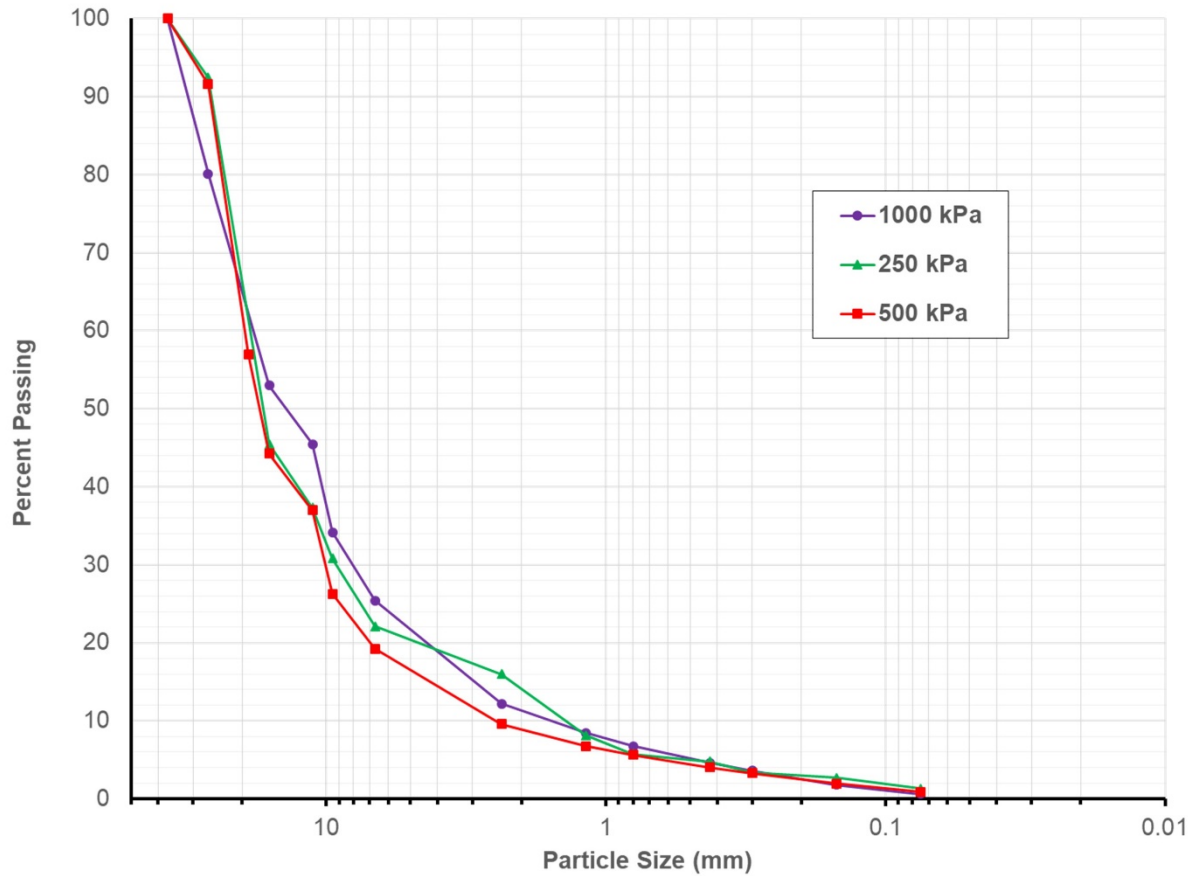


Figure 4-19 Particle size distributions of sheared waste rock samples

The results are inconclusive – observed variation in the curves is less than the natural variability that would be expected between samples. It should be noted that the curves here represent the entire sample and are not restricted to the immediate vicinity of the shear plane on the interface between the two halves of the box. Consequently, breakage on the shear plane may be more evident in reality than indicated here.

4.7 Discussion

The results show that filtered tailings and waste rock blends behave as predominantly frictional materials, with shear strength increasing as rock content increases. Blends with

a rock to tailings ratio (R) of 1.8 and 1 had approximate friction angle of 40° , the $R=0.4$ blend had a friction angle of approximately 38° and filtered tailings alone had a friction angle of approximately 35° . The strength of the rock alone was found to be reduced at high stress. This is generally consistent with the observed behaviour for rockfills (Leps 1970), which are typically considered to behave as frictional materials with non-linear strength functions due to increasing particle breakage effects at higher stresses. However, 1000 kPa would typically be considered a low stress for particle breakage to occur; this suggests that the test result is an anomaly, as supported by the stress – strain curve. Blends of waste rock and filtered tailings may also be stronger than rock alone at high stresses. This is because the tailings particles occupying the void space between the rock particles reduce the stresses at the clast to clast contacts and therefore reduce breakage of rock particles.

Borja Castillo (2019) performed 150 mm tri-axial tests on “Geowaste” (filtered tailings and waste rock blend sourced from the same mine as the materials tested in this research) with a mix ratio R of 1.2 up to a confining stress of 500 kPa. The tangent friction angle was reported to be 32° , with the secant friction angle increasing with confining stress. This is significantly lower than this study, which suggests that the larger rock particles have a very significant influence.

Figure 4-20 shows the shear tests (after consolidation but prior to shearing) plotted on the material property boundary diagram introduced in Section 2.7.

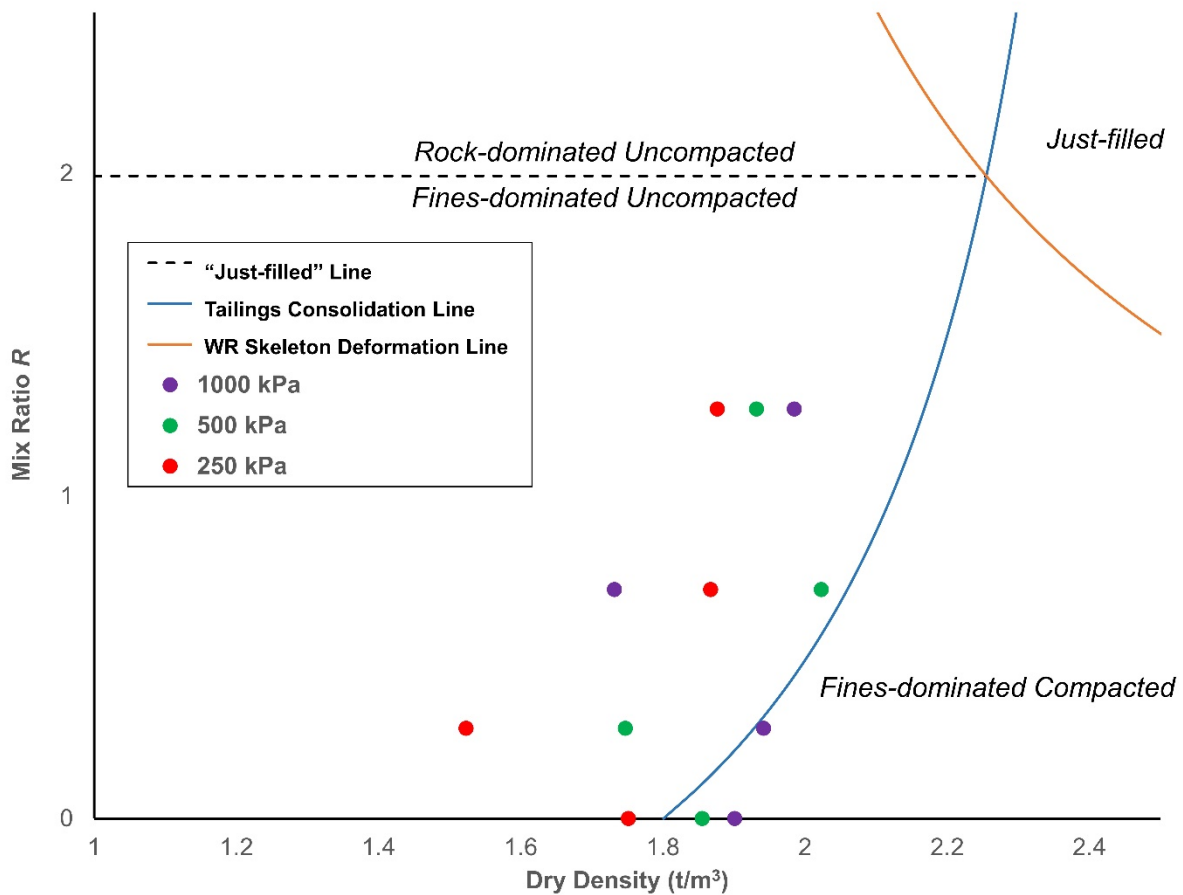


Figure 4-20: Direct shear tests plotted on property boundary chart

Figure 4-20 shows that all of the mix ratios tested fall well within the fines-dominated or “floating” condition, and the majority of the tests fall within the “fines-dominated uncompacted” blend configuration. This shows that “floating” rock particles have a significant influence on the shear strength of a blend, even if the blend does not have a continuous rock phase in clast-to-clast contact throughout. This is understandable, when one considers that even if the compression behaviour of the blend is dominated by fines, the influence it may have on the shear behaviour is likely to be significant, for the shear band is still forced to take an increasingly tortuous path around and through the rock particles, even if the rock particles are not initially in clast to clast contact.

Another noteworthy observation from Figure 4-20 is that even at a normal stress of 1000 kPa (the highest tested here, equating to a stack height of approximately 56 m), blended materials that have been placed loose and self-weight compacted are likely to still be in the unsaturated condition.

Given that the sample is initially unsaturated, it is possible that matric suction has some influence on the shear strength. It is generally accepted that negative pore pressure can increase the shear resistance of soils (Bishop and Blight 1963, Fredlund, Morgenstern and Widger 1978). Table 4-10 presents calculated degree of saturation values for the tests. Considerable scatter is seen in the data, which may be due to error in calculation of the global properties of the sample from a small sub-sample. Nevertheless, in the majority of cases the tailings alone are shown to be fully saturated at the end of the test. The materials tested consist of a heterogenous blend of rock particles, filtered tailings lumps and large air voids. The tailings lumps are understood to be generally at or close to 100% saturation. Figure 4-9 shows the SWCC for the tailings sample; the air entry value was shown to be around 10 kPa. This implies that suction within the fine tailings is generally low (<10 kPa) and unlikely to have a significant influence on the shear strength. Low global degree of saturation measured for the sample does not necessarily imply a high suction, due to heterogenous nature of the sample.

To investigate the possible influence of matric suction on the results, one of the tests presented in this chapter ($R=1$ blend at 500 kPa confining stress) was repeated using a wet test. To ensure full saturation, the sample was placed in the shear box and then

immersed in water for 3 days prior to testing. A comparison between the results of the wet test and the unsaturated test is presented in Figure 4-21.

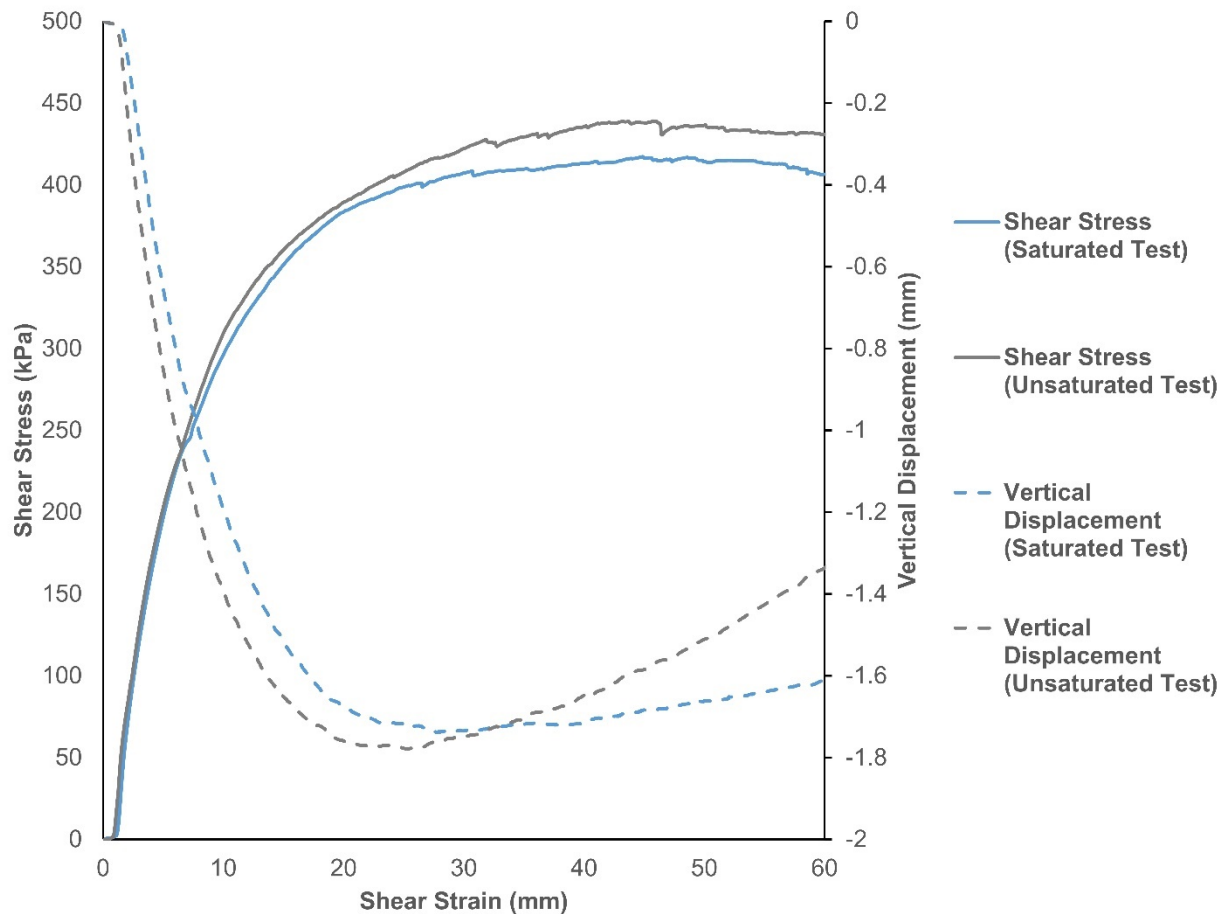


Figure 4-21: Comparison between saturated and unsaturated direct shear box test results ($R=1$ blend, 500 kPa confining stress)

The results show generally the same behaviour between the two materials. The measured peak shear stress of the unsaturated samples is 22 kPa greater than that of the wet sample, which approximates to an increase in friction angle of 1.4° .

4.8 Conclusions

The results show that the addition of even a relatively small amount of rock to a filtered tailings dry stack can significantly increase the shear strength. The shear strength increases with increasing the mix ratio up to a limiting value of around 1:1 by dry mass. At higher stresses, blends of rock and filtered tailings have a higher shear strength than rock alone, because the tailings prevent the breakage of rock particles. The stress above which this occurs will depend upon the strength of the rock and can easily be determined by testing on the rock alone.

References

- Alfaro, M., N. Miura and D. Bergado (1995). "Soil-Geogrid Reinforcement Interaction by Pullout and Direct Shear Tests."
- Bauer, G. and Y. Zhao (1993). "Shear Strength Tests for Coarse Granular Backfill and Reinforced Soils."
- BISHOP, A. W., and BLIGHT, G. E. 1963. Some aspects of effective stress in saturated and unsaturated soils. *Geotechnique*, 13, pp. 177-197.
- Borja Castillo, R. N. (2019). UNDRAINED SHEAR BEHAVIOUR AND CRITICAL STATE ANALYSIS OF MIXED MINE WASTE ROCK AND TAILINGS, Colorado State University. Libraries.
- Brawner, C. and J. Argall, GA (1978). Concepts and experience for subsurface storage of tailings. Proceedings of the 2nd International Tailings Symposium, Tailings Disposal Today, Denver, Colo.
- Cerato, A. and A. Lutenecker (2006). "Specimen Size and Scale Effects of Direct Shear Box Tests of Sands."
- D. G. Fredlund, N. R. Morgenstern, and R. A. Widger. (1978) The shear strength of unsaturated soils. *Canadian Geotechnical Journal*. 15(3): 313-321.
- Habte, K. and K. Bocking (2017). Co-disposal practice in mine waste management. Tailings and Mine Waste '17. Banff, Alberta, Canada.
- Hawley, M. and J. Cunniff (2017). Guidelines for Mine Waste Dump and Stockpile Design, CSIRO Publishing.
- Jehring, M. M. and C. A. Bareither (2016). "Tailings composition effects on shear strength behaviour of co-mixed mine waste rock and tailings." *Acta Geotechnica* **11**(5): 1147-1166.
- Khalili, A., D. Wijewickreme and G. W. Wilson (2010). "Mechanical response of highly gap-graded mixtures of waste rock and tailings. Part I: Monotonic shear response." *Canadian Geotechnical Journal* **47**(5): 552-565.
- Leps, T. M. (1970). "Review of shearing strength of rockfill." *Journal of Soil Mechanics & Foundations Div.*
- Lord, E. R. F. and B. A. A. Isaac (1989). "Geotechnical investigations of dredged overburden at the Syncrude oil sand mine in northern Alberta, Canada." *Canadian Geotechnical Journal* **26**(1): 132-153.

Malgesini, M., L. Aubone, R. Hunsaker and W. Boyd (2017). Tailings and Mine Waste 2017. Keystone, CO.

Morgenstern, N., S. Vick and D. Van Zyl (2015). "Report on Mount Polley tailings storage facility breach." Report of independent expert engineering investigation and review panel. Prepared on behalf of the Government of British Columbia and the Williams Lake and Soda Creek Indian Bands.

Morgerstern, N., S. Vick and B. Watts (2016). Fundão Tailings Dam Review Panel Report on the Immediate Causes of the Failure of the Fundão Dam.

Robertson, P., L. de Melo, D. Williams and G. Wilson (2019). Report of The Expert Panel on the Technical Causes of the Failure of Feijão Dam 1.

Roscoe, K. H. (1970). "The influence of strains in soil mechanics." Geotechnique **20**(2): 129-170.

Scarpelli, G. and D. M. Wood (1982). "Experimental observations of shear patterns in direct shear tests." NASA STI/Recon Technical Report N **83**.

Stone, K. J. and D. M. Wood (1992). "Effects of dilatancy and particle size observed in model tests on sand." Soils and Foundations **32**(4): 43-57.

Thevanayagam, S. (2007). "Intergrain contact density indices for granular mixes—I: Framework." Earthquake engineering and engineering vibration **6**(2): 123.

Vick, S. G. (1990). Planning, design, and analysis of tailings dams, BiTech.

Wickland, B. and S. Longo (2017). Mine waste case examples of stacked tailings and co-disposal. Tailings and Mine Waste '17. Banff, Alberta, Canada.

Wickland, B. E. (2006). Volume change and permeability of mixtures of waste rock and fine tailings, University of British Columbia.

Wijewickreme, D., A. Khalili and G. W. Wilson (2010). "Mechanical response of highly gap-graded mixtures of waste rock and tailings. Part II: Undrained cyclic and post-cyclic shear response." Canadian Geotechnical Journal **47**(5): 566-582.

Williams, D. (1997). Effectiveness of co-disposing coal washery wastes. Proceedings of the 4th International Conference on Tailings and Mine Waste.

Xu, Y., D. J. Williams and M. Serati (2017). Effect of Scalping on Shear Strength of Aggregate. 51st U.S. Rock Mechanics/Geomechanics Symposium. San Francisco, California, USA, American Rock Mechanics Association.

Yu, X., S. Ji and K. D. Janoyan (2006). "Direct Shear Testing of Rockfill Material." Soil and Rock Behaviour and Modeling.

5 CO-DISPOSAL IN THE OIL SANDS: GEOTECHNICAL TESTING ON CLEARWATER SHALE AND FLUID FINE TAILINGS BLENDS

5.1 Introduction

The Athabasca oil sands in Northern Alberta present significant tailings management challenges; most notably the very large volumes of fine tailings that have thus far proven very resistant to dewatering by normal methods. As of 2016, the industry as a whole managed an inventory of Fluid Fine Tailings (FFT), estimated to be 1.13 billion m³ (AER 2016). Unlike conventional metal mine tailings, which can be effectively dewatered by filtration, the dewatering of FFT remains a significant, largely unresolved challenge and represents a barrier to reclamation and closure. Whilst most approaches for dewatering FFT currently in use or under development aim to increase the solids content of the FFT by removing water, co-disposal with overburden increases the solids content by adding solids. This has great potential because of the high water demand of the clay shale overburden material found in the region. Upon mixing, water transferred from the FFT to the shale, promoting rapid dewatering and strength gain. Co-disposal is perhaps the only method currently under development that has demonstrated the potential to produce “dry stacks” of oil sand tailings quickly (Mikula, Wang et al. 2016, Wang, Cleminson et al. 2017), although it has yet to be implemented commercially at a large scale. Whilst successful stacking of clay shale – FFT blends has been demonstrated, the geotechnical properties of the material are still not well understood. There is a particular need to

understand the compression behaviour and the build-up and dissipation of excess pore pressures during stacking.

5.2 Background

5.2.1 *Geological background*

Published works on co-disposal in the oil sands industry are focussed predominately on mixing fine tailings with overburden material from the Clearwater formation. The Clearwater formation is the predominant deposit overlying the McMurray (oil sand) formation, in the main surface minable region on the West side of the Athabasca River. It is well described and characterised in the literature (Isaac, Dusseault et al. 1982, O'Donnell and Jodrey 1984, Shafie Zadeh and Chalaturnyk 2015); a brief summary is given here. It consists mainly of silts (around 50%), marine clay shales (around 44%) and some beach and shoreface sands (around 6%), deposited in a mixed marine and continental environment. The clay fraction is mainly composed of illite and smectite. The Clearwater formation on Syncrude's lease was found to consist of seven sub-layers, each readily identifiable by a distinct geophysical response. These are informally identified by Syncrude as Kcw, a, b, c, d, e and f. During the process of the field trials, Kca, Kcb and Kcc were identified by Syncrude as those most suitable for co-disposal (Wang, Cleminson et al. 2017).

It is noteworthy that the in-situ moisture content of the Clearwater formation is generally at or below the plastic limit. This is significant because it implies that the shale has a high water demand; upon mixing it will draw the water out of the tailings, causing rapid dewatering and strength gain.

5.2.2 Previous studies on Clearwater shale – FFT blends

It is interesting to note that some of the earliest published work on the co-disposal of mine wastes originates in the oil sands. Several studies were carried out in the 1980s to investigate the properties of clay shale overburden lumps blended with fluid tailings. The focus of the study was assessing the feasibility of building hydraulically placed overburden dumps rather than on tailings disposal, which at the time was not given the same priority it is today. However, the early work is worthy of re-examination in this context.

During the summers of 1985 and 1986, field scale trials were conducted on Syncrude's lease to assess the feasibility of creating stable, hydraulically placed overburden dumps using dredging techniques (Lord and Isaac 1989). To do this, 12,100 m³ of Pleistocene lacustrine clay and 13,600 m³ of Kcc Clearwater shale, considered representative of the overburden materials found on the lease at the time, were dredged and deposited into test cells ranging from 1.5 to 6 m deep. The main focus was to determine the geotechnical properties of the deposits. Results from the Clearwater shale tests are of most concern because that is the predominant overburden material at present and in the future. Both tailings pond water and FFT were used as transport fluids. The FFT had a solids content of approximately 30% and a bitumen content ranging between 2 and 3%. The final deposits had solids contents around 75%.

Density tests performed immediately upon deposition showed many air voids. However, tests performed after 20 days showed almost zero air voids with saturation in excess of 97%; this implies that the initial macro porosity was sealed off by the swelling of the shale

lumps. Unfortunately, no settlement data was published since all of the instrumentation was destroyed during deposition. The undrained shear strength was found to vary between 6 and 35 kPa; the effective stress parameters were in the range of $\phi'=20^{\circ}$ - 27° $c'=0$ -10 kPa. The dissipation of excess pore pressure in response to surcharge loading was observed to be slow; only 10% dissipation occurred in 100 days, irrespective of the transport fluid used.

Dusseault and Ash (1987) carried out laboratory tests on shale – FFT mixtures. Swedish drop cone tests on a 50/50 volumetric mix at 24 and 72 hours gave average undrained shear strengths of 30 and 33 kPa, respectively. They also carried out “Nylon stocking” tests to study the moisture transfer process; shale lumps were lowered into an excess of tailings sludge for a specified time and then re-weighed. It was found that a steady state was reached in two to four days with a typical mass increase of 20%. To put this result in some perspective, if a 50/50 volumetric mix is assumed, and the same amount of swelling of the shale lumps is achieved, this would equate to an increase in the solids content of the sludge from 30 to 55%, corresponding to a significant amount of dewatering. Mimura (1990) investigated the shear strength of the Clearwater shale “lump” structure, carrying out 42 consolidated undrained (CU) tri-axial tests using a range of mixing fluids, confining stresses and “softening” durations. All of the tri-axial tests showed high cohesion intercepts (up to 62 kPa) and low friction angles (less than 8°). High positive pressures were measured during shearing, although unconsolidated shale lumps may have developed negative pressures. The mixing fluid had no significant impact on the strength, but mixes made with FFT were observed to have very slow consolidation times because of the low permeability. Six “softening” tests were also carried out, where clay lumps were

placed in a consolidation cell, which was topped up with pond water. The objective was to determine the vertical confining stress at which the clay lump structure was no longer free draining. It was found that the lump structure deformed to a limiting void ratio of around 0.7 at around 60 kPa.

More recently, in 2015, Syncrude constructed self-supporting, trafficable test piles of blended FFT and Clearwater overburden, using conveyors for blending and stacking (Mikula, Wang et al. 2016, Wang, Cleminson et al. 2017). No data has been published relating to the geotechnical performance of the piles. However, the supporting patent contains laboratory test data on Clearwater shale – FFT blends at a range of mix ratios and shale lithologies. The mix ratios used were 0.2 : 1, 0.4 : 1 and 0.6 : 1 FFT : shale based on bulk volume; the lithologies used were Kca, Kcb, Kcc, Kcw and a composite sample consisting of 0.5 : 0.3 : 0.2 Kca : Kcb : Kcc. Undrained shear strength was measured at five time intervals (1, 2, 3, 7 and 14 days) after mixing, and testing was repeated for fine and coarse shale lumps. It was found that undrained strength increased with increasing shale content and that generally Kca had higher strength than the other shale types. The Kca sample at the highest mix ratio achieved an undrained strength of 33 kPa with fine lumps and 22 kPa with coarse lumps. All Kca samples tested at all mix ratios were above 5 kPa. The shale lump size had a mixed effect on shear strength: a notable increase was observed for Kca at higher mix ratios; otherwise, no great difference was observed. Contrary to expectation, no significant change in shear strength with time was observed for the time intervals tested. It is likely that the majority of the shear strength gain occurred in the first 24 hours, and if smaller time steps had been selected, strength gain with time would have been observed. Additional tests were carried out on compacted

samples; compaction was found to increase the undrained shear in all cases for the highest mix ratio (0.2) and for the Kca blends at all mix ratios. In addition to shear strength testing, testing using a variety of methods was carried out to evaluate the rate of moisture transfer from FFT to shale and to measure the suction. It was found that the suction generally correlated well to the undrained shear strength; suction increased with solids content, and suction increased with respect to time up to around 24 hours, whereupon it remains steady.

5.3 Mix design theory for Clearwater Shale – FFT blends

This section discusses the application of the co-disposal mix design theory to the special case of Clearwater shale – FFT blends used for co-disposal of oil sands tailings and extends that theory where applicable. The same principles may be applied to other co-disposal operations where the waste rock or overburden materials have a fines content or are prone to weathering.

5.3.1 *Blend structure and configuration*

In practice, blends of shale overburden and FFT are not perfectly mixed but consist of “lumps” of shale with FFT and/or air occupying the void space between lumps. The same approach used by Wickland, Wilson et al. (2006) may be applied here, by likening the waste rock particles to shale “lumps”. This is shown schematically in Figure 5-1.

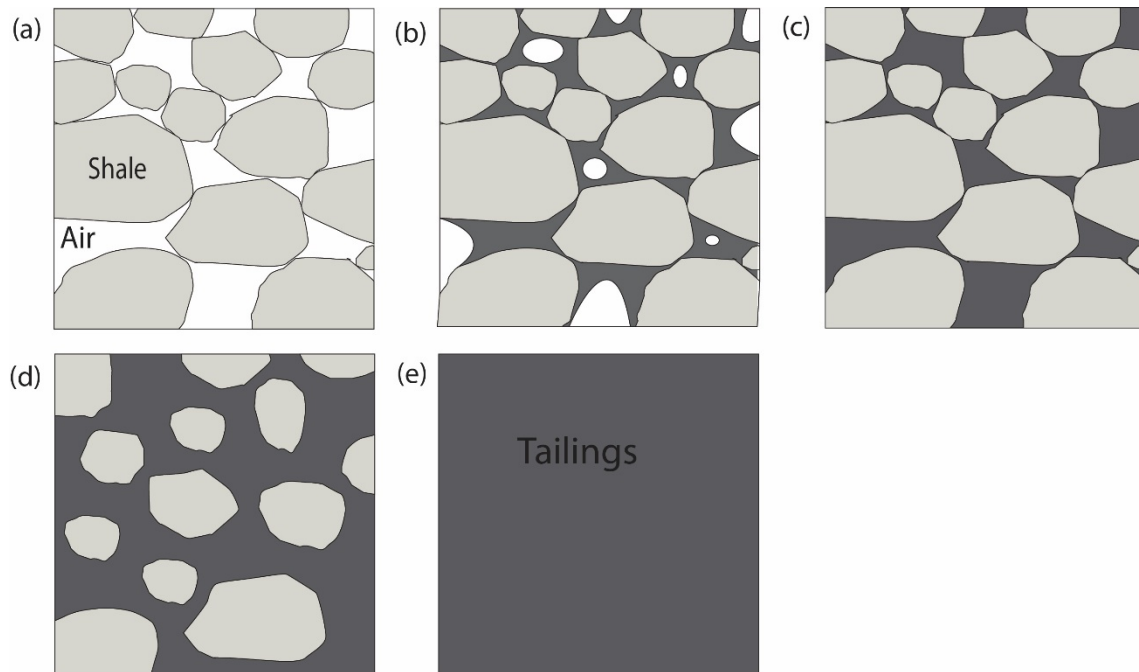


Figure 5-1: Particle structure configurations for Clearwater shale - FFT blends: (a) Shale lumps only; (b) Shale lump matrix partly filled with FFT; (c) "Just filled" condition; (d) "Floating" shale lumps in an FFT matrix; (e) FFT only

At the time of blending, the shale lumps are unsaturated and contain shale solids, porewater, and air voids. The internal structure of a shale lump is shown schematically in Figure 5-2.

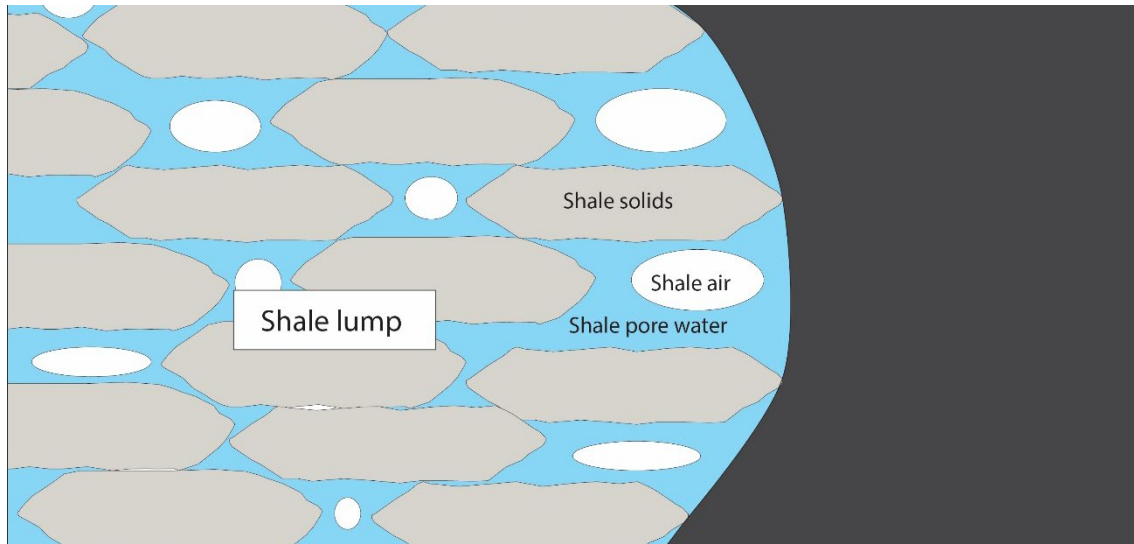


Figure 5-2: Schematic showing internal structure of shale “lump”

It is convenient and often reasonable to assume that the tailings are fully saturated. However, experience has shown that the tailings often contain entrained air bubbles; this is particularly true in the case of centrifuge cakes. This may be considered a separate air phase in the conceptual model. In summary, three air phases are proposed as follows: air in the unsaturated shale pores, occluded air in the fluid tailings and “macro”-scale air voids.

5.3.2 Phase relationships

A comprehensive guide to phase relationships and material property definitions for conventional oil sand tailings, which has been widely adopted by the industry, is given by Scott (2003). Definitions used in this thesis are consistent with those given by Scott (2003) and where applicable are extended to suit the case of co-disposal materials. Figure 5-3 shows the extended phase diagram for Clearwater shale – FFT blends.

Mass M	Shale mass M_r	Shale solids M_{rs}
		Shale water M_{rw}
	Tailings mass M_t	Mineral solids M_{ts}
		Tailings water M_{tw}
		Bitumen M_{bit}

Volume V	Shale volume V_r	Shale solids V_{rs}
		Shale water V_{rw}
		Shale air voids V_{ra}
	Tailings volume V_t	Mineral solids V_{ts}
		Tailings water V_{tw}
		Tailings air voids V_{ta}
		Bitumen V_{bit}
	Macro air voids V_{ma}	

Figure 5-3: Phase diagram for Clearwater shale – FFT blends

Blends may be characterised using the same void ratios described in Section 2.3. In the case of Clearwater shale – fluid fine tailings blends, the global ratio e is defined as:

$$e = \frac{\text{Total volume of voids}}{\text{Total volume of solids}} \quad \text{or} \quad e = \frac{V_{rw} + V_{tw} + V_{ta} + V_{ma}}{V_{rs} + V_{ts} + V_{bit}} \quad (5-1)$$

The “macro scale”, or shale lump skeleton void ratio, is defined as:

$$e_r = \frac{V_t + V_{ma}}{V_r} \quad (5-2)$$

The tailings void ratio is defined as:

$$e_t = \frac{V_{tw} + V_{ta} + V_{bit}}{V_{ts}} \quad (5-3)$$

In addition, the internal shale lump void ratio may also be defined as follows:

$$e_s = \frac{V_{sw} + V_{sa}}{V_{ss}} \quad (5-4)$$

5.3.3 Mix ratio

For the purposes of this thesis, when dealing with oil sands tailings, the mix ratio is defined as follows:

$$R = \frac{\text{Mass of shale solids}}{\text{Mass of tailings mineral solids} + \text{Mass of bitumen}} \quad \text{or} \quad R = \frac{M_{ss}}{M_{ts} + M_{bit}} \quad (5-5)$$

If this mix ratio definition is used, then equations 3.10 and 3.11 are still valid.

Gravimetric moisture content (w_r and w_t) are defined as follows:

$$w_r = \frac{\text{Mass of rock pore water}}{\text{Mass of rock solids}} = \frac{M_w}{M_{rs}} \quad (5-6)$$

$$w_t = \frac{\text{Mass of tailings pore water}}{\text{Mass of tailings solids} + \text{Mass of bitumen}} = \frac{M_{tw}}{M_{ts} + M_{bit}} \quad (5-7)$$

Bitumen content (b), is defined as follows:

$$b = \frac{\text{Mass of bitumen}}{\text{Mass of tailings solids} + \text{Mass of bitumen}} = \frac{M_{bit}}{M_{ts} + M_{bit}} \quad (5-8)$$

Given that the gravimetric moisture content and bitumen content of the constituents of the blend can easily be measured, it is straightforward to calculate the mass proportion of a blend at a given mix ratio. Figure 5-4 shows the mass proportion diagram for a typical Clearwater shale - FFT blend.

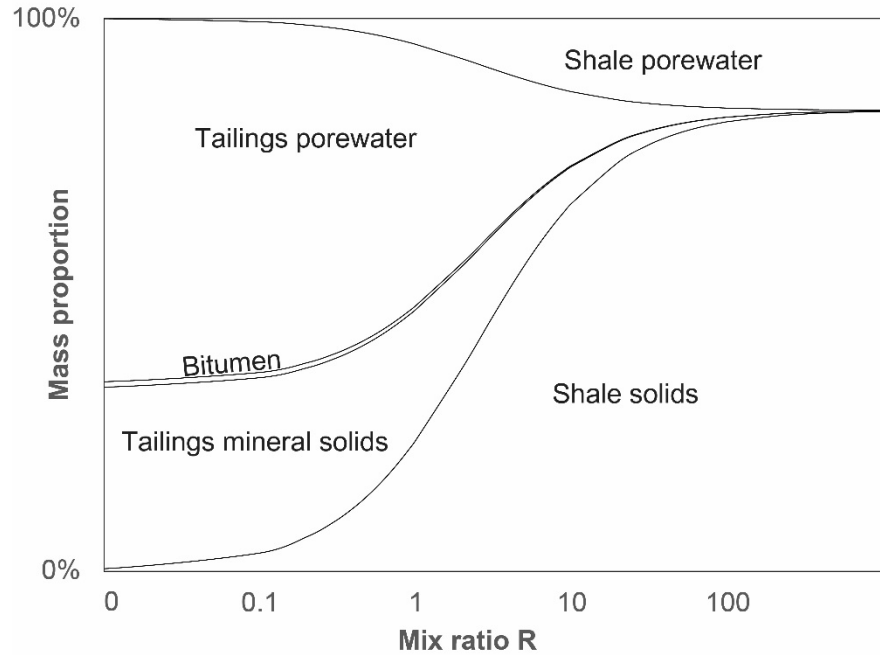


Figure 5-4: Mass proportion with respect to mix ratio for a typical FFT – Clearwater shale blend

Solids content (s or s_m) is widely used in the oil sands industry to characterise tailings. It is therefore useful to express the mix ratio in terms of the final solids content, as follows:

$$S = \frac{M_{ss} + M_{ts} + M_{bit}}{M_{ss} + M_{ts} + M_{sw} + M_{tw} + M_{bit}} \quad (5-9)$$

$$s_m = \frac{M_{ss} + M_{ts}}{M_{ss} + M_{ts} + M_{sw} + M_{tw} + M_{bit}} \quad (5-10)$$

Figure 5-5 shows the relationships between the different mix ratio parameters for a typical Clearwater shale – FFT blend.

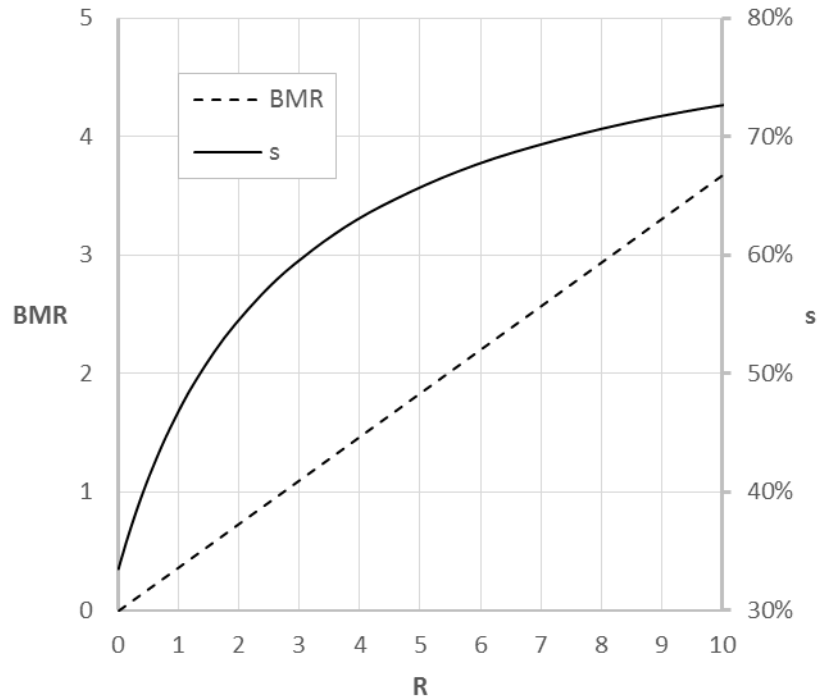


Figure 5-5: Bulk Mass Ratio (BMR) and solids content (s) with respect to dry mass ratio (R) for a typical FFT-Clearwater shale blend ($w_s = 20\%$, $w_t = 200\%$, $b = 8\%$)

5.3.4 Predicting blend configuration from mix ratio

In general, the model proposed in Section 2.7 is not applicable to blends composed of Clearwater shale lumps or other highly weatherable rock types. In contrast to waste rock particles, shale lumps are highly compressible due to the deformation and breakdown of the lumps. Consequently, it is difficult to predict the maximum void ratio of the shale lump skeleton. An alternative, experimental procedure to predict the critical void ratio based upon compaction tests is given in Section 5.4.2

5.4 Experimental Investigations

This section presents the methodology, results and a discussion of the experimental investigations into Clearwater shale and FFT blends undertaken as part of this research.

The materials were collected from an open pit oil sands operation in Alberta. Section 5.4.1 gives details of the sampling and the basic characterisation of the materials. Two experimental investigations are presented. Section 5.4.2 presents a simple experimental methodology for the prediction of the critical mix ratio of Clearwater shale – FFT blends, based upon compaction testing. Section 5.4.3 presents the compression testing that investigates the geotechnical behaviour of the Clearwater shale – FFT stacks.

5.4.1 Material Characterisation

The materials tested consist of FFT, centrifuge cake and Kca, Kcb and Kcc Clearwater shale. The samples were collected by Syncrude on their Mildred Lake Mine site and shipped to the University of Alberta.

5.4.1.1 Moisture content

As received gravimetric moisture contents are given in Table 5-1.

Table 5-1: Gravimetric moisture content of oil sands materials

Material	w (%)
FFT	210.9
Centrifuge Cake	94.1
Kca	21.1
Kcb	20.3
Kcc	16.9

5.4.1.2 Atterberg Limits

Atterberg limits for the Syncrude centrifuge cake used in this study are given by Schafer (2018) and are summarised in Table 5-2. These are likely to be equivalent to the FFT used.

Table 5-2 Atterberg limits of Syncrude centrifuge cake (after Schafer 2018)

Property	Value (%)
Liquid limit	57
Plastic limit	26
Plasticity index	31

The Atterberg limits of the Clearwater shale samples used in this study were not tested. Atterberg limits for the Clearwater formation, based on the results of 80 tests presented by Zadar and Chalaturnyk (2015), are given in Table 5-3.

Table 5-3 Atterberg limits for the Clearwater formation (after Zadar and Chalaturnyk 2015)

Property	Number of Tests	Minimum	Maximum	Average	Standard Deviation
Liquid Limit (%)	60	27.9	109.1	61	24.1
Plastic Limit (%)	60	14.5	44.5	26.2	5.6
Plasticity Index (%)	60	9.2	78	35.6	23.1

5.4.1.3 Particle size distribution

The particle size distributions for the Clearwater shale samples were determined using the sieve and hydrometer method. The results are plotted in Figure 5-6.

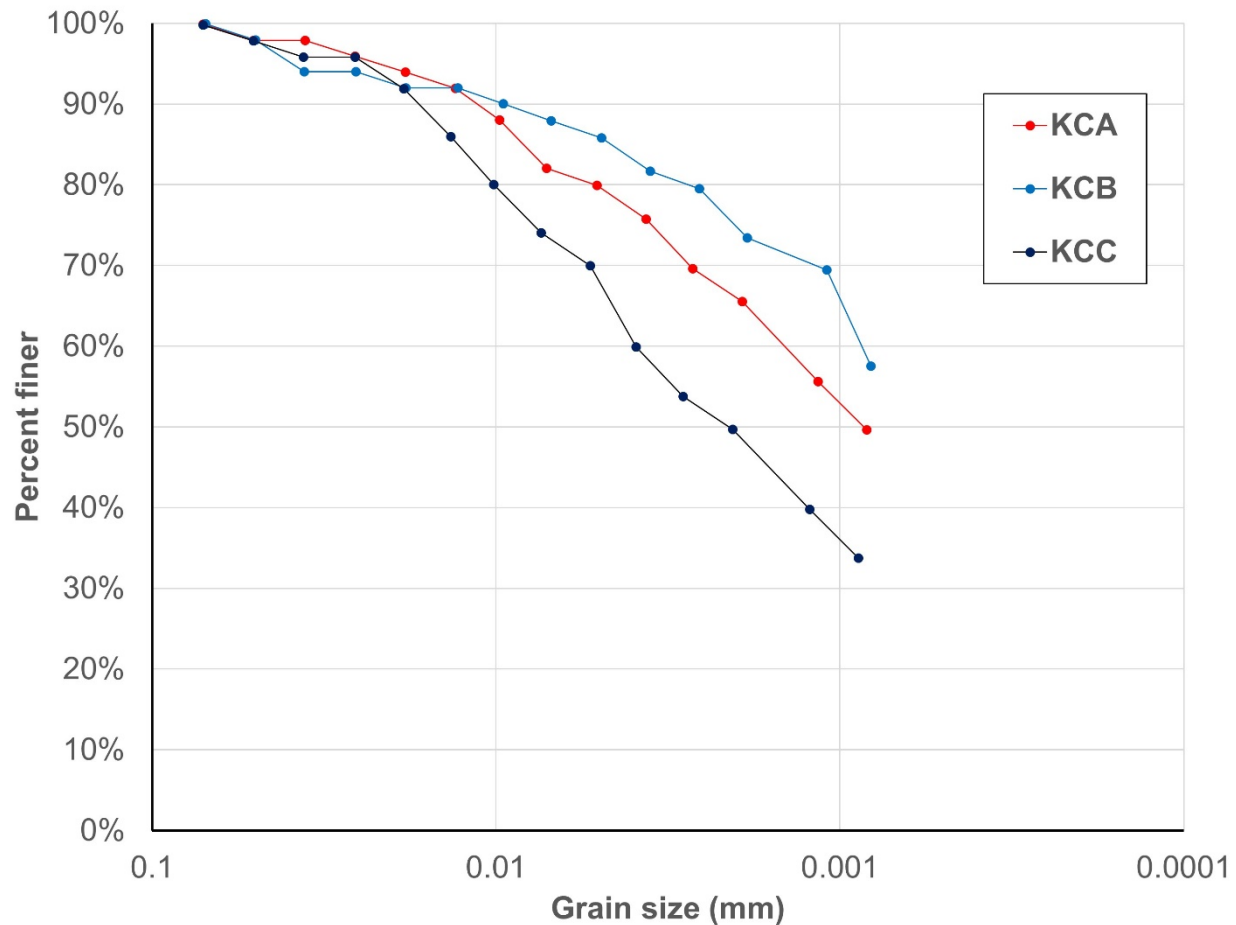


Figure 5-6: Particle size distribution for Clearwater shale samples

The particle size distribution for the Syncrude centrifuge cake used in this study is given in Figure 5-7, after Schafer (2018).

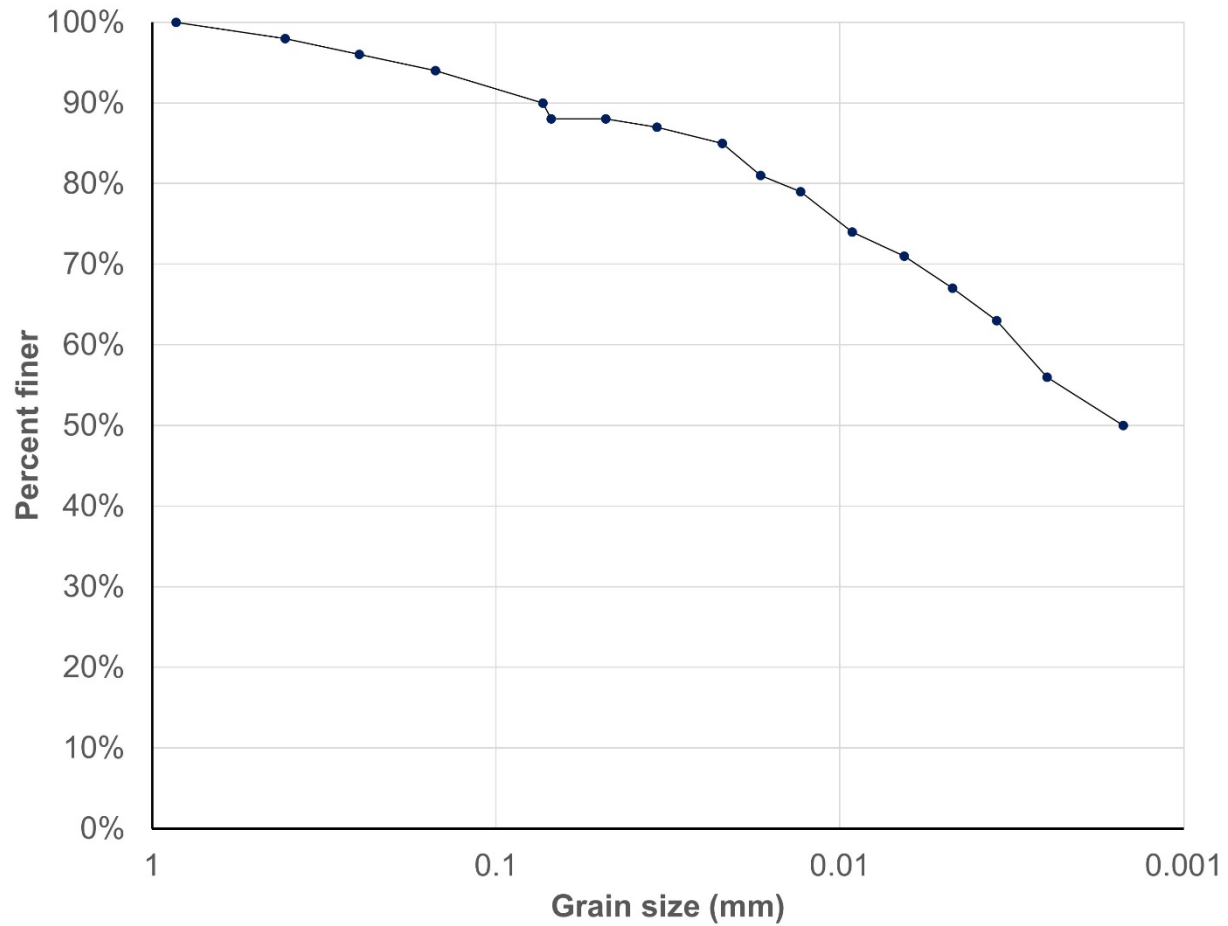


Figure 5-7: Particle size distribution for Syncrude centrifuge cake (after Schafer 2018)

It is understood that the particle size distribution of the FFT provided is similar to the particle size distribution of the centrifuge cake.

5.4.1.4 Specific gravity of solids

The specific gravity of soil solids was measured using a helium pycnometer. The results are given in Table 5-4. The specific gravity of the tailings solids was not measured and was assumed to be 2.65.

Table 5-4: Specific gravity of solids for oil sands materials

Material	G_s
Kca	2.57
Kcb	2.62
Kcc	2.62

5.4.1.5 Clay mineralogy

Mikula, Wang et al. (2016) report x-ray diffraction (XRD) analysis for Clearwater shale and FFT materials collected from Syncrude's Mildred Lake Mine site and methylene blue index (MBI) for Clearwater shale.

MBI testing measures the absorption of methylene blue dye by a clay sample and is a simple index used to give an indication of clay activity (Kaminsky 2014). The MBI for Clearwater shale is given in Table 5-5

Table 5-5: MBI for Clearwater shale (after Mikula, Wang et al. 2016)

Material	Average MBI (meq/100 g)
Kca	34.7
Kcb	37.8
Kcc	18.2

The clay mineralogy by XRD for both bulk fraction and clay sized fraction are given in Table 5-6, after Mikula, Wang et al. (2016).

Table 5-6: XRD analysis for Clearwater shale and FFT (after Mikula, Wang et al. 2016)

Material	Fraction	Weight (%)	Kaolinite	Chlorite	Illite	Montmorillonite
Kca	Bulk	100	6	5	6	30
	Clay	17.5	5	4	23	63
Kcb	Bulk	100	7	5	7	30
	Clay	22.5	12	11	16	58
Kcc	Bulk	100	9	9	22	5
	Clay	19.5	20	25	30	16
FFT	Bulk	100	41	0	21	0
	Clay	83	34	0	21	0

5.4.1.6 Bitumen content

The bitumen content of the the FFT was measured using the Dean and Stark (1920) method. The results are given below in Table 5-7.

Table 5-7: Dean Stark test results for oil sands tailings

Material	Bitumen content <i>b</i> (%) ^(a)
FFT	7.51
Centrifuge cake	3.94

(a) Defined as mass of bitumen / mass of bitumen + mineral solids x 100%

5.4.2 *Mixing trial*

5.4.2.1 *Introduction*

This section describes a simple experimental procedure for the prediction of the critical mix ratio based on the widely-used Proctor compaction test. Whereas the waste rock skeleton void ratio (e_m) for blends composed of hard rock and tailings can generally be assumed, that is not the case for Clearwater shale-FFT blends or other blends composed of soft, soil-like rocks.

Obtaining experimental measurements of the macro-scale void ratio (e_m), internal shale lump void ratio (e_s) and tailings void ratio (e_t) of a blend is difficult. However, prior to mixing, e_t can easily be calculated based on tailings moisture content. At initial conditions, e_s may be assumed to be equal to the in-situ void ratio of the shale. Tailings may be assumed to be fully saturated. Given these assumptions, the full volumetric proportions may then be back-calculated from the measurement of total volume.

The Standard Proctor Test (ASTM D698) is a useful means of evaluating the properties of blends of different mixture ratios because it is quick, simple, well established in geotechnical practice and allows for easy volume measurement.

5.4.2.2 *Methodology*

Tests were conducted on a Kca Clearwater shale – centrifuge cake blend, starting with pure Kca at its natural moisture content. Blends used for subsequent tests were wetted by adding centrifuge cake and mixed by hand. In all cases, the Kca was passed through a No. 4 sieve prior to mixing. At each stage, the blend was compacted using the Standard Proctor method, and the bulk mass and gravimetric moisture content were measured.

Given that the volume of the mold is known, the bulk density can easily be calculated. The test was repeated using the modified Proctor method.

5.4.2.3 Results and discussion

The standard Proctor compaction curve is shown in Figure 5-8. The dashed lines represent global degrees of saturation (S_r) of 100% and 80%.

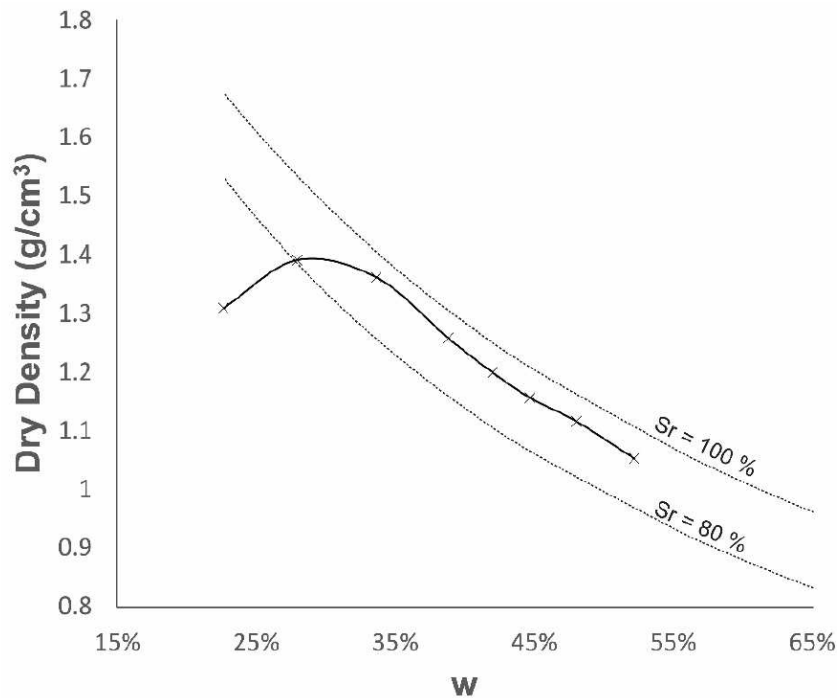


Figure 5-8: Standard Proctor compaction curve for Clearwater shale – FFT blend

Given that the water content of the final blend, the water contents of the shale and tailings and the bitumen content of tailings are known, if perfect mixing is assumed, the mass proportion of all of the phases can be evaluated and the mixture ratio can be back-calculated. Figure 5-9 shows the dry density with respect to mix ratio. Theoretical curves representing the fully saturated condition, and zero “macro” air voids, using an assumed e_s of 0.7 and assuming the tailings are fully saturated, are plotted.

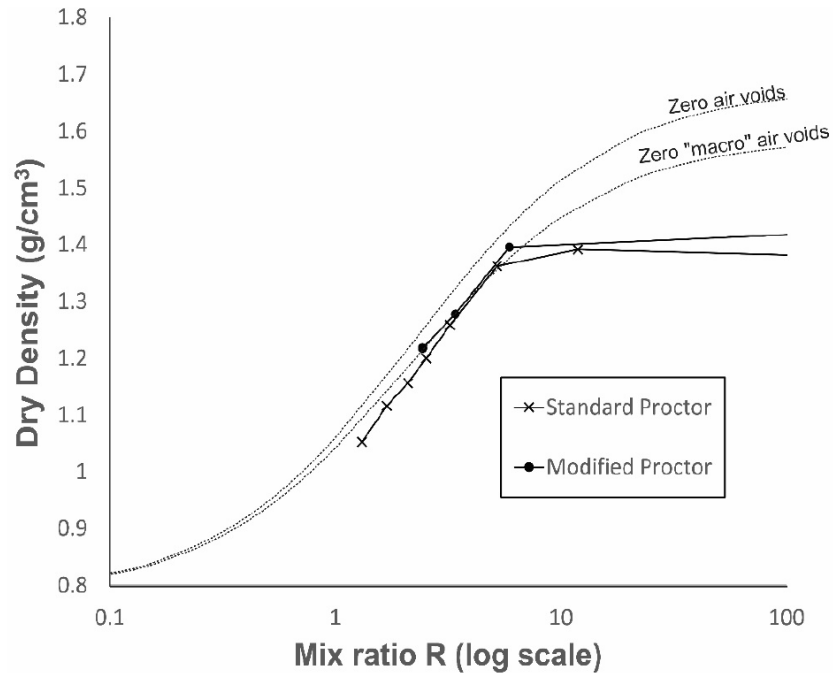


Figure 5-9: Dry density with respect to mix ratio for Centrifuge cake – KCA Clearwater shale blends compacted using the standard and modified Proctor method

If the points plot on the zero macro air voids line, that implies that the blend is in either the “floating” or “just filled” configuration (Figure 5-1 (c) and (d)). If the points are below the line, that implies that they are in an unsaturated configuration (Figure 5-1 (b)). Based on the conceptual model, it is expected that points would not plot above this line irrespective of the degree of compaction. In other words, 100% saturation will not be achieved, because the floating shale lumps remain unsaturated.

In general, the results show the expected behaviour. At low mix ratios the blends are in the “floating” configuration: shale lumps floating in a fine tailings matrix. When the mix ratio is higher than a critical value ($R_{critical}$) the blends consist of shale lumps, fine tailings and macro scale air voids. The point where the blends become unsaturated with increasing mix ratio represents the “just filled” point, where the blend has optimum

density. As might be expected, the critical mix ratio is slightly higher for the modified Proctor than the standard, suggesting that $R_{critical}$ is a function not only of the material properties, but also of the degree of compaction or confining stress. The critical mix ratio for these material appears to be around $R = 6$, corresponding to a final solids content (s_m) of around 75% and a Bulk Mass Ratio (BMR) of 3 : 1 shale : tailings. This suggests that blends optimised for tailings disposal will generally be in the “floating” configuration.

It should be noted that the conceptual model discussed here is generally only valid at initial conditions. Upon blending, moisture is transferred from the tailings to the shale under a suction gradient, and the shale lumps will swell. Nevertheless, the test method presented herein provides a useful methodology for the evaluation of the critical mix ratio for fine tailings blended with clayey overburden material or weak rocks, that is quick and inexpensive to perform.

5.4.3 Slurry consolidometer testing

5.4.3.1 Introduction

Chapter 3 of this thesis presented a new method of simulating the self-weight consolidation of tailings stacks, using Controlled Rate of Loading (CRL) tests where an incrementally increasing load rate is applied as the stress increases, to account for the increase in drainage path length as the tailings stack rises in the field. A procedure for calculating a series of load rates to simulate the required deposition rate was given, and the results of experimental trials on filtered gold tailings intended to verify this approach were presented. The results of the experimental trial showed how this method could be applied to simulate the placement of “dry stacked” blends of filtered tailings and waste

rock, and to predict the pore pressure response. The objective of this testing is to apply this approach to the special case of “dry stacks” constructed from Clearwater shale – FFT blends. In particular, the objective was to predict the pore pressure response of rapidly-placed stacks, since that is critical to stability.

5.4.3.2 Methodology

The cell used in this study was a slurry consolidometer, custom built to the specifications of the University of Queensland by Wille Geotechnik of Germany. The cell has an internal diameter of 150 mm and is capable of accommodating samples up to 300 mm high. An axial load is applied via a 10 kN high precision electromechanical load frame. It is equipped with two load cells: one located on the loading piston that measures the applied load and one located at the base of the sample. The vertical displacement of the loading ram is measured via an LVDT; this is used to measure the settlement of the sample. The device is fully computer controlled, and any sequence of load steps and load rates may be applied. The device is shown in Figure 5-11 and shown schematically in Figure 5-10.

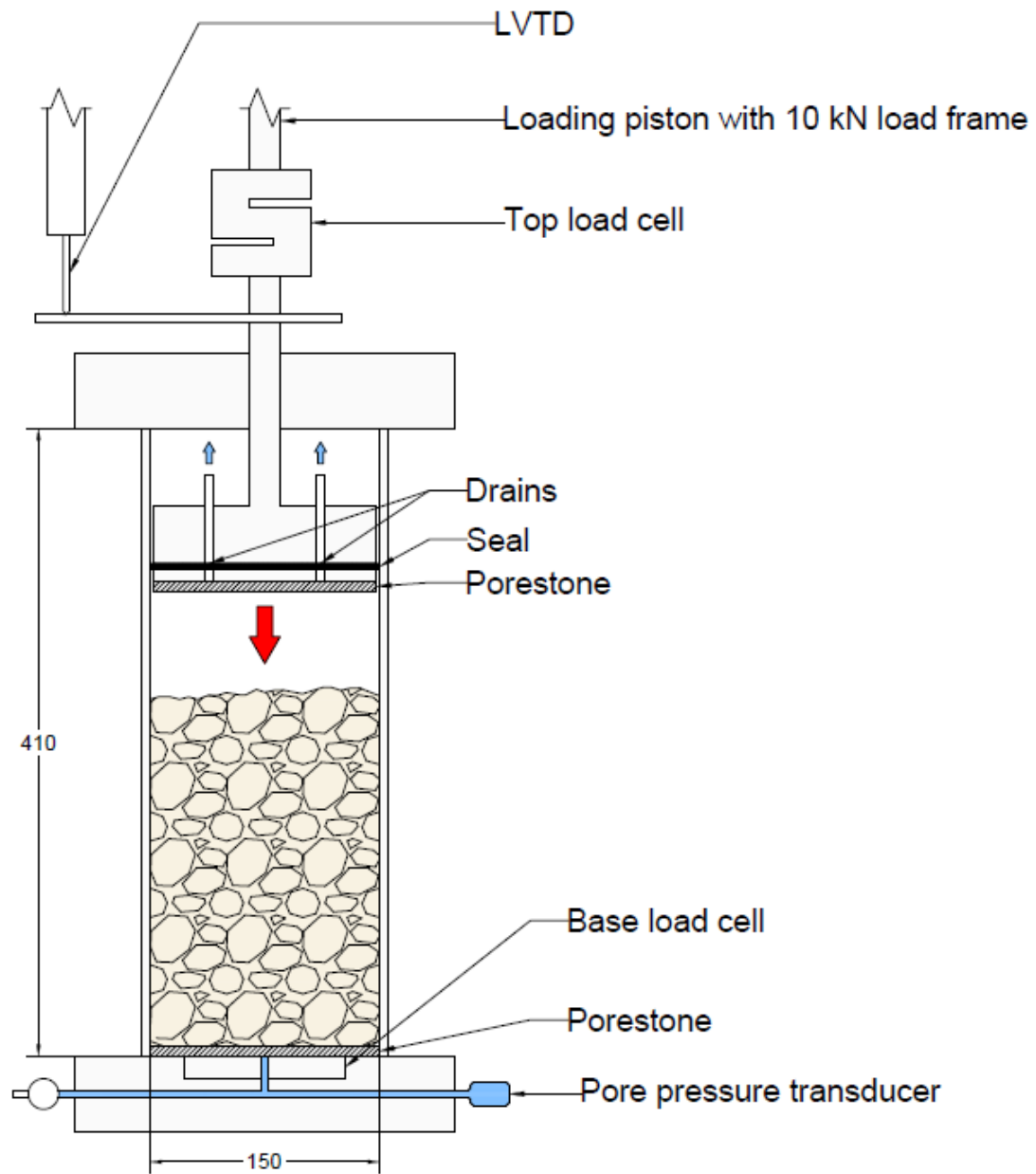


Figure 5-10: Slurry consolidometer schematic (dimensions in mm)

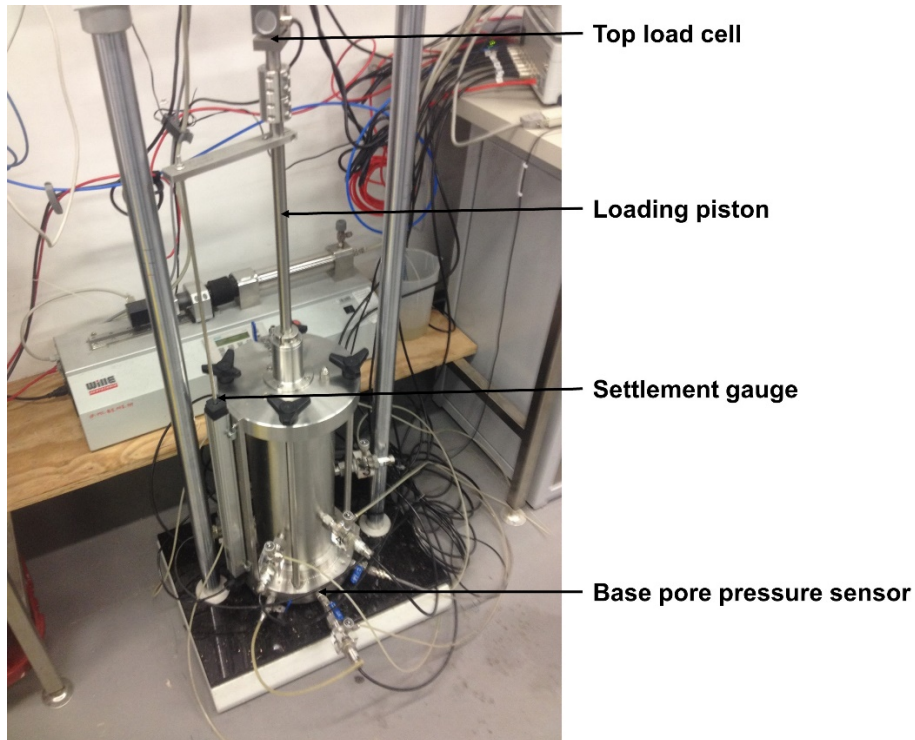


Figure 5-11: Slurry consolidometer

The testing considered a scenario where blended materials were placed rapidly in a 15 m high stack, whereupon the stack was moved elsewhere, and the stack was left to sit for an extended period of time. This scenario is intended to be representative of how a commercial-scale oil sands co-disposal project might operate. The scenario was simulated in the slurry consolidometer by applying a vertical stress rapidly in single step. A loading rate of 100 kPa/minute was used.

The tests were performed with a range of mix ratios, sample heights and loading conditions. The tests performed are summarised in Table 5-8.

Table 5-8: Summary of slurry consolidometer tests on oil sand materials

Test	Applied Load (kPa)	Shale Type	Mix ratio		Sample height (mm)
			<i>R</i>	Solids content s	
Test 1	270	Kc/b/c	9.3	72.2%	108
Test 2	290	Kc/b/c	7.8	70.6%	104
Test 3	290	Kc/b/c	8.1	71.0%	264
Test 4	340	Kc/b/c	7.9	70.7%	35
Test 5	270	Kc/b/c	9.2	72.1%	192
Test 6 ^(a)	270	Kc/b/c	9.4	72.3%	191

(a) Test 6 was left to “cure” under an applied load of 10 kPa for a period of one week, prior to rapid loading to 270 kPa

The tests were carried out using a composite sample of Kca, Kcb and Kcc Clearwater shale in the proportion of 5 : 3 : 2 by bulk mass, because this is approximately representative of their relative proportion in the deposit (Mikula, Wang et al. 2016). Tests 1 and 2 investigate the effect of the mix ratio. Tests 3 and 4 investigate the influence of the sample height. Tests 5 and 6 investigate the effect of the sample “curing” for a week prior to stacking. The total weight of blended material placed in the cell was measured, to allow calculation of initial parameters. The gravimetric moisture content of the blend at initial conditions was measured. The mix ratios stated in Table 5-8 are back-calculated from the gravimetric moisture content.

5.4.3.3 Results

The initial and final moisture contents, void ratios and test durations are given in Table 5-9.

Table 5-9: Initial and final void ratios for oil sands slurry consolidometer tests

Test	Test Duration (hours)	Void ratio e	
		Initial	Final
Test 1	23.4	1.0	0.68
Test 2	22.1	1.2	0.76
Test 3	19.5	1.1	0.91
Test 4	0.55	1.3	0.74
Test 5	24.1	1.0	0.76
Test 6	48.1	1.0	0.70

Figure 5-12 through Figure 5-17 show the output of the tests, plotted against time. The applied stress is shown by the red line. The stress measured at the base of the sample is shown by the green line. The pore pressure measured at the base of the sample is shown by the blue line. The void ratio is calculated from measured settlement and is plotted on a secondary axis.

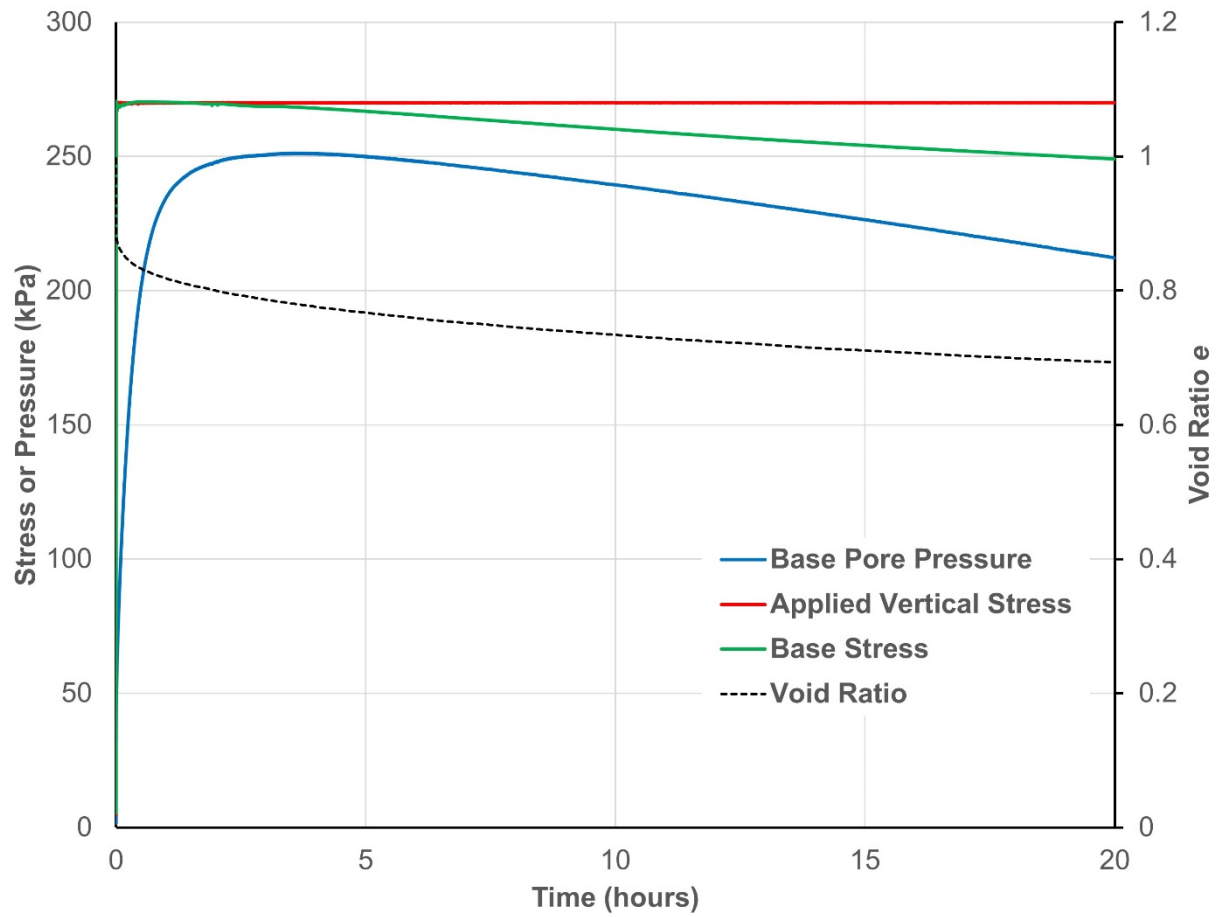


Figure 5-12: Test 1 – 72% solids 108 mm sample height

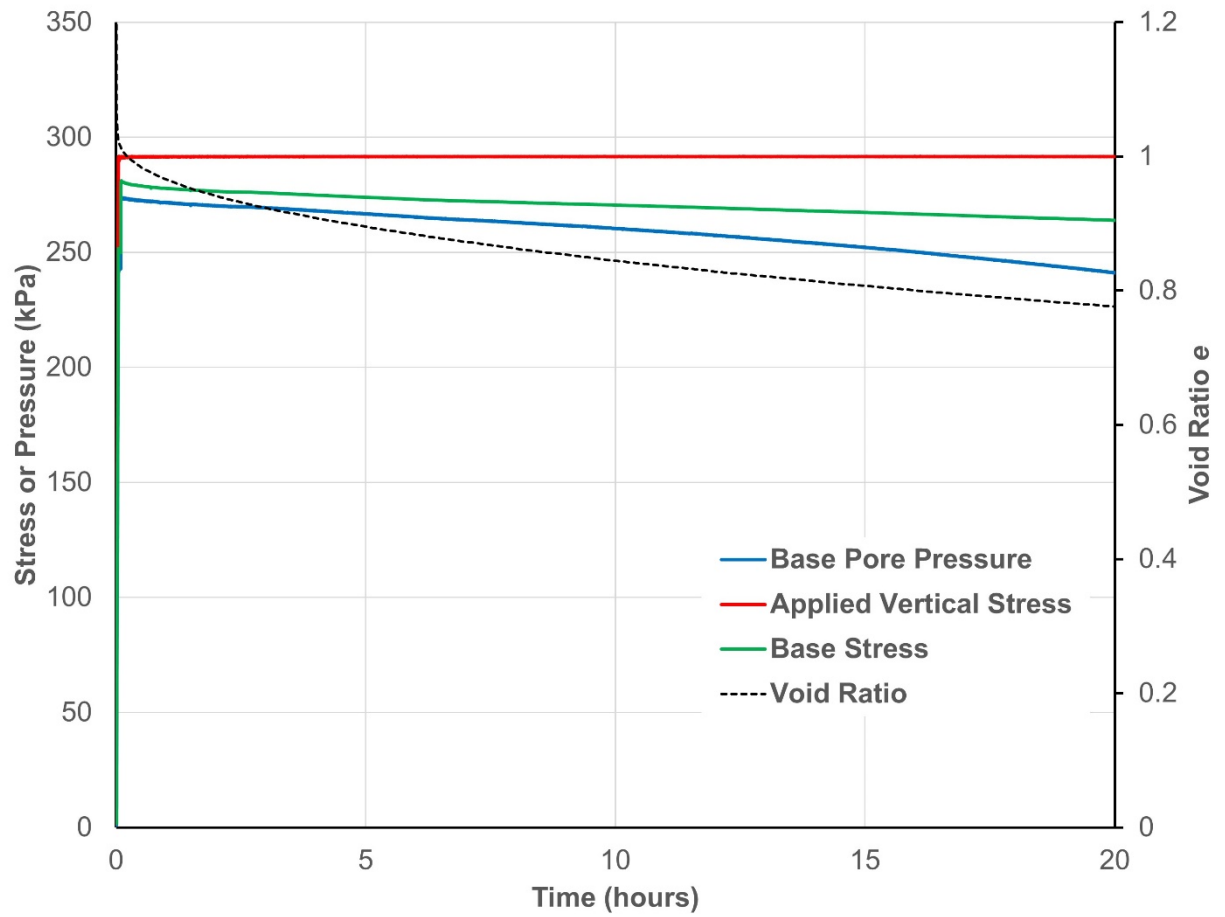


Figure 5-13: Test 2 – 71% solids 104 mm sample height

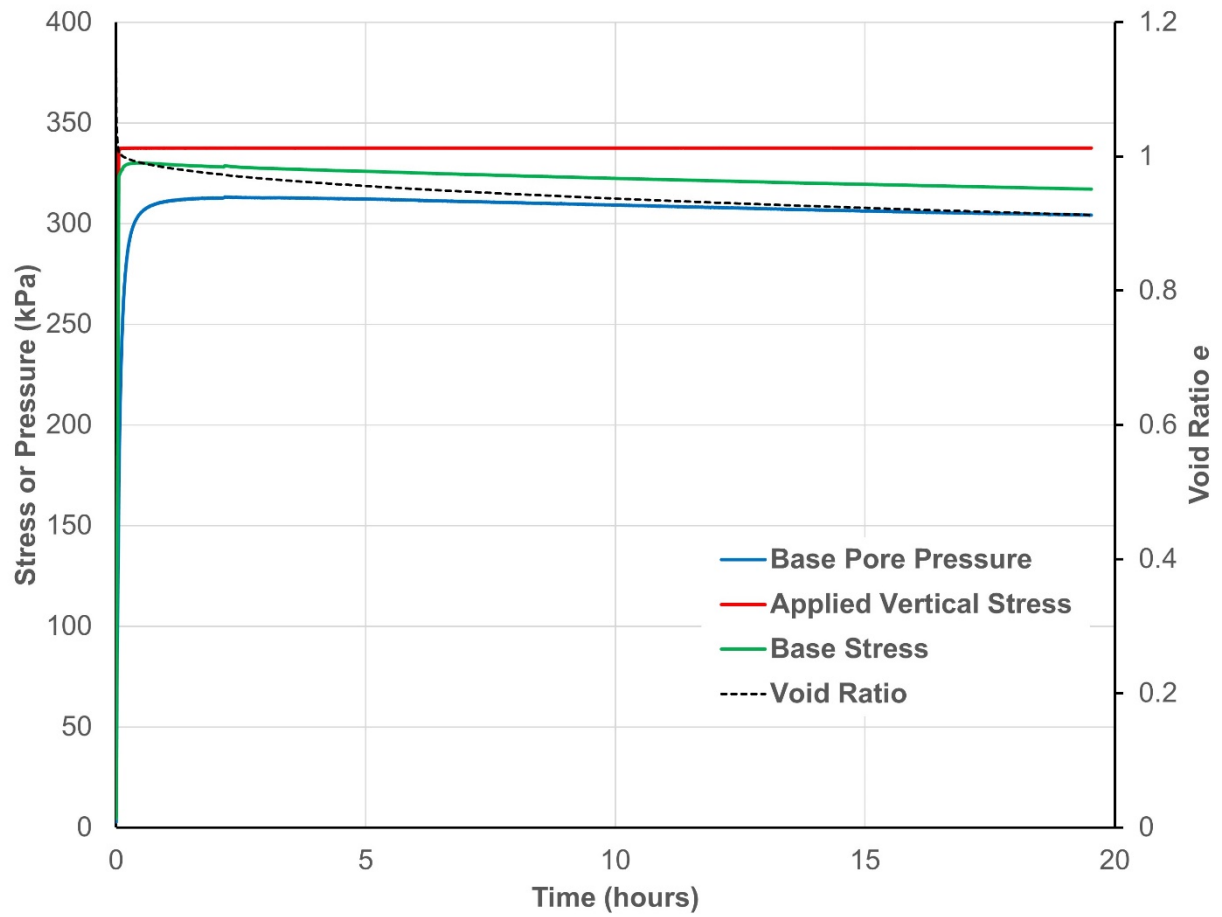


Figure 5-14: Test 3 – 71% solids 264 mm sample height

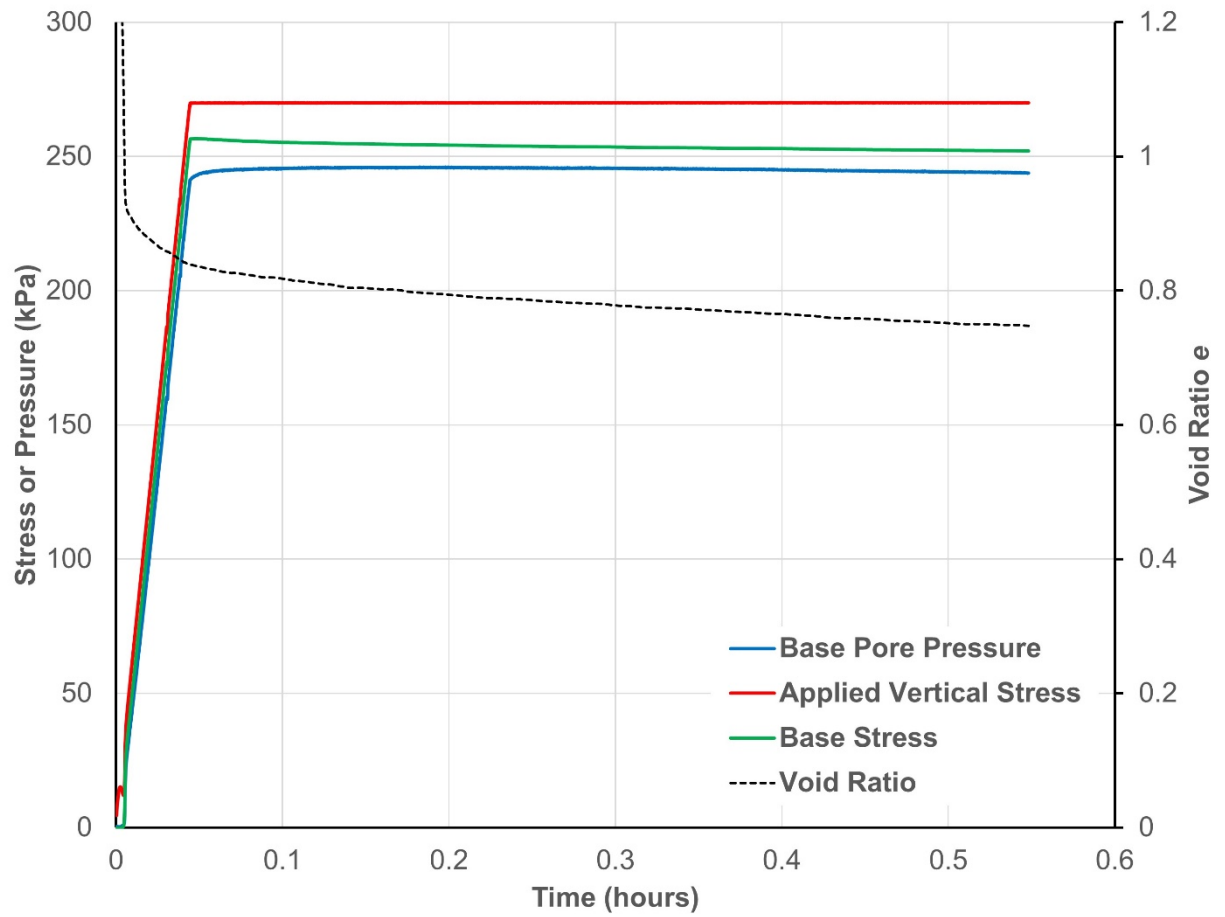


Figure 5-15: Test 4 – 71% solids 35 mm sample height

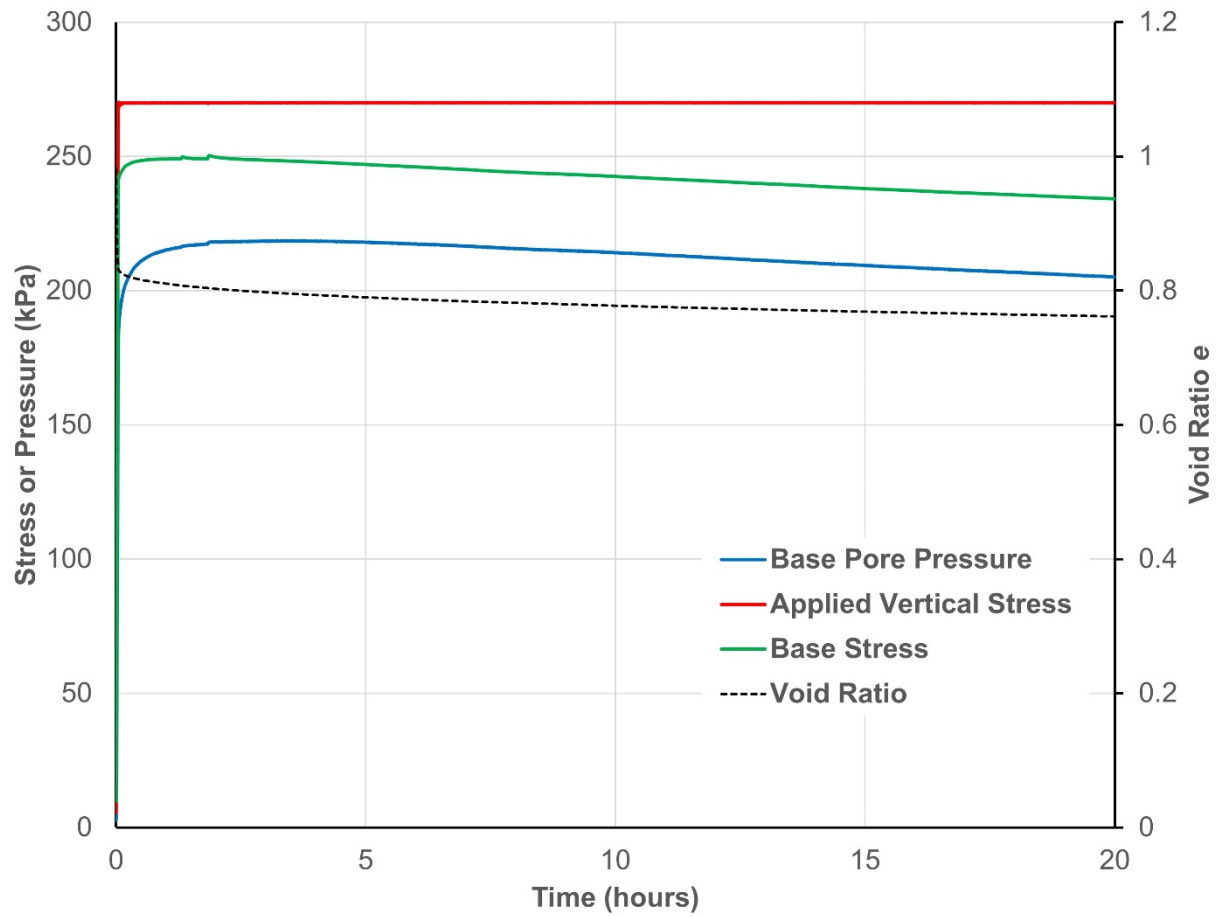


Figure 5-16: Test 5 – 72% solids 191 mm sample height

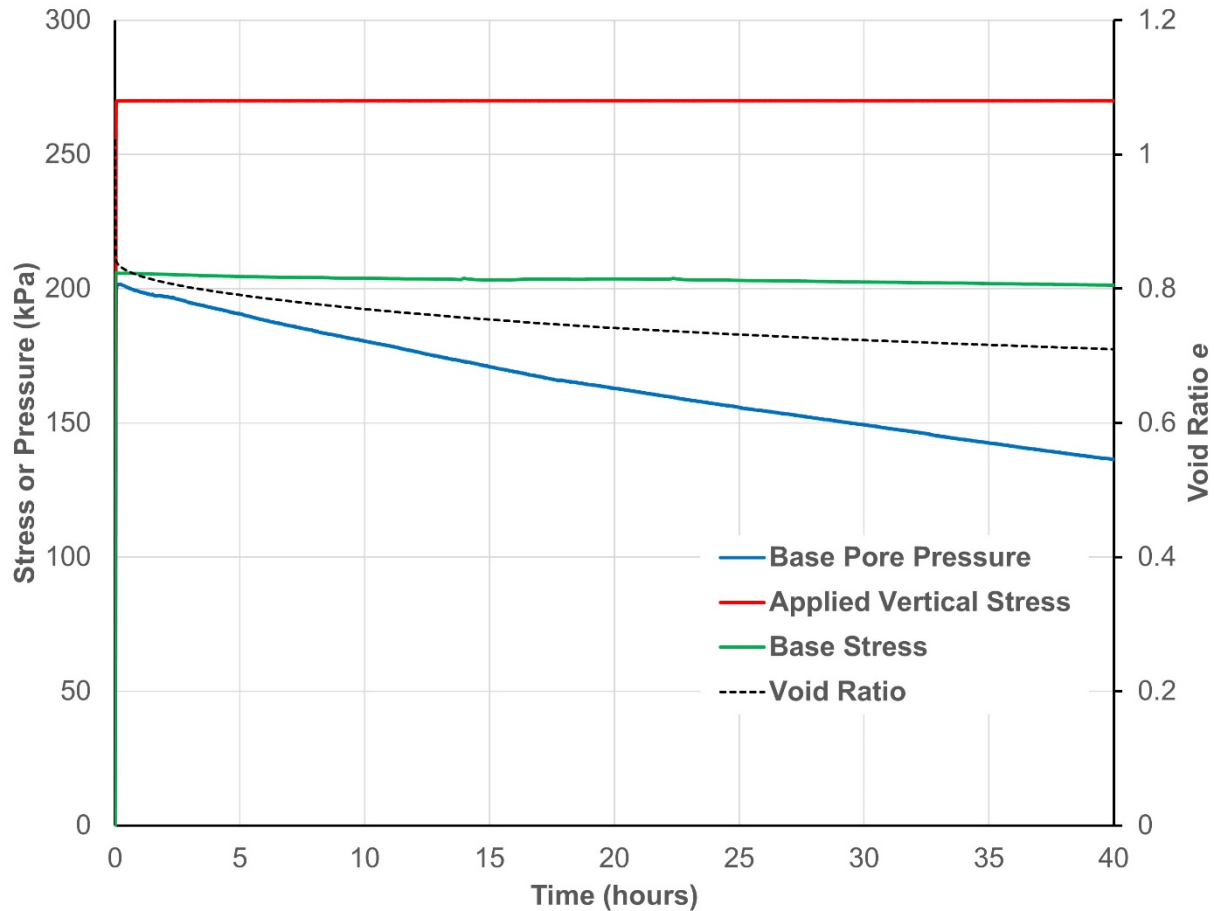


Figure 5-17: Test 6 – 72% solids 192 mm sample height (left to cure for 1 week prior to test)

5.4.3.4 Discussion

The stacking behaviour of oil sands dry stacks is markedly different from filtered gold tailings (presented in Section 3). Clearwater shale – FFT blends are characterised by much greater generation of excess pore pressures with minimal dissipation.

The mix ratio, sample height and curing time were all observed to have an influence on the results. Figure 5-18 shows the base pore pressure normalised with respect to base stress for Test 1 and Test 2, two otherwise similar test specimens with varying mix ratios.

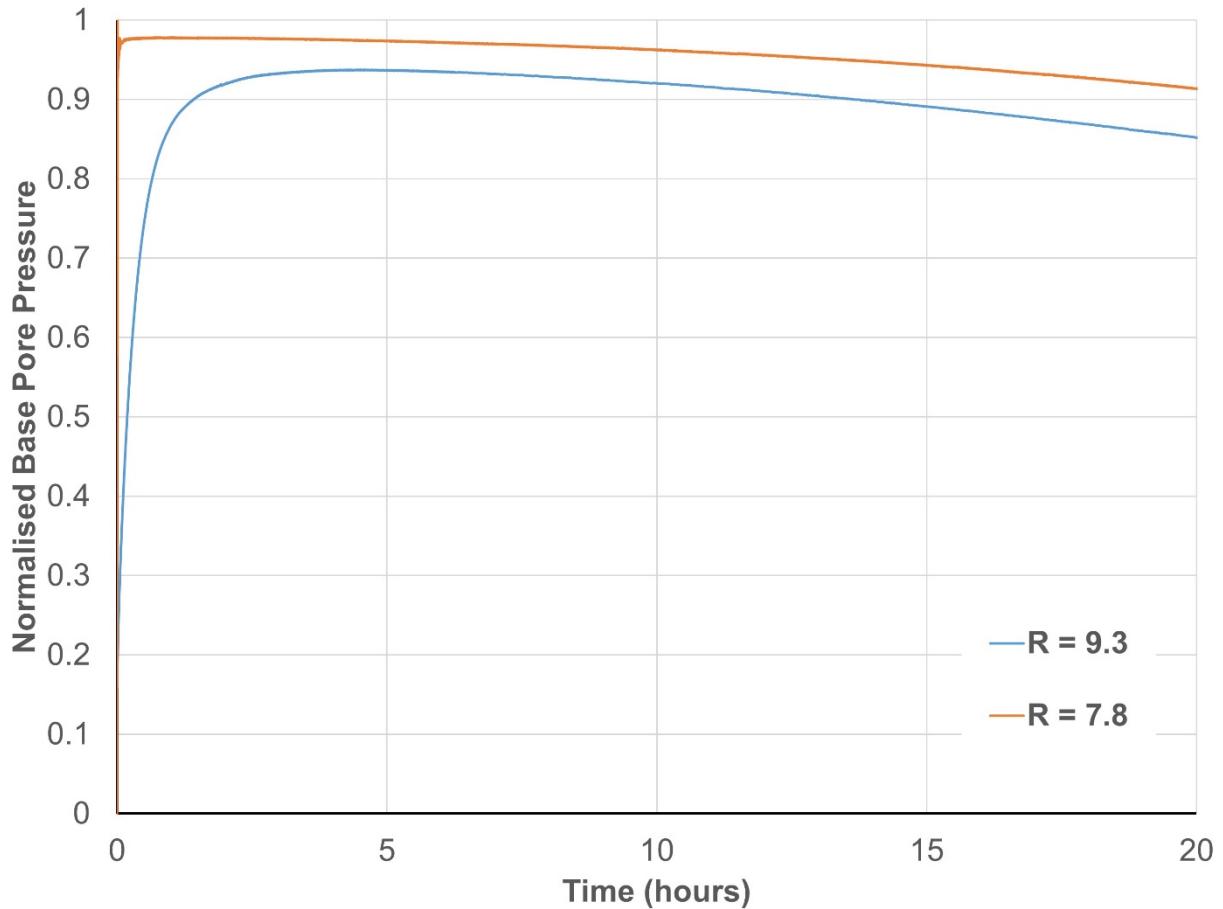


Figure 5-18: Normalised base pore against time for Test 1 and Test 2

Increasing the mix ratio appears to cause a reduction in excess pore pressure generated at the base of the stack, faster dissipation of pore pressure and an increased lag time in the measurement of excess pore pressure. This is most likely due to increased shale content, increasing the rate of moisture transfer from the FFT into the shale lumps. This suggests that when the material is loaded, excess pore pressure is generated in the tailings, which is then dissipated by drainage of water from the FFT into the shale lumps. Given the importance of the moisture transfer process to the dissipation of excess pore pressure, the “time scaling” procedure given in Chapter 3, based on drainage path length,

is clearly not appropriate for Clearwater shale – FFT blends or blends containing other weak rocks with high clay content. Nevertheless, if this method were to be applied to these results, it would be evident that, based on single drainage and consolidation alone, excess pore pressure would dissipate during a practical time period.

Figure 5-19 shows the base pore pressure normalised with respect to base stress for Test 2, Test 3 and Test 4. These tests have three different sample heights and otherwise similar mix ratios and loading conditions.

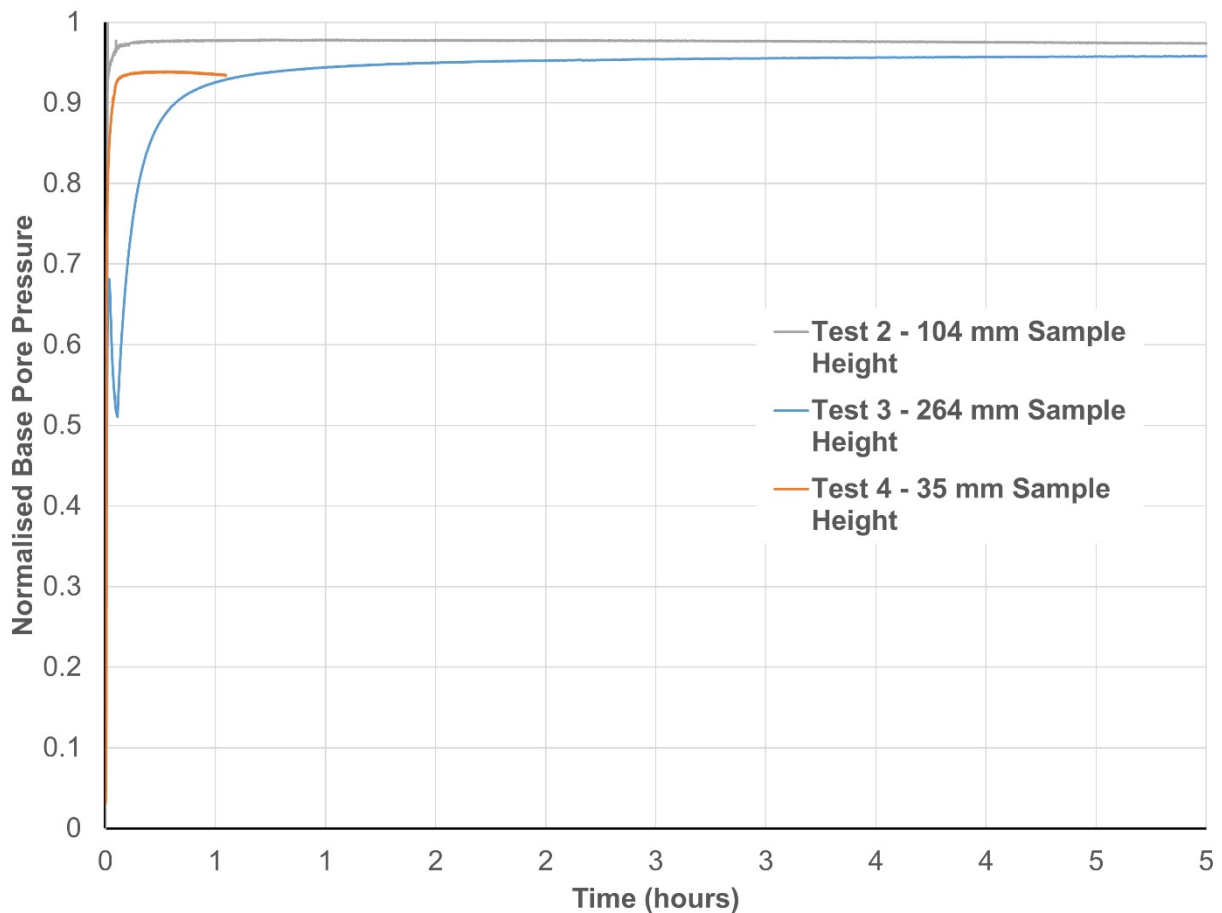


Figure 5-19: Normalised base pore pressure against time for samples at a range of sample heights

It can be seen from Figure 5-19 that, as expected, faster dissipation of the excess pore pressure is observed in the thinner sample. This is due to the shorter drainage path and shows that consolidation has an influence on pore pressure dissipation, in addition to moisture transfer.

Tests 5 and 6 investigated the influence of “curing time”. Two samples were prepared to 72% solids and 190 mm in sample height. One sample was then tested immediately upon mixing. The other sample was left for a period of one week under a nominal load of 10 kPa before testing.

Figure 5-20 shows the base pore pressure plotted against time for Test 5 and Test 6.

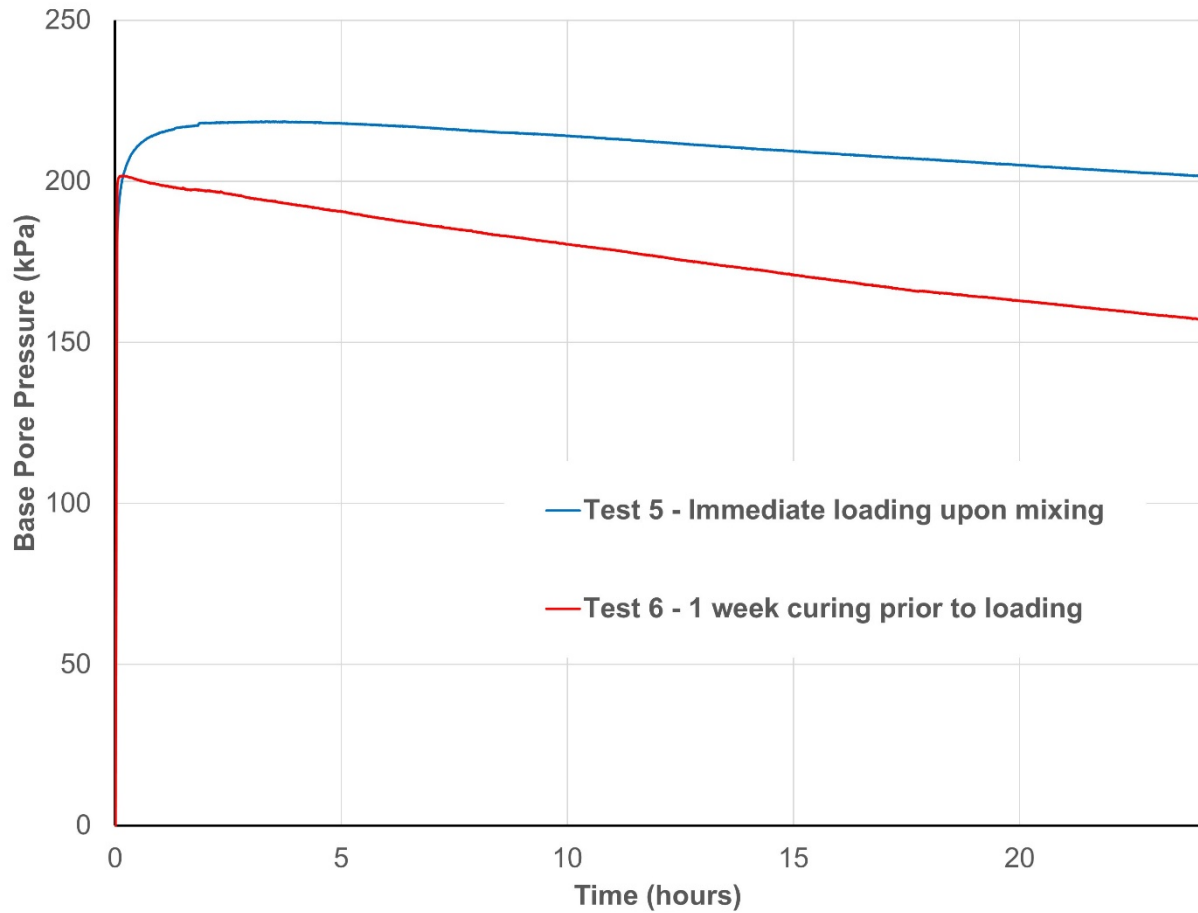


Figure 5-20: Base pore pressure against time for Test 5 and Test 6

It can be seen that the sample loaded immediately upon mixing generates higher excess pore pressure than the cured sample.

Figure 5-21 shows the pore pressure response normalised with respect to base stress for Test 4 and Test 5.

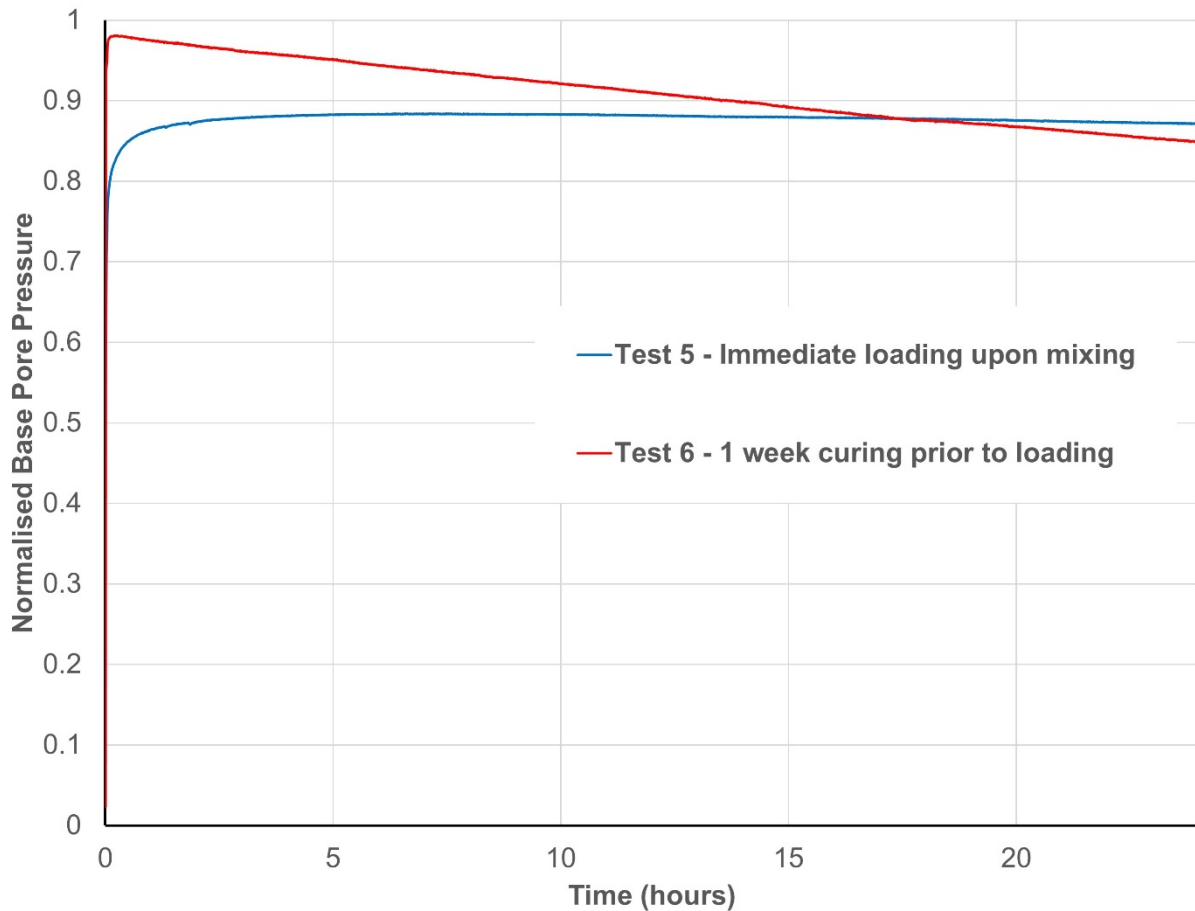


Figure 5-21: Normalised base pore pressure against time for Test 5 and Test 6

When normalised with respect to the base stress, the cured sample has a higher pore pressure response. In contrast to the uncured sample, the cured sample appears to demonstrate the behaviour of a fully saturated material. This suggests that the overall degree of saturation of the mix is increasing as the shale lumps take on water from the FFT and swell.

The overall magnitude of the measured pore pressure at the base is lower for the cured sample, because the vertical stress measured at the base is lower. This due to increased wall friction in the cured sample. The phenomenon of “wall friction”, or horizontal earth

pressure, is likely to be caused by shearing of the sample. The increased wall friction is caused by the development of strength and stiffness due to the transfer of moisture from the FFT to the shale lumps.

5.5 Further discussion and conclusions

Co-disposal of fine tailings and waste rock or overburden material is an emerging technology which has the potential to significantly improve the way mine waste is managed. In the oil sands, this approach could offer an effective and economical way of dewatering and managing the large volumes of fine tailings that have thus far proven problematic. A conceptual model, based on the approach used by Wickland et al. (2006), has been developed. It is proposed that the mix ratio can be used as the principle parameter to control the properties of a blend and that the conceptual model can be used to predict the properties of a blend of a given mix ratio. It is shown how simple compaction tests can be used to estimate the relationship between the mix ratio and configuration at the time of placement.

The mix ratio, sample height and curing time all have an influence on the behaviour of “dry-stacked” blends of Clearwater shale and FFT. The following indicative conclusions can be drawn from the observation of the consolidometer tests. The process of pore pressure dissipation is governed by the process of moisture transfer into the shale lumps and by consolidation. By consolidation alone, the stack would take many years for significant dissipation of excess pore pressure to occur. This implies that the moisture transfer process is the dominant factor in controlling the pore pressure response. Consequently, the type of shale used for stacking is likely to be critically important to

performance. The geotechnical performance of the stack can also be improved by increasing the shale content.

The development of a rigorous mathematical model is required to further characterise the behaviour of these materials. Double-porosity consolidation models have been developed for “lumpy” clay fills (Yang, Tan et al. 2002, Yang and Tan 2005, Shi, Herle et al. 2018). These have been demonstrated to be effective in saturated conditions. A study on the applicability of these models to the characterisation of Clearwater shale – FFT blends and an extension of these models to consider unsaturated soils is beyond the scope of this thesis, but it is proposed as a recommendation for future research.

References

AER (2016). Alberta Energy Regulator Mineable Oil Sands Fluid Tailings Status Report, 2014 and 2015. Calgary, Alberta.

Ash, P. O. (1987). Improvement of oil sands tailings sludge disposal behaviour with overburden material. MSc, Waterloo.

Dean, E. and D. Stark (1920). "A Convenient Method for the Determination of Water in Petroleum and Other Organic Emulsions." Industrial & Engineering Chemistry **12**(5): 486-490.

Isaac, B. A., M. B. Dusseault, G. D. Lobb and J. D. Root (1982). Characterization of the Lower Cretaceous overburden for oil sands surface mining within Syncrude Canada Ltd. Leases 17 and 22.

Kaminsky, H. (2014). DEMYSTIFYING THE METHYLENE BLUE INDEX.

Lord, E. R. F. and B. A. A. Isaac (1989). "Geotechnical investigations of dredged overburden at the Syncrude oil sand mine in northern Alberta, Canada." Canadian Geotechnical Journal **26**(1): 132-153.

Mikula, R., N. Wang and R. Cleminson (2016). Overburden/tailings mixtures for engineered tailings deposit control, Canadian Patent 2 825 518 Issued: 10/11/2016.

Mimura, D. W. (1990). Shear strength of hydraulically placed clay shale. MSc, University of Alberta.

O'Donnell, N. and J. Jodrey (1984). Geology of the Syncrude mine site and its application to sampling and grade control, Syncrude Canada Ltd., Edmonton, Alberta.

Schafer, H. L. (2018). Freezing Characteristics of Mine Waste Tailings and their Relation to Unsaturated Soil Properties. Master's, University of Alberta.

Scott, J. D. (2003). "Definitions and Conversion Equations for Oil Sands Tailings."

Shafie Zadeh, N. and R. Chalaturnyk (2015). "Geotechnical Characterization of Clearwater Clay Shale and Comparison of the Properties With Other Cretaceous Clay Shales in North America." Journal of Canadian Petroleum Technology **54**.

Shi, X. S., I. Herle and D. M. Wood (2018). "A consolidation model for lumpy composite soils in open-pit mining." Géotechnique **68**(3): 189-204.

Wang, N., R. Cleminson and J. Lorentz (2017). Co-mixing of Fluid Fine Tailings and Clearwater Overburden. COSIA Oil Sands Innovation Summit. Calgary, AB.

Wickland, B. E., G. W. Wilson, D. Wijewickreme and B. Klein (2006). "Design and evaluation of mixtures of mine waste rock and tailings." Canadian Geotechnical Journal **43**(9): 928-945.

Yang, L.-A. and T.-S. Tan (2005). "One-dimensional consolidation of lumpy clay with non-linear properties." Géotechnique **55**(3): 227-235.

Yang, L.-A., T.-S. Tan, S.-A. Tan and C.-F. Leung (2002). "One-dimensional self-weight consolidation of a lumpy clay fill." Géotechnique **52**(10): 713-725.

6 CONCLUSIONS AND RECOMMENDATIONS

6.1 Conclusion

The general objective of the research was to advance the understanding of the geotechnical behaviour of dry stacked, blended mine wastes. Two specific materials were studied: filtered gold tailings blended with waste rock, and oil sands FFT blended with Clearwater shale overburden. The research comprises three principle components: a literature review, a theoretical component and a laboratory-based experimental study. The waste rock, gold tailings, FFT and clay shale used in the study were taken from working mines and were not modified in any way except for the scalping of oversized rock particles.

“Dry stacking”, or the placement of tailings on land in self-supporting piles without the need for a dam or impoundment, is a growing trend in the mining industry. In general, the results of this study support the hypothesis that mixing tailings with waste rock or overburden material can be an effective means of improving the stability of a “dry stacked” tailings deposit.

Conclusions specific to the filtered tailings and waste rock examined are summarised below:

- Blends of waste rock and tailings, with a fines dominated matrix, were observed to have higher drained shear strength than waste rock alone. The shear strength was observed to increase with rock content, up to a limiting value of 1 : 1 rock to tailings

by dry mass. At higher stresses, or with weaker rocks, the strength of the blend has the potential to be higher than rock alone.

- The addition of waste rock to filtered tailings reduces the build-up of pore pressure when loaded in compression with an incrementally increasing load. This suggests that the co-disposal of filtered tailings with rock will reduce the build-up of pore pressure during stacking, improving stability and allowing more rapid deposition or deposition in higher lifts.

Conclusions specific to the Clearwater shale and FFT examined are summarised below:

- The blending of FFT with Clearwater shale overburden is a promising technology that has the potential to enable FFT to be disposed of in trafficable, terrestrial landforms that can be constructed rapidly.
- The volume change behaviour and pore pressure response of Clearwater shale – FFT blends under compression is a complex, time-dependent process, governed by both consolidation and by the transfer of moisture from the FFT into the shale lumps. Further study is required to characterise this process.

6.2 Contributions of the thesis

Contributions of the research include:

- An up-to-date, comprehensive literature review on the geotechnical properties of blended waste rock and tailings, focussed specifically on Clearwater shale – FFT blends and waste rock – filtered tailings blends.

- A methodology for the application of ternary diagrams to characterise blends of waste rock and tailings blends. These diagrams provide a useful method for quickly evaluating the properties of a blend of a given mix ratio and tailings solids content, and may assist in high-level tailings planning and design.
- A conceptual model to describe the behaviour of filtered tailings and waste rock blends, based upon the particle packing arrangement. The model may be used to predict the structure and behaviour of the blend, based on mix ratio and density.
- An innovative testing method to simulate tailings deposition and predict the development of pore pressure at the base of the stack for a given rate of rise.
- A practical demonstration of the potential advantages of the application of co-disposal to improve the performance of dry stacked tailings, including improved shear strength and reduced build up of pore pressures during stacking. These findings support the view that dry stacking of blended tailings and waste rock may offer significant economic advantages over established dry stacking methods, which generally require compaction of filtered tailings.
- Identification of knowledge gaps for further study.

6.3 Recommendations for further research

Recommendations for further research include:

- The development of a rigorous mathematical model to characterise the behaviour of filtered tailings and waste rock blends. The model would be required to model compaction, consolidation and waste rock skeleton “creep” processes, and would

have to consider both saturated and unsaturated conditions. The theoretical framework developed in Chapter 2.7 could be used as the basis for the model.

- Field-scale trials, or meso-scale column trials, should be undertaken to study the stacking behaviour of filtered tailings and waste rock blends to verify the experimental findings.
- A further study of the development of wall friction in the slurry consolidometer cell. This could involve numerical stress-deformation modelling to predict the state of stress throughout the sample.
- The development of an unsaturated, double-porosity consolidation numerical consolidation model, which is suitable for simulating the behaviour of Clearwater shale – FFT blends.

REFERENCES (COMBINED)

- Åberg, B. (1992). "Void ratio of noncohesive soils and similar materials." Journal of geotechnical engineering **118**(9): 1315-1334.
- AER (2016). Alberta Energy Regulator Mineable Oil Sands Fluid Tailings Status Report, 2014 and 2015. Calgary, Alberta.
- Alfaro, M., N. Miura and D. Bergado (1995). "Soil-Geogrid Reinforcement Interaction by Pullout and Direct Shear Tests."
- AMEC. (2008). "Rosemont Copper Company Filtered Tailings Dry Stacks Current State of Practice Final Report." from <https://www.rosemonteis.us/files/technical-reports/012312.pdf>.
- Amoah, N. (2019). Large-Scale Tailings Filtration and Dry Stacking at Karara Magnetite Iron Ore Operation. Tailings and Mine Waste 2019, Vancouver, Canada.
- Antonaki, N., T. Abdoun and I. Sasanakul (2018). "Centrifuge Tests on Comixing of Mine Tailings and Waste Rock." Journal of Geotechnical and Geoenvironmental Engineering **144**(1): 04017099.
- Ash, P. O. (1987). Improvement of oil sands tailings sludge disposal behaviour with overburden material. MSc, Waterloo.
- ASTM (2011). D2435/D2435M-11 Standard Test Methods for One-Dimensional Consolidation Properties of Soils Using Incremental Loading, ASTM International.
- ASTM (2016). ASTM D4254-16 Standard Test Methods for Minimum Index Density and Unit Weight of Soils and Calculation of Relative Density.
- Bareither, C. A., J. Gorakhki, J. Scalia and M. Jacobs (2018). Compression Behaviour of Filtered Tailings and Waste Rock Mixtures: Geowaste. Tailings and Mine Waste 2018. Keystone, CO.
- Bauer, G. and Y. Zhao (1993). "Shear Strength Tests for Coarse Granular Backfill and Reinforced Soils."
- BISHOP, A. W., and BLIGHT, G. E. 1963. Some aspects of effective stress in saturated and unsaturated soils. *Geotechnique*, 13, pp. 177-197.
- Blight, G. and O. Steffen (1979). "Geotechnics of Gold Mine Waste Disposal, Current Geotechnical Practice in Mine Waste Disposal." Geotech. Eng. Div., American Society of Civil Engineers.

Bolton, M. D. (1986). "The strength and dilatancy of sands." Géotechnique **36**(1): 65-78.

Borja Castillo, R. N. (2019). UNDRAINED SHEAR BEHAVIOUR AND CRITICAL STATE ANALYSIS OF MIXED MINE WASTE ROCK AND TAILINGS, Colorado State University. Libraries.

Brawner, C. and J. Argall, GA (1978). Concepts and experience for subsurface storage of tailings. Proceedings of the 2nd International Tailings Symposium, Tailings Disposal Today, Denver, Colo.

Bussiere, B. (2007). "Colloquium 2004: Hydrogeotechnical properties of hard rock tailings from metal mines and emerging geoenvironmental disposal approaches." Canadian Geotechnical Journal **44**(9): 1019-1052.

Butikofer, D., B. Erickson, A. Marsh, R. Friedel, L. Murray and M. J. Piggot (2017). Filtered Tailings Disposal Case History: Operation and Design Considerations Part II. Tailings and Mine Waste 2017. Banff, AB.

Butterfield, R. (2000). "SCALE-MODELLING OF FLUID FLOW IN GEOTECHNICAL CENTRIFUGES." Soils and Foundations **40**(6): 39-45.

Cerato, A. and A. Lutenecker (2006). "Specimen Size and Scale Effects of Direct Shear Box Tests of Sands."

Charles, M. and R. Charles (1971). The use of heavy media in the pipeline transport of particulate solids. Advances in Solid-Liquid Flow in Pipes and its Application, Elsevier: 187-197.

COE (2019). Urgent request for information concerning tailings management.

COSIA (2012). Technical Guide for Fluid Fine Tailings Management.

Crystal, C. and C. Hore (2018). Filter-Pressed Dry Stacking: Design Considerations Based on Practical Experience. Tailings and Mine Waste 2018. Keystone, CO.

Davies, M. P. and S. Rice (2001). "An alternative to conventional tailings management—"dry stack" filtered tailings." Proceeding of Tailings and Mine Waste'01: 411-420.

Davison, L. R. and J. H. Atkinson (1990). "Continuous loading oedometer testing of soils." Quarterly Journal of Engineering Geology and Hydrogeology **23**(4): 347-355.

Dean, E. and D. Stark (1920). "A Convenient Method for the Determination of Water in Petroleum and Other Organic Emulsions." Industrial & Engineering Chemistry **12**(5): 486-490.

Fahey, M., M. Helinski and A. Fourie (2010). "Consolidation in accreting sediments: Gibson's solution applied to backfilling of mine stopes." Géotechnique **60**(11): 877-882.

- D. G. Fredlund, N. R. Morgenstern, and R. A. Widger. The shear strength of unsaturated soils. *Canadian Geotechnical Journal*. 15(3): 313-321.
- Gibson, R. E. (1958). "The Progress of Consolidation in a Clay Layer Increasing in Thickness with Time." *Géotechnique* **8**(4): 171-182.
- Green, P. (1981). "De-watering coal refuse." *Coal Age* **86**: 145-157.
- Habte, K. and K. Bocking (2017). Co-disposal practice in mine waste management. *Tailings and Mine Waste '17*. Banff, Alberta, Canada.
- Hawley, M. and J. Cunning (2017). Guidelines for Mine Waste Dump and Stockpile Design, CSIRO Publishing.
- Isaac, B. A., M. B. Dusseault, G. D. Lobb and J. D. Root (1982). Characterization of the Lower Cretaceous overburden for oil sands surface mining within Syncrude Canada Ltd. Leases 17 and 22.
- Jehring, M. M. and C. A. Bareither (2016). "Tailings composition effects on shear strength behaviour of co-mixed mine waste rock and tailings." *Acta Geotechnica* **11**(5): 1147-1166.
- Jewell, R. J. and A. B. Fourie (2006). Paste and thickened tailings: A guide, Australian Centre for Geomechanics, The University of Western Australia.
- Kaminsky, H. (2014). DEMYSTIFYING THE METHYLENE BLUE INDEX.
- Khalili, A., D. Wijewickreme and G. W. Wilson (2010). "Mechanical response of highly gap-graded mixtures of waste rock and tailings. Part I: Monotonic shear response." *Canadian Geotechnical Journal* **47**(5): 552-565.
- Lambe, T. W. and R. V. Whitman (1969). Soil Mechanics. New York, John Wiley and Sons.
- Lara, J., E. Pornillos and H. Muñoz (2013). Geotechnical-geochemical and operational considerations for the application of dry stacking tailings deposits—state-of-the-art. Proceedings of the 16th International Seminar on Paste and Thickened Tailings, Belo Horizonte, Brazil, June 17–20.
- Latham, J.-P., A. Munjiza and Y. Lu (2002). "On the prediction of void porosity and packing of rock particulates." *Powder Technology* **125**(1): 10-27.
- Leps, T. M. (1970). "Review of shearing strength of rockfill." Journal of Soil Mechanics & Foundations Div.

Lord, E. R. F. and B. A. A. Isaac (1989). "Geotechnical investigations of dredged overburden at the Syncrude oil sand mine in northern Alberta, Canada." Canadian Geotechnical Journal **26**(1): 132-153.

Malgesini, M., L. Aubone, R. Hunsaker and W. Boyd (2017). Tailings and Mine Waste 2017. Keystone, CO.

Marachi, N. D. (1969). "Strength and Deformation. Characteristics of Rockfill Materials." Report No. TE-69-5 to State of California Department of Water Resources.

Marsal, R. J. (1973). Embankment dam engineering : casagrande volume. A. Casagrande, R. C. Hirschfeld, S. J. Poulos and G. E. Bertram. New York :, Wiley.

Mikula, R., N. Wang and R. Cleminson (2016). Overburden/tailings mixtures for engineered tailings deposit control, Canadian Patent 2 825 518 Issued: 10/11/2016.

Mimura, D. W. (1990). Shear strength of hydraulically placed clay shale. MSc, University of Alberta.

Mittal, H. K. and N. R. Morgenstern (1976). "Seepage control in tailings dams." Canadian Geotechnical Journal **13**(3): 277-293.

Morgenstern, N., S. Vick and D. Van Zyl (2015). "Report on Mount Polley tailings storage facility breach." Report of independent expert engineering investigation and review panel. Prepared on behalf of the Government of British Columbia and the Williams Lake and Soda Creek Indian Bands.

Morgerstern, N., S. Vick and B. Watts (2016). Fundão Tailings Dam Review Panel Report on the Immediate Causes of the Failure of the Fundão Dam.

Newman, L., K. Arnold and D. Wittwer (2010). Dry stack tailings design for the Rosemont Copper project. International Conference on Tailings & Mine Waste. Tailings and Mine Waste.

O'Donnell, N. and J. Jodrey (1984). Geology of the Syncrude mine site and its application to sampling and grade control, Syncrude Canada Ltd., Edmonton, Alberta.

Oldecop, L. and E. Alonso (2017). "Measurement of Lateral Stress and Friction in Rockfill Oedometer Tests Enabling the Analysis of the Experimental Results in the p'-q Space." Geotechnical Testing Journal **40**(5): 822-832.

Olson, R. (1986). State of the Art: Consolidation Testing. STP34606S Consolidation of Soils: Testing and Evaluation. R. Yong and F. Townsend. West Conshocken, PA, ASTM International: 7-70.

- Parkin, A. and G. Adikari (1981). Rockfill deformation from large-scale tests. Proceedings of the 10th International Conference Soil Mechanical and Foundations Engineering Stockholm.
- Parkin, A. K. (1991). Through and Overflow Rockfill Dams. Advances in Rockfill Structures. E. M. das Neves. Dordrecht, Springer Netherlands: 571-592.
- Penman, A. and J. Charles (1976). "The quality and suitability of rockfill used in dam construction. Dams and embankments, Practical Studies from the BRE." London: The Construction Press **6**: 72-85.
- Peronius, N. and T. Sweeting (1985). "On the correlation of minimum porosity with particle size distribution." Powder technology **42**(2): 113-121.
- Robertson, P., L. de Melo, D. Williams and G. Wilson (2019). Report of The Expert Panel on the Technical Causes of the Failure of Feijão Dam 1.
- Robertson, P. K., A. V. da Fonseca, B. Ulrich and J. Coffin (2017). "Characterization of unsaturated mine waste: a case history." Canadian Geotechnical Journal **54**(12): 1752-1761.
- Roscoe, K. H. (1970). "The influence of strains in soil mechanics." Geotechnique **20**(2): 129-170.
- Rousé, P. C., R. J. Fannin and D. A. Shuttle (2008). "Influence of roundness on the void ratio and strength of uniform sand." Géotechnique **58**(3): 227-231.
- Rowe, P. W. and L. Barden (1966). "A New Consolidation Cell." Géotechnique **16**(2): 162-170.
- Scarpelli, G. and D. M. Wood (1982). "Experimental observations of shear patterns in direct shear tests." NASA STI/Recon Technical Report N **83**.
- Schafer, H. L. (2018). Freezing Characteristics of Mine Waste Tailings and their Relation to Unsaturated Soil Properties. Master's, University of Alberta.
- Schiffman, R. L. and R. E. Gibson (1964). "Consolidation of non-homogeneous clay layers." Journal of the Soil Mechanics and Foundations Division ASCE **5**(90): 1-30.
- Scott, J. D. (2003). "Definitions and Conversion Equations for Oil Sands Tailings."
- Shafie Zadeh, N. and R. Chalaturnyk (2015). "Geotechnical Characterization of Clearwater Clay Shale and Comparison of the Properties With Other Cretaceous Clay Shales in North America." Journal of Canadian Petroleum Technology **54**.
- Shi, X. S., I. Herle and D. M. Wood (2018). "A consolidation model for lumpy composite soils in open-pit mining." Géotechnique **68**(3): 189-204.

- Shokouhi, A. and D. J. Williams (2015). Settling and consolidation behaviour of coal tailings slurry under continuous loading. Tailings and Mine Waste 2015. Vancouver, BC.
- Stone, K. J. and D. M. Wood (1992). "Effects of dilatancy and particle size observed in model tests on sand." Soils and Foundations **32**(4): 43-57.
- Taylor, R. N. (1995). Geotechnical Centrifuge Technology, Taylor & Francis.
- Terzaghi, K. (1943). Theoretical soil mechanics, J. Wiley and Sons, inc.
- Terzaghi, K. and O. K. Fröhlich (1936). Theorie der Setzung von Tonschichten: eine Einführung in die analytische Tonmechanik, Franz Deuticke.
- Thevanayagam, S. (2007). "Intergrain contact density indices for granular mixes—I: Framework." Earthquake engineering and engineering vibration **6**(2): 123.
- Tsirel, S. (1997). "Methods of granular and fragmented material packing density calculation." International Journal of Rock Mechanics and Mining Sciences **34**(2): 263-273.
- Vick, S. G. (1990). Planning, design, and analysis of tailings dams, BiTech.
- von Fay, K. and C. Cotton (1986). Constant-Rate-of-Loading (CRL) Consolidation Test. STP34618S Consolidation of Soils: Testing and Evaluation, ASTM International.
- Wang, C., D. Harbottle, Q. Liu and Z. Xu (2014). "Current state of fine mineral tailings treatment: A critical review on theory and practice." Minerals Engineering **58**: 113-131.
- Wang, N., R. Cleminson and J. Lorentz (2017). Co-mixing of Fluid Fine Tailings and Clearwater Overburden. COSIA Oil Sands Innovation Summit. Calgary, AB.
- Wickland, B. and S. Longo (2017). Mine waste case examples of stacked tailings and co-disposal. Tailings and Mine Waste '17. Banff, Alberta, Canada.
- Wickland, B. E. (2006). Volume change and permeability of mixtures of waste rock and fine tailings, University of British Columbia.
- Wickland, B. E. and G. W. Wilson (2005). "Self-weight consolidation of mixtures of mine waste rock and tailings." Canadian Geotechnical Journal **42**(2): 327-339.
- Wickland, B. E., G. W. Wilson and D. Wijewickreme (2010). "Hydraulic conductivity and consolidation response of mixtures of mine waste rock and tailings." Canadian Geotechnical Journal **47**(4): 472-485.
- Wickland, B. E., G. W. Wilson, D. Wijewickreme and B. Klein (2006). "Design and evaluation of mixtures of mine waste rock and tailings." Canadian Geotechnical Journal **43**(9): 928-945.

Wijewickreme, D., A. Khalili and G. W. Wilson (2010). "Mechanical response of highly gap-graded mixtures of waste rock and tailings. Part II: Undrained cyclic and post-cyclic shear response." Canadian Geotechnical Journal **47**(5): 566-582.

Williams, D. (1997). Effectiveness of co-disposing coal washery wastes. Proceedings of the 4th International Conference on Tailings and Mine Waste.

Williams, M., K. Seddon, T. Fitton, A. Fourie, R. Jewell, P. Slatter and A. Paterson (2008). Surface disposal of Paste and Thickened Tailings—A brief history and current confronting issues. 11th Int. Seminar on Paste and Thickened Tailings.

Xu, Y., D. J. Williams and M. Serati (2017). Effect of Scalping on Shear Strength of Aggregate. 51st U.S. Rock Mechanics/Geomechanics Symposium. San Francisco, California, USA, American Rock Mechanics Association.

Yang, L.-A. and T.-S. Tan (2005). "One-dimensional consolidation of lumpy clay with non-linear properties." Géotechnique **55**(3): 227-235.

Yang, L.-A., T.-S. Tan, S.-A. Tan and C.-F. Leung (2002). "One-dimensional self-weight consolidation of a lumpy clay fill." Géotechnique **52**(10): 713-725.

Youd, T. (1973). Factors controlling maximum and minimum densities of sands. Evaluation of relative density and its role in geotechnical projects involving cohesionless soils. American Society for Testing and Materials STP 523. Philadelphia, PA: 98-112.

Yu, A. and N. Standish (1993). "A study of the packing of particles with a mixture size distribution." Powder Technology **76**(2): 113-124.

Yu, X., S. Ji and K. D. Janoyan (2006). "Direct Shear Testing of Rockfill Material." Soil and Rock Behaviour and Modeling.

Znidarčić, D., R. L. Schiffman, V. Pane, P. Croce, H. Y. Ko and H. W. Olsen (1986). "The theory of one-dimensional consolidation of saturated clays: part V, constant rate of deformation testing and analysis." Géotechnique **36**(2): 227-237.

DERIVATION OF EQUATION (3.2)

Given (Terzaghi 1943):

$$\frac{u_b}{u_i} = \sum_{m=0}^{m=\infty} \frac{2}{M} (\sin M) \exp(-M^2 T_v) \quad (1)$$

Where:

$$M = \frac{\pi}{2} (2m + 1)$$

$$T_v = \frac{c_v t}{d^2}$$

u_b = excess pore pressure at base

u_i = initial excess pore pressure at base

For a homogenous material of a given c_v , the degree of dissipation of excess pore pressure (u_b/u_i) is a function of t/d^2 .

Consider 2 samples of identical material with different drainage path lengths. For a given u_b/u_i , we can say:

$$\frac{t_1}{d_1^2} = \frac{t_2}{d_2^2} \quad (2)$$

Where d_1 and d_2 are the drainage path lengths of each stack, and t_1 and t_2 are the times for each stack to reach the given u_b/u_i .

We can use this principle to simulate consolidation of a stack in field, using a smaller sample in the laboratory. Let T = laboratory (actual) time, t = field (simulated) time, h = laboratory drainage path length (sample height), d = field drainage path length (stack height). Substitution into (2) gives:

$$\frac{t}{d^2} = \frac{T}{h^2} \quad (3)$$

Rearranging gives:

$$\frac{T}{t} = \frac{h^2}{d^2} \quad (4)$$

RAPID DEPOSITION CASE – WORKED EXAMPLE

Consider the case of a stack being raised rapidly to a height of 15m, with single drainage from the top only. In this case, we assume that because the stack is constructed rapidly, the load is applied instantaneously. If we wish to simulate this stack in the laboratory using a sample 0.3 m high,

Sample height, $h = 0.3\text{m}$

Field drainage path length, $d = 15\text{m}$

By re-arranging equation (3), we can calculate the stress that must be applied rapidly to the sample in the laboratory:

$$\sigma = \frac{\sigma}{d} d = 18 \text{ kNm}^{-3} \times 15 \text{ m} = 270 \text{ kPa}$$

From equation (2), we can calculate the time scaling factor,

$$\text{Time scaling factor } (T_s) = \frac{T}{t} = \frac{h^2}{d^2} = \frac{0.3^2}{15^2} = 0.0004$$

Thus, if we run the test for 1 hour of actual, laboratory time (T) and observe dissipation of excess pore pressure due to the consolidation process, the time which we have simulated in the field (t), can be calculated:

$$t = T/T_s = 1/0.0004 = 2500 \text{ hours or } 104.17 \text{ days}$$

SLOW RATE OF DEPOSITION – WORKED EXAMPLE

Consider the case of a stack that rises at a constant rate of 1m/day to a final height of 15m, with single drainage from the top only.

The problem may be approximated by dividing it up into a series of load steps, and applying a constant load rate for the duration of each step. For this example, we will use 10 steps of equal load, given below:

Appendix A

Derivations and worked examples

Load step	Load (kPa)
1	27
2	54
3	81
4	108
5	135
6	162
7	189
8	216
9	243
10	270

The field drainage path length (d) at the end of each load step can be calculated using equation (3):

$$d = \frac{\sigma}{\gamma}$$

Load step	Load (kPa)	d (m)
1	27	1.5
2	54	3
3	81	4.5
4	108	6
5	135	7.5
6	162	9
7	189	10.5
8	216	12

Appendix A

Derivations and worked examples

9	243	13.5
10	270	15

The time factor (T_s) at the end of each load step can be calculated using equation (2):

$$T_s = \frac{h^2}{d^2}$$

For a sample height (h) of 0.1 m:

Load step	Load (kPa)	d (m)	T_s
1	27	1.5	4.44E-03
2	54	3	1.11E-03
3	81	4.5	4.94E-04
4	108	6	2.78E-04
5	135	7.5	1.78E-04
6	162	9	1.23E-04
7	189	10.5	9.07E-05
8	216	12	6.94E-05
9	243	13.5	5.49E-05
10	270	15	4.44E-05

The “field time” of each load step can then be calculated using equation (5):

$$t = \frac{\Delta d}{m} = \frac{1.5 \text{ m}}{1 \text{ m/day}} = 1.5 \text{ days}$$

The laboratory (actual) time of each load step (T) can then be calculated by rearranging equation (2):

$$T = t \times T_s$$

Appendix A

Derivations and worked examples

Load step	Load (kPa)	d (m)	T _s	T (minutes)
1	27	1.5	4.44E-03	9.60
2	54	3	1.11E-03	2.40
3	81	4.5	4.94E-04	1.07
4	108	6	2.78E-04	0.60
5	135	7.5	1.78E-04	0.38
6	162	9	1.23E-04	0.27
7	189	10.5	9.07E-05	0.20
8	216	12	6.94E-05	0.15
9	243	13.5	5.49E-05	0.12
10	270	15	4.44E-05	0.10

The loading rate ($\Delta\sigma / \Delta T$) for each step can then easily be calculated:

Load step	Load (kPa)	d (m)	T _s	T (minutes)	Loading rate (kPa/min)
1	27	1.5	4.44E-03	9.60	2.81
2	54	3	1.11E-03	2.40	11.25
3	81	4.5	4.94E-04	1.07	25.31
4	108	6	2.78E-04	0.60	45.00
5	135	7.5	1.78E-04	0.38	70.31
6	162	9	1.23E-04	0.27	101.25
7	189	10.5	9.07E-05	0.20	137.81
8	216	12	6.94E-05	0.15	180.00
9	243	13.5	5.49E-05	0.12	227.81
10	270	15	4.44E-05	0.10	281.25

Appendix A

Derivations and worked examples

The load steps are programmed into the testing apparatus. Note that while the above is an approximation which assumes constant sample height, when analysing test data, continuous time factors can be calculated from actual sample height, and the “field time” t is a summation of field time calculated from each time step (in this case the time step is the data recording interval of the apparatus).